EVALUATION OF PLATINUM SILICIDE AND INDIUM ANTIMONIDE AS DETECTOR MATERIALS FOR SPACE-BASED REMOTE SENSING IN THE 3.0-TO-5.0 MICROMETER WAVELENGTH BAND

THESIS

Ralph R. Sandys
Captain, USAF
AFIT/GSO/ENP/ENS/89D-6

DEPARTMENT OF THE AIR FORCE
AIR UNIVERSITY
AIR FORCE INSTITUTE OF TECHNOLOGY

Wright-Patterson Air Force Base, Ohio

AFIT/GSO/ENP/ENS/89D-6

EVALUATION OF PLATINUM SILICIDE AND INDIUM ANTIMONIDE AS DETECTOR MATERIALS FOR SPACE-BASED REMOTE SENSING IN THE 3.0-TO-5.0 MICROMETER WAVELENGTH BAND

THESIS

Presented to the Faculty of the School of Engineering
of the Air Force Institute of Technology
Air University
In Partial Fulfillment of the
Requirements for the Degree of
Master of Science in Space Operations

Ralph R. Sandys
Captain, USAF

December 1989

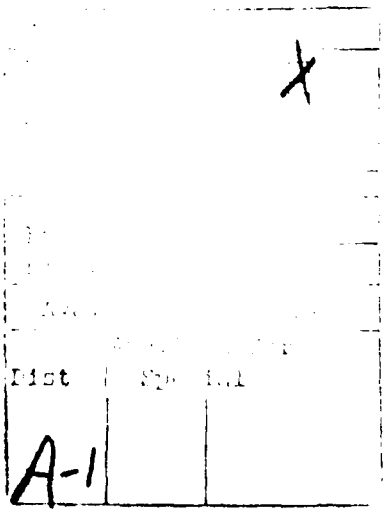

Approved for public release; distribution unlimited

Preface

A great deal of time and effort was put into this thesis. Many, many, many hours were spent in front of my computer crunching numbers. The assistance and understanding I received from several people, technical and otherwise, was of great importance in completing this thesis as well as AFIT. First, a thank you goes to my advisor Major James J. Lange for the expertise and knowledge he contributed to this effort. Moreover, I'd like to thank him for keeping me in check. I'd also like to thank Major T.S. Kelso for helping me keep things in perspective. Finally, a big thank you goes to Roz for understanding and putting up with me throughout this research and my stay at AFIT.

Ralph R. Sandys

Table of Contents

List of Figures

List of Tables

Abstract

Platinum Silicide and Indium Antimonide are evaluated as detector materials for space-based remote sensing of man-made ground targets in the 3.0-to-5.0 μm band. The evaluation compares a generic target to each of four backgrounds including vegetation, snow, sand, and soil. A spectral count rate for the target and each background is calculated taking into account the material's quantum efficiency, the source's reflectivity/emissivity, and the atmospheric transmission. A baseline case and nine excursions were examined. The baseline case has the target and backgrounds at a temperature of 298°K. The atmospheric transmission used in this case is for a rural setting with a 23 km visibility and a vertical path through the atmosphere. The nine additional cases are produced by varying the baseline one parameter at a time — target and background temperatures, target reflectivity, and atmospheric humidity. Based on these cases, an evaluation was made of the remote sensing potential of each material as the various parameters were varied. In addition, an assessment was made of the multiband remote sensing possibilities in the 3.0-to-5.0 μm band available for each material.

I. Introduction

Space-based infrared (IR) remote sensing has been in existence for over 29 years — almost from the days following the first satellite launch in 1957. Civilian applications of space-based IR remote sensing include earth resources monitoring and weather forecasting. In addition to these two applications, military applications also include surveillance, early warning, reconnaissance, and arms control verification (10:22,13:108).

Historically the 8.0-to-12.0 micrometer (μm) and 0.7-to-3.0 μm regions of the IR have been the bands of choice for most space-based IR remote sensing applications. The primary reason for this choice is directly related to the available detector technology. Recent advances, however, in staring focal plane array sensor technology now make space-based remote sensing in the 3.0-to-5.0 μm band a viable alternative.

The 3.0-to-5.0 μm band, also known as the middle wavelength IR (MWIR), has recently been compared to the 8.0-to-12.0 μm band for various IR remote sensing applications (13:106). Past MWIR remote sensing applications have centered around air- and ground-based systems, for example, air-to-air detection of aircraft, ground-to-air missile seekers, and telescopes for astronomy.

The MWIR band is interesting — at these wavelengths, both target and background signatures (characteristic

radiation from a particular target or background) transition from being mostly reflected solar to being mostly thermally emitted. In fact, it could be that this characteristic will make the MWIR the most important portion of the IR band, since it allows for the exploitation of both types of radiation from a target, instead of just one.

Remote sensing in the MWIR has become easier due to important advances in detector technology. Of particular importance in exploiting the MWIR are the advances in producing two-dimensional focal plane arrays (FPA) of platinum silicide (PtSi) detectors. For example, some state-of-the-art PtSi FPAs contain 262,144 and 311,040 pixels, or individual detectors, arranged in 512 x 512 and 486 x 640 arrays, respectively. In fact, Hughes Aircraft is planning on using PtSi detectors on the US Army's new Non-Line-Of-Sight Missile. The low cost of producing PtSi detectors even has Strategic Defense Initiative (SDI) officials interested. Hesitation by these same officials to commit to this detector arises from the fact that there is little information concerning whether or not a space sensor can be developed (11:51).

Research by the US Air Force's Rome Air Development Center (RADC) and the Lincoln Laboratory have primarily focused on ground- and air-based applications of this technology. Moreover, Schoon, in his thesis, indicates that evaluation of space-based sensors in the MWIR is

non-existent (32:1). Schoon evaluates PtSi as well as indium antimonide (InSb) as detector materials for space-based remote sensing applications in the MWIR. His research indicated that both detectors show promise in this band. Specifically, PtSi is more suited for detecting reflected solar radiation from a target, while InSb is more responsive in detecting a target's thermal radiation during the day. Although this work indicates both detectors may be usable in the MWIR, it is far from being complete. In order to detect a target, the detector must be able to distinguish between the radiation from the target and that from its background, the latter of which is often not insignificant.

The purpose of this investigation is to further evaluate the space-based remote sensing potential of PtSi and InSb as detector materials in the 3.0-to-5.0 μm band of the electromagnetic spectrum by calculating sensor (detector) outputs for standard targets against a variety of backgrounds and scenarios, to include different lighting (day and night) and atmospheric conditions. A determination is also made of the remote sensing possibilities, including multiband remote sensing, available within the 3.0-to-5.0 μm band.

Chapter II contains a review of the background material necessary to understand the methodology involved in this investigation. This chapter gives a definition of remote sensing, the physics of remote sensing pertinent to this

research, the types of sensors available, and the detector materials available.

Chapter III discusses the methodology used in this investigation. It includes the sensor output equations, the target, the backgrounds, and the cases explored.

Chapter IV presents the results of this investigation. Finally, Chapter V discusses the conclusions and presents some recommendations.

II. Background

Introduction

In order to assess the potential of space-based remote sensing as well as air-to-ground applications in the MWIR using the recent advances in sensor technology, an understanding of several topics is necessary. This chapter will include a basic definition of remote sensing, the physics of remote sensing pertinent to this research, the types of sensors available, and the detector materials available.

Definition of Remote Sensing

Space-based remote sensing is the process of detecting and collecting electromagnetic radiation (energy) from objects, scenes, or events at the earth's surface from space, without being in direct contact with the item in question. In many applications of remote sensing, the objective is often to identify and track a target. This encompasses collecting radiation from both the target and its background, and then somehow discriminating the target from the background for identification.

Physics of Remote Sensing

Target Radiation. Radiation from a source is typically a combination of reflected solar and thermally emitted energy. A target or background can be characterized and

identified by the energy emanating from it. Reflected solar energy from a target is a function of the target's material and surface properties and is characterized by its reflectance or reflectivity. Emitted thermal energy from a target is a function of the target's material properties and is characterized by its emissivity parameter and temperature (21:37-42; 9:16-19). As a result of their dependence on these characteristics, both solar reflectance and thermal emission vary with wavelength. The characteristic, and in many cases, unique variation with wavelength of radiation from a target is often called a signature. Signatures are used to distinguish between a target and its background and, more importantly, to specifically classify or identify the target.

Atmospheric Propagation of IR Radiation. In order for radiation or light from a scene to reach a space-based sensor, it must pass through the atmosphere. Propagation of light through the atmosphere is affected by three processes: 1) extinction, 2) turbulence, and 3) refraction (8:445). For the purposes of this investigation, only extinction, which is the most important to this application, will be considered. Extinction results from the interaction of light with other matter. Light particles (photons) can either be absorbed or scattered as a result of interaction, thereby reducing the amount of light reaching a space-based sensor. In the IR region of the electromagnetic spectrum,

water vapor (H_2O), carbon dioxide (CO_2), and ozone (O_3) molecules are the primary cause of absorption, while interaction with atmospheric particles such as haze, smog, and smoke can cause scattering (9:20; 29:28-29). Attenuation due to absorption causes large portions of the electromagnetic spectrum to be unusable for remote sensing due to low or no transmission of radiation. The portions that are usable are called atmospheric windows. The MWIR band is an atmospheric window in the IR portion of the electromagnetic spectrum. Figure 1 shows the typical percentages of transmission in the MWIR. To conduct remote sensing, an atmospheric window must be used.

MWIR Characteristics. In addition to being an atmospheric window, the MWIR has another interesting feature. For wavelengths less than 3.0 μm, radiation is predominantly reflected solar for scenes on the earth's surface having a typical temperature of 298°K (77°F). For wavelengths greater than 5.0 μm, radiation from a typical scene is predominantly thermally emitted. However, radiation from a scene between 3.0 and 5.0 μm has components of both types as shown in Figure 2. It is therefore important to consider both when remote sensing is conducted in this region.

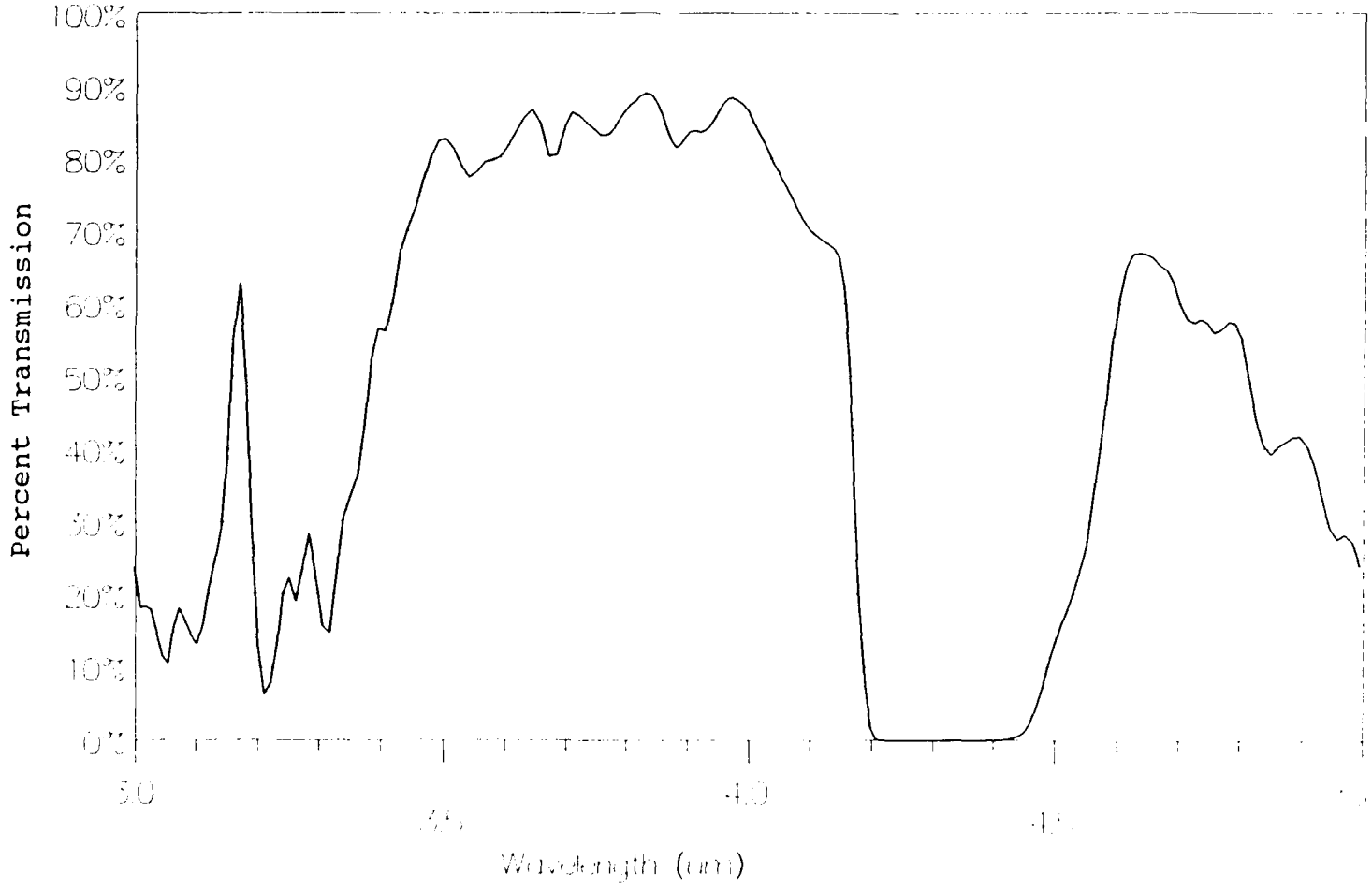

Figure 1. Atmospheric Transmission in the MWIR

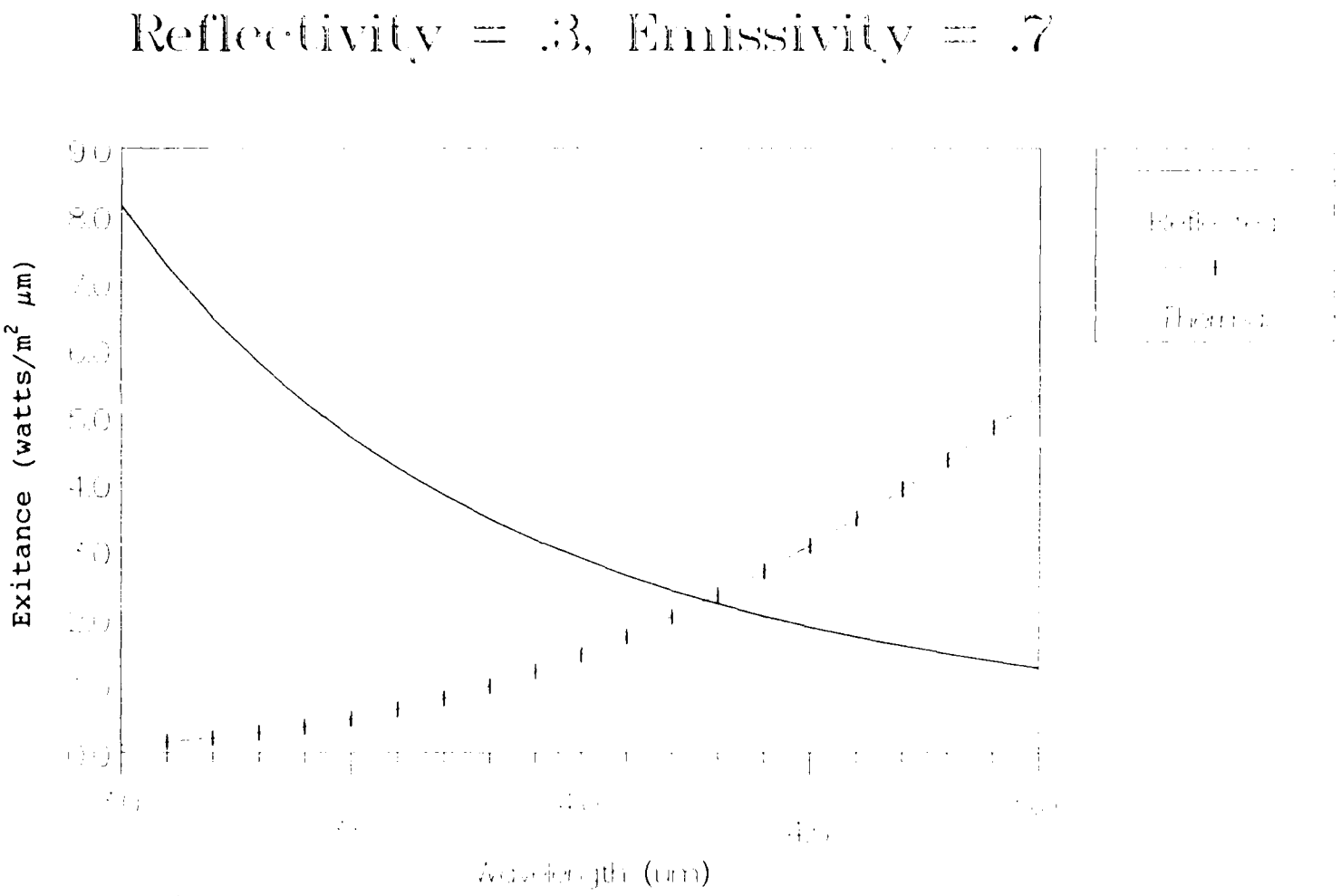

Figure 2. Reflected vs Thermal Radiation in the MWIR

Sensors

After propagating through the atmosphere, the radiation from a scene reaching a space-based satellite is collected by some form of optics. The optics, usually consisting of a lens or mirror or some combination of lenses and/or mirrors, focus incident radiation onto a sensor, located at the focal plane. There are two basic types of sensors, a scanning sensor and a staring sensor. Both types of sensors rely on the interaction of photons (radiation) with individual detector elements. Photons from a target, impinging a detector element, are converted into an electrical signal which is then processed along with the signals from other individual detector elements to form an image of the scene (22:856).

A typical scanning sensor consists of a linear focal plane array (FPA) of detector elements which mechanically scans or sweeps across the scene under observation. A staring sensor, having no moving parts, relies on large, two-dimensional focal plane arrays of detectors to observe the same scene. Staring sensors have advanced from single detectors to focal planes of high numbers and densities of detectors (5:60; 30:14). The lack of moving parts and potentially higher sensitivities are two of the reasons staring focal plane arrays are now being used for IR remote sensing (22:855).

Sensitivity. Selection of a sensor for remote sensing applications depends on the type of target, background, and what portion of the electromagnetic spectrum is being used. In general, scanning sensors are used to detect targets which are much brighter or much dimmer than the background. On the other hand, because staring sensors can potentially be more sensitive than scanning sensors, they do not necessarily have to depend on as bright a signature for target detection as a scanning sensor. This high sensitivity characteristic of staring sensors is useful for remote sensing in any spectral band where the contrast between target intensity and background intensity may be low with the target slightly brighter than the background or slightly dimmer than the background (24:84).

Photon Collection Efficiency. When there is low intrinsic scene contrast, caused by similar electromagnetic responses of the target and background, a large number of photons must be collected and processed, in order to measure the relatively small number of photons that make up the target signature (20:271; 28:144-145; 30:7). Therefore, one requirement for high sensitivity in a sensor is a high photon collection efficiency. For a staring focal plane array, incoming photons are captured by all of its detectors simultaneously, which leads to a high collection efficiency. In contrast, a scanning sensor captures only a portion of the incoming photons (4:13). Because of this low collection

efficiency, the quantum efficiency (how well radiation is converted into electrons) of a scanning sensor must be relatively high, while the quantum efficiency for a staring sensor can be lower. The quantum efficiency for a sensor is determined by the material(s) used in constructing a sensor's detectors, a characteristic which is discussed later in this chapter.

Photo Response Uniformity. The other requirement for high sensitivity in staring focal plane arrays is high photo (photon) response uniformity. Although large numbers of photons are collected, unless the signals that are produced by their interactions with each detector element are uniform, the resulting output image will be distorted, and therefore, will not properly represent the observed target and/or background. This requires that the response (of each individual detector) to impinging photons be uniform from detector element to detector element (22:855; 34:98). High photo response uniformity is a function of detector material(s), focal plane array device design, and focal plane array fabrication technology. Recent advances in these areas provide focal plane arrays with the high photo response uniformity required for the high sensitivity needed in MWIR remote sensing.

Resolution. In addition to the high sensitivity provided by staring focal plane arrays, high image resolution is another potential benefit. The long photon

collection times (integration times) inherent to staring focal plane arrays not only give a high photon collection efficiency, but when coupled with the high photo response uniformity possible with staring focal plane arrays, can lead to increased resolution of the target (5:62).

Detector Materials

There are many different types of materials that are used for remote sensing detectors. Of these, only a few readily lend themselves to MWIR remote sensing. Factors such as the sensitivity and resolution requirements of the remote sensing application as well as the device design and fabrication technology of staring focal plane arrays tend to restrict the types of materials available. Some of the more common detector materials that are under investigation for MWIR staring focal plane array sensors include indium antimonide (InSb), mercury cadmium telluride (HgCdTe), platinum silicide (PtSi), iridium silicide (IrSi), and platinum iridium silicide (PtIrSi) (4:13; 33:147; 37:100). The following paragraphs discuss the MWIR remote sensing potential of each of these materials.

Indium Antimonide (InSb). InSb, under development for over 20 years as an IR detector, is a good material for remote sensing in the MWIR in that it has a high quantum efficiency (14:429; 40:579). However, employment of these detectors has been limited to applications such as

ground-based astronomy, air-to-air missiles, and ground-to-air missiles (14:429). One current InSb sensor has a 128 x 128 array of detector elements (2). In addition to the fairly large number of detector elements, InSb also has a high quantum efficiency. For the 3.0-to-5.0 μm band, InSb's quantum efficiency is constant at about 0.6-to-0.7 across the band (4:13; 15:50-51; 26:413; 32:38). In addition, InSb focal plane arrays can be manufactured at a reasonable cost using current fabrication technology (15:57). Because of these factors, InSb focal plane arrays may be suitable for space-based MWIR remote sensing.

Mercury Cadmium Telluride (HgCdTe). HgCdTe, under development for over 15 years as an IR detector, currently competes with InSb for many MWIR remote sensing applications (7:12). Arrays of 128 x 128 detector elements are available for MWIR remote sensing (7:9). Although having the same number of detector elements as current InSb sensors, HgCdTe has a lower quantum efficiency of about 0.4-to-0.5 across the 3.0-to-5.0 μm band (4:13). In addition, the characteristics of the material itself make the manufacture of HgCdTe focal plane arrays with high photo response uniformity difficult (12:60). Furthermore, only one out of 100 HgCdTe focal plane arrays manufactured is usable due to dead detector elements on the array (25:70). As a result of these manufacturing problems, HgCdTe focal plane arrays are

not only expensive but are probably unsuitable for space-based MWIR remote sensing.

Platinum Silicide (PtSi). Silicide focal plane arrays for MWIR use were first suggested in 1973 using Schottky-barrier detector technology (34:98). The first PtSi focal plane array, developed in 1979, contained 1250 detector elements arranged in a 25 x 50 element array (19:1564). The largest current PtSi focal plane array is a 512 x 512-element sensor developed by the Mitsubishi Electric Corporation (16:1124; 35:6). The rapid advance in PtSi focal plane array technology is due to its utilization of standard silicon very large scale integrated circuit (VLSIC) technology (17:11; 34:98). Because PtSi focal plane arrays are based on silicon technology, manufacturing costs are low and large arrays can be constructed. Furthermore, approximately 35-to-40% of PtSi arrays manufactured are usable, in contrast to the 1% for HgCdTe arrays (25:70). On the other hand, the quantum efficiency of PtSi is extremely low in the MWIR. Starting with about 0.03 at 3.0 μm, it quickly drops to about 0.002 at 5.0 μm (4:13; 32:39). However, PtSi's low quantum efficiency is offset by the high photon collection efficiency provided by the large number of detector elements intrinsic to large, two-dimensional arrays (4:13). In addition, high photo response uniformity, resulting from the use of standard silicon technology, also offsets the low quantum efficiency (6:279; 17:11; 23:225;

34:98). Based on these attributes, PtSi focal plane arrays appear suitable for space-based MWIR remote sensing.

Iridium Silicide (IrSi). A "strong interest in extending the response of Schottky-barrier detectors into the" 8.0-to-14.0 μm region of the electromagnetic spectrum has lead to the development of two other silicide materials applicable to MWIR remote sensing (27:93; 37:100). The first of these is IrSi. Under development since 1982, IrSi is projected to have a slightly higher quantum efficiency than PtSi, starting with about 0.1 at 3.0 μm, and dropping to about 0.04 at 5.0 μm (4:13). However, problems in forming IrSi currently prevent the fabrication of the large focal plane arrays required for MWIR remote sensing (27:96; 37:100).

Platinum Iridium Silicide (PtIrSi). The second material resulting from the interest to extend the response of Schottky-barrier detectors to longer wavelengths is PtIrSi. Although Tsaur suggests that PtIrSi has a better quantum efficiency than either PtSi or IrSi, it appears that the PtSi and IrSi devices that he used in the comparison may not be the most current available (37). Moreover, fabrication of large focal plane arrays using this material needs to be demonstrated before space-based MWIR remote sensing applications are considered.

Of the five different materials under development for MWIR remote sensing, the first three, InSb, HgCdTe, and

PtSi, currently show the most promise. Of these three, InSb and PtSi show the most potential for space-based MWIR remote sensing applications and will be used for this investigation. Because the quantum efficiency of InSb and HgCdTe are both nearly constant in the MWIR, most of the results and conclusions for InSb should be applicable to HgCdTe.

III. Methodology

Introduction

The approach used in evaluating PtSi and InSb as detector materials is presented in this chapter. The evaluation involves calculating sensor outputs for each material. The sensor output calculation is based on the phenomenology of radiation from a target and its background traveling through the atmosphere to reach the sensor. This phenomenology is captured in a single equation, explained below, which is the basis for this investigation.

Scaled Count Rate Equation

The sensor output calculation is based on the fact that radiation from a source reaching a sensor is converted to electrons. The number of electrons created by the sensor is calculated by the following equation:

$$N = \frac{A_R \ \Omega_R}{\pi \ h \ c} \int_{\lambda_1}^{\lambda_2} \eta(\lambda) \ G(\lambda) \ M_\lambda(\lambda) \ \tau_{ATM}(\lambda) \ \tau_{OPT}(\lambda) \ \lambda \ d\lambda \qquad (1)$$

where

N	is the count rate in electrons per unit time;
A_R	is the effective collecting area of the sensor's front-end optics;
Ω_R	is the field of view of the sensor;
h	is Planck's constant;

c	is the speed of light;
λ	is the wavelength of incident radiation;
hc/λ	is the energy of a photon;
$\eta(\lambda)$	is the quantum efficiency of the detector material in the spectral bandpass between λ_1 and λ_2;
$G(\lambda)$	is the gain of the sensor in the spectral bandpass between λ_1 and λ_2;
$M_\lambda(\lambda)$	is the spectral exitance of the target or background between λ_1 and λ_2, assuming a Lambertian, or diffuse, reflection or emission;
$\tau_{ATM}(\lambda)$	is the atmospheric transmission in the spectral bandpass between λ_1 and λ_2; and
$\tau_{OPT}(\lambda)$	is the transmission of all the sensor optics in the spectral bandpass between λ_1 and λ_2 (21:216-224; 32:35-36; 36:423-430; 39:109-120).

This equation assumes that the radiation from a source fills the field of view of a single detector.

In order to keep the evaluation non-sensor specific, the count rate, N, is divided by all the variables pertaining to the optics and electronics in Equation 1. In so doing, the assumption that $G(\lambda)$ and $\tau_{OPT}(\lambda)$ are constant across the spectral bandpass is used. This results in the following scaled count rate (SCR) equation:

$$SCR \equiv \frac{N \pi h c}{A_R \Omega_R G \tau_{OPT}} = \int_{\lambda_1}^{\lambda_2} \eta(\lambda) M_\lambda(\lambda) \tau_{ATM}(\lambda) \lambda \, d\lambda \qquad (2)$$

Evaluation of the integral in Equation 2 is done using the following summation:

$$SCR \simeq \sum_{i=1}^{n} \eta(\lambda_i)\ M_\lambda(\lambda_i)\ \tau_{ATM}(\lambda_i)\ <\lambda_i>\ \Delta\lambda_i \qquad (3)$$

$$= \sum_{i=1}^{n} SCR_\lambda(\lambda_i)\ \Delta\lambda_i$$

where

SCR_λ	is the spectral scaled count rate;
$\eta(\lambda_i)$	is the quantum efficiency at each wavelength λ_i;
$M_\lambda(\lambda_i)$	is the spectral exitance of the target or background at each wavelength λ_i, assuming a Lambertian, or diffuse, emission or reflection;
$\tau_{ATM}(\lambda_i)$	is the atmospheric transmission at each wavelength λ_i;
$<\lambda_i>$	is the average wavelength over the band λ_i to λ_{i+1}; and
$\Delta\lambda_i$	is the bandwidth between λ_i and λ_{i+1} (32:36).

Quantum Efficiency

The quantum efficiency, η, of a material is a measure of how well the material converts radiation into electrons. For PtSi, the quantum efficiency, shown in Figure 3, is evaluated using the following equation:

$$\eta(\lambda) = .31\left[1 - \frac{.21\lambda}{1.24}\right]^2 \frac{h\ c}{e\ \lambda} \qquad (4)$$

Figure 3. Platinum Silicide Quantum Efficiency

where

$\eta(\lambda)$ is the number of electrons created per incident photon at λ,

λ is the wavelength in μm,

h is Planck's constant in joule sec,

c is the speed of light in μm/sec, and

e is the charge of an electron and the conversion factor from joules to electron volts (32:38).

The quantum efficiency for InSb, on the other hand, is essentially constant at 0.65 across the 3.0-to-5.0 μm band (32:38).

Spectral Exitance

Calculation of the spectral exitance from both the target and background assumes a Lambertian source. The spectral exitance calculations first required the calculation of the ideal or black body exitance given in general by

$$B_\lambda(\lambda) = \frac{2 \pi h c^2}{\lambda^5 \left[\exp\left[\frac{h c}{\lambda k_B T} \right] - 1 \right]} \quad (5)$$

where

$B_\lambda(\lambda)$ is the black body exitance at λ and has units of watts per m^2 of emitting area per m of spectral bandpass;

h is Planck's constant;

k_B is Boltzmann's constant;

c is the speed of light in m/sec;

λ is the wavelength in meters; and

T is the temperature in °K (21:7).

For wavelengths in units of μm, Equation 5 reduces to

$$B_\lambda(\lambda) = \frac{3.74 \times 10^8}{\lambda^5 \left[\exp\left[\frac{1.44 \times 10^4}{\lambda \ T} \right] - 1 \right]} \qquad (6)$$

where

$B_\lambda(\lambda)$ has units of watts per m^2 per μm,

λ is the wavelength in μm, and

T is the temperature in °K (21:7).

The reflected exitance from a source is calculated by

$$M_{\lambda R}(\lambda) = B_\lambda(\lambda, T_{sun}) \left[\frac{R_{sun}}{R_{1AU}} \right]^2 \rho(\lambda) \ \tau_{ATM}(\lambda) \qquad (7)$$

where

$B_\lambda(\lambda, T_{sun})$ is the black body exitance of the sun at λ;

T_{sun} is the surface temperature of the sun, T_{sun} = 6000°K;

R_{sun} is the average radius of the sun, R_{sun} = 695,950 km;

R_{1AU} is the distance between the sun and the earth, R_{1AU} = 149,599,650 km;

$\rho(\lambda)$ is the reflectivity of a target or background at λ; and

$\tau_{ATM}(\lambda)$ is the atmospheric transmission at λ.

The thermal exitance from a source is calculated by

$$M_{\lambda T}(\lambda) = B_{\lambda}(\lambda, T_{source})\ \epsilon(\lambda) \qquad (8)$$

where

$B_{\lambda}(\lambda, T_{source})$ is the black body exitance of the target or background at λ and

$\epsilon(\lambda)$ is the emissivity of the target or background at λ, where $\epsilon(\lambda) = 1 - \rho(\lambda)$.

The summation of the reflected and thermal exitances gives the daytime exitance of a source, while the thermal exitance gives the nighttime exitance.

Targets and Backgrounds

The emissivity or reflectivity required for the exitance calculations is a function of the source as described in Chapter II. In this case, the sources include a target and four backgrounds. The target used for this investigation is a generic target comprised of 20 different coatings (32:40). This target was selected for two reasons, 1) to keep the calculations generic (unclassified) and 2) to continue the efforts started by Schoon. Table I contains a list of the coatings used along with their average reflectivities across the 3.0-to-5.0 μm band. Figure 4 has plots of the target's average reflectivity and average emissivity across the 3.0-to-5.0 μm band, respectively. The

Table I. Target Coatings

Coating	Average Reflectance
Alkyd Resin	.181
Epoxy Resin	.614
Lacquer Resin	.615
Nylon Resin	.277
Polyurethane Resin	.608
Polyvinyl Chloride Resin	.921
Titanium Dioxide	.108
Lead Molybdenum Tetraoxide	.152
Manganese Oxide	.522
Silicon Nitride	.428
Vanadium Oxide	.254
Zirconium Oxide	.506
Zirconium Silicate	.365
Titanium Dioxide Pigmented	.076
Aluminum Pigmented	.408
Antimony Oxide Pigmented	.055
Carbon Pigmented	.075
Strontium Molybdate Pigmented	.235
Zinc Chromate Pigmented	.147
Zinc Oxide Pigmented	.202

Adapted from (32:42)

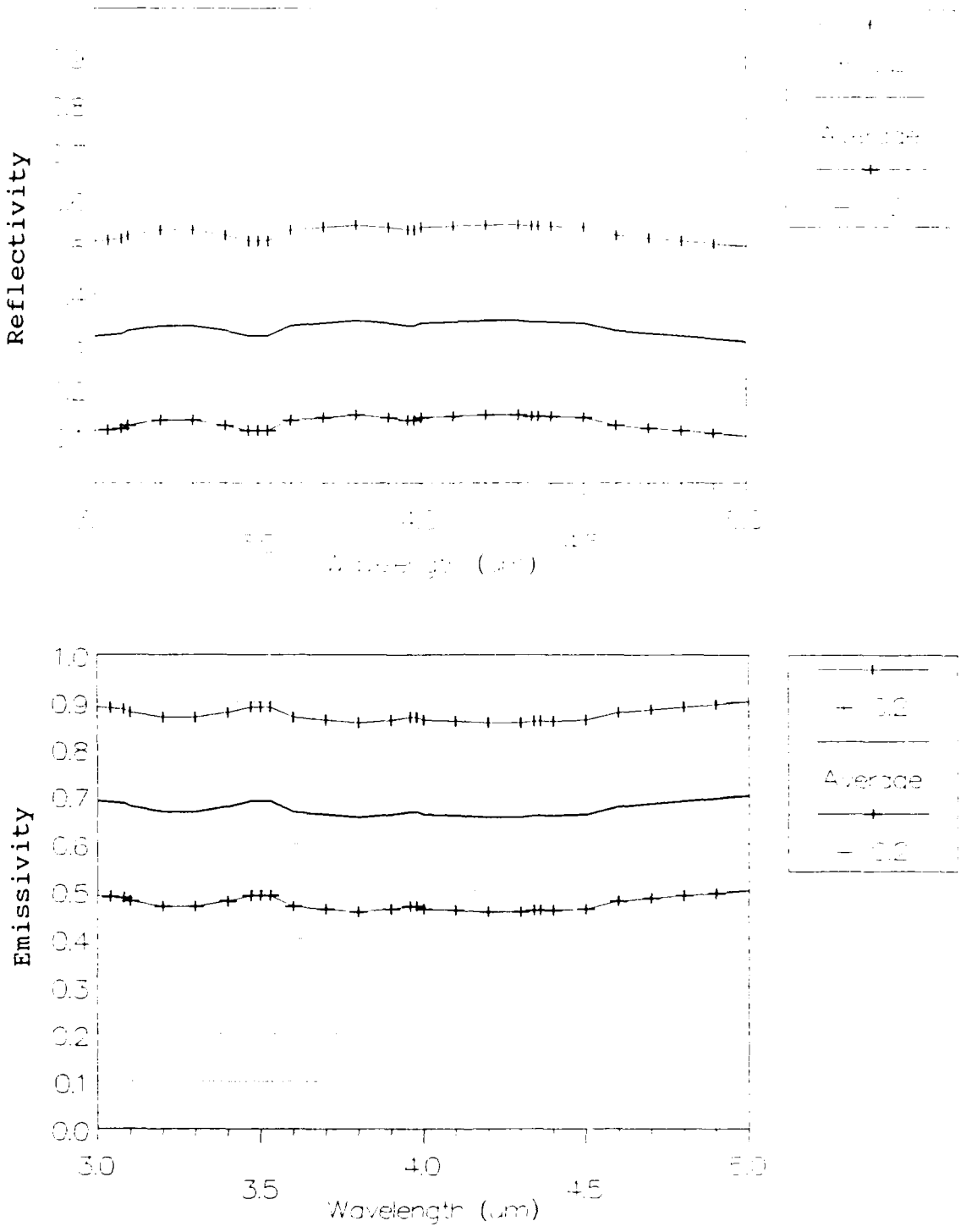

Figure 4. Spectral Reflectivity and Emissivity of the Target Adapted from (32:43)

plus or minus 0.2 deviations closely approximate that of one standard deviation for each of the average plots.

Backgrounds selected for this investigation include vegetation, snow, sand, and soil. Collection of emissivity data was difficult in that such data for the 3.0-to-5.0 μm band is fairly scarce. Nevertheless, data for all but one of the backgrounds was found.

The spectral emissivity for vegetation used in this investigation is an average of actual spectral emissivity measurements made of grass, green coniferous twigs, and maple leaves (38:92,93,95). Figure 5 plots all four vegetation emissivities.

Literature searches reveal no actual emissivity measurements of snow for the 3.0-to-5.0 μm band, only calculated emissivity values based on an equation developed and plotted by Berger (3:7). A plot of this emissivity is shown in Figure 6. For comparison, emissivity measurements of ice in the 3.0-to-5.0 μm band by both Alkezweeny and Schaaf result in similar values as those calculated for snow (1:1084; 31:727).

The spectral emissivity of sand used in this investigation is an average of actual spectral emissivity measurements made of natural gypsum sand and russian sand (38:12). Figure 7 plots all three sand emissivities.

The soil spectral emissivity used in this investigation is an average of actual spectral emissivity measurements

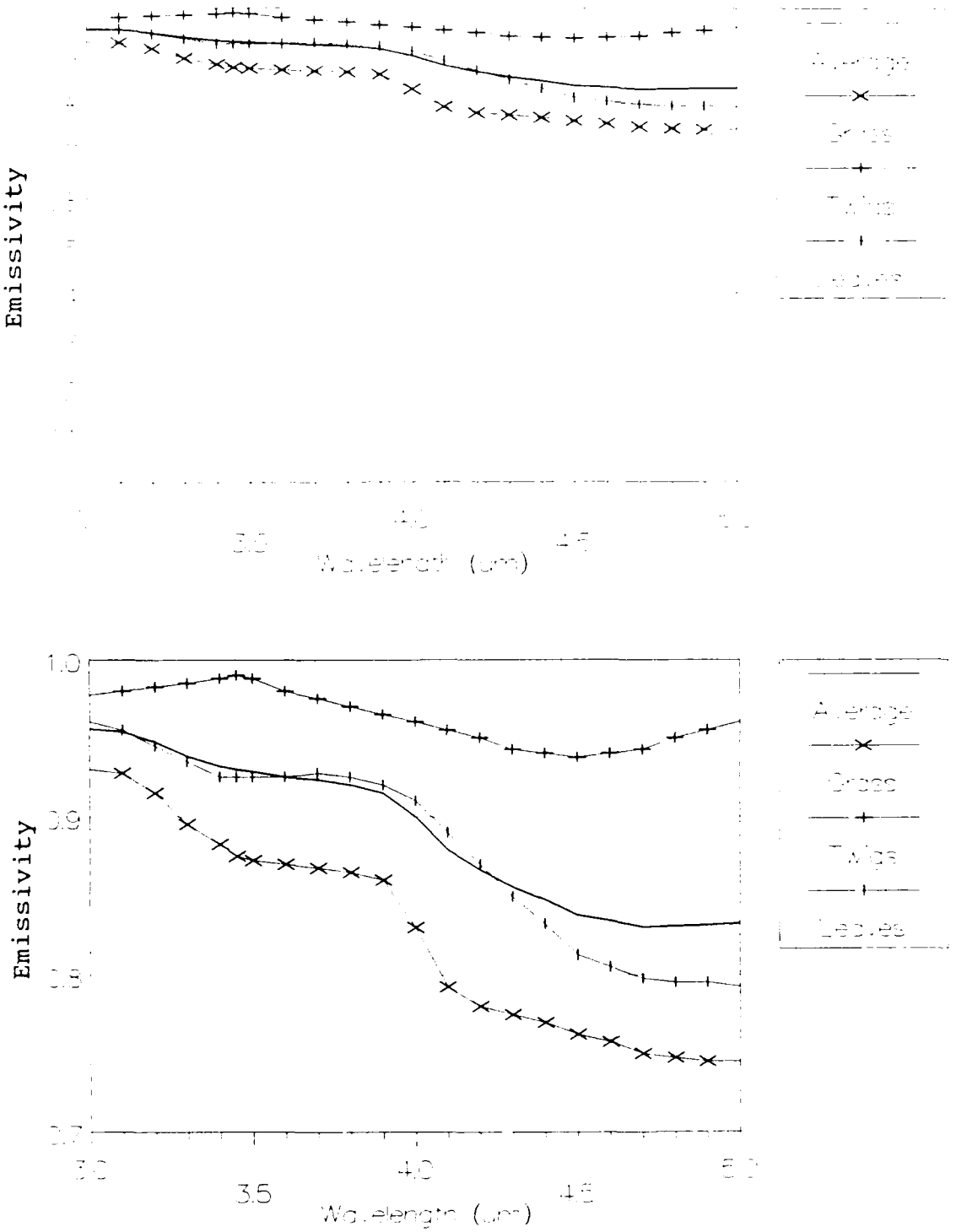

Figure 5. Spectral Emissivity of Vegetation
Adapted from (38:92,93,95)

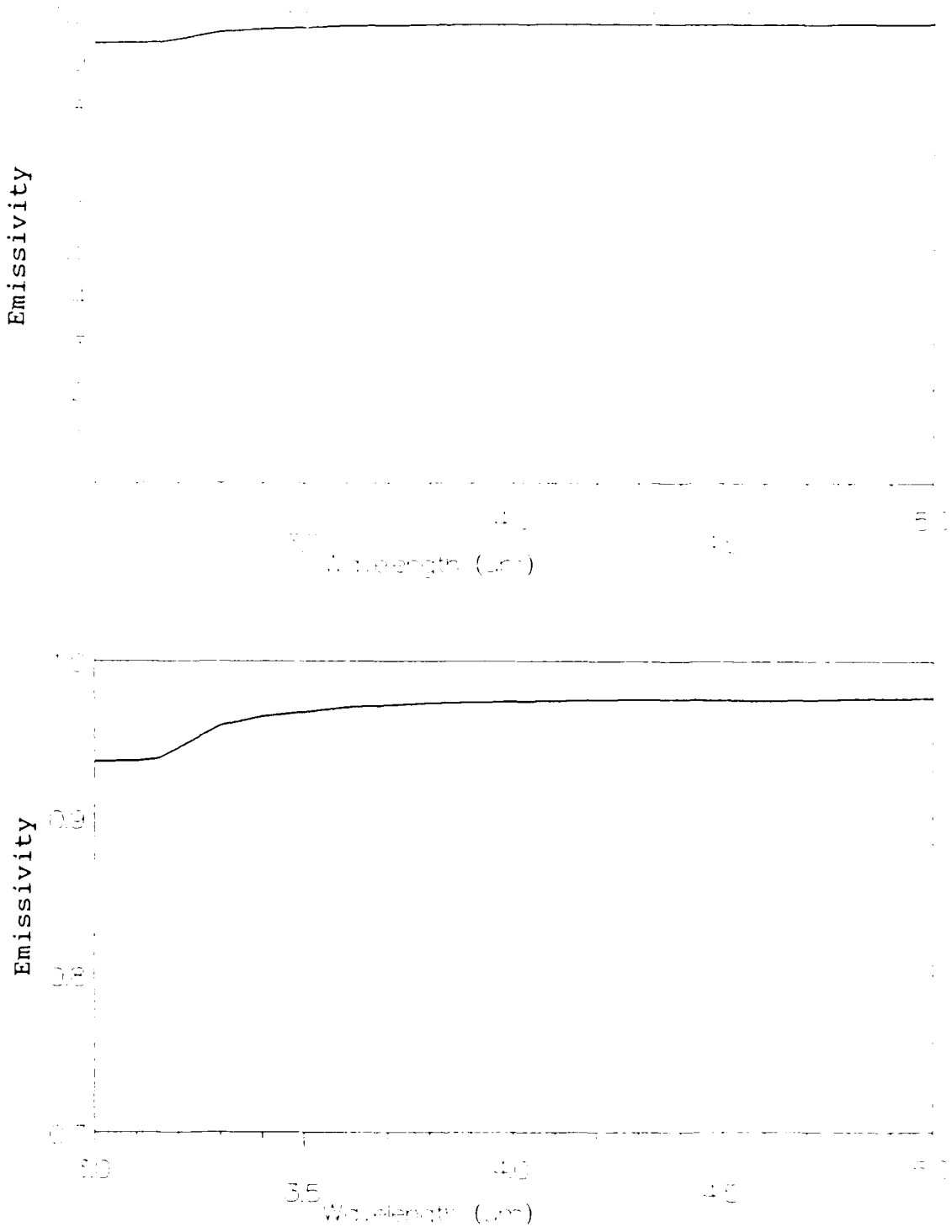

Figure 6. Spectral Emissivity of Snow
Adapted from (3:7)

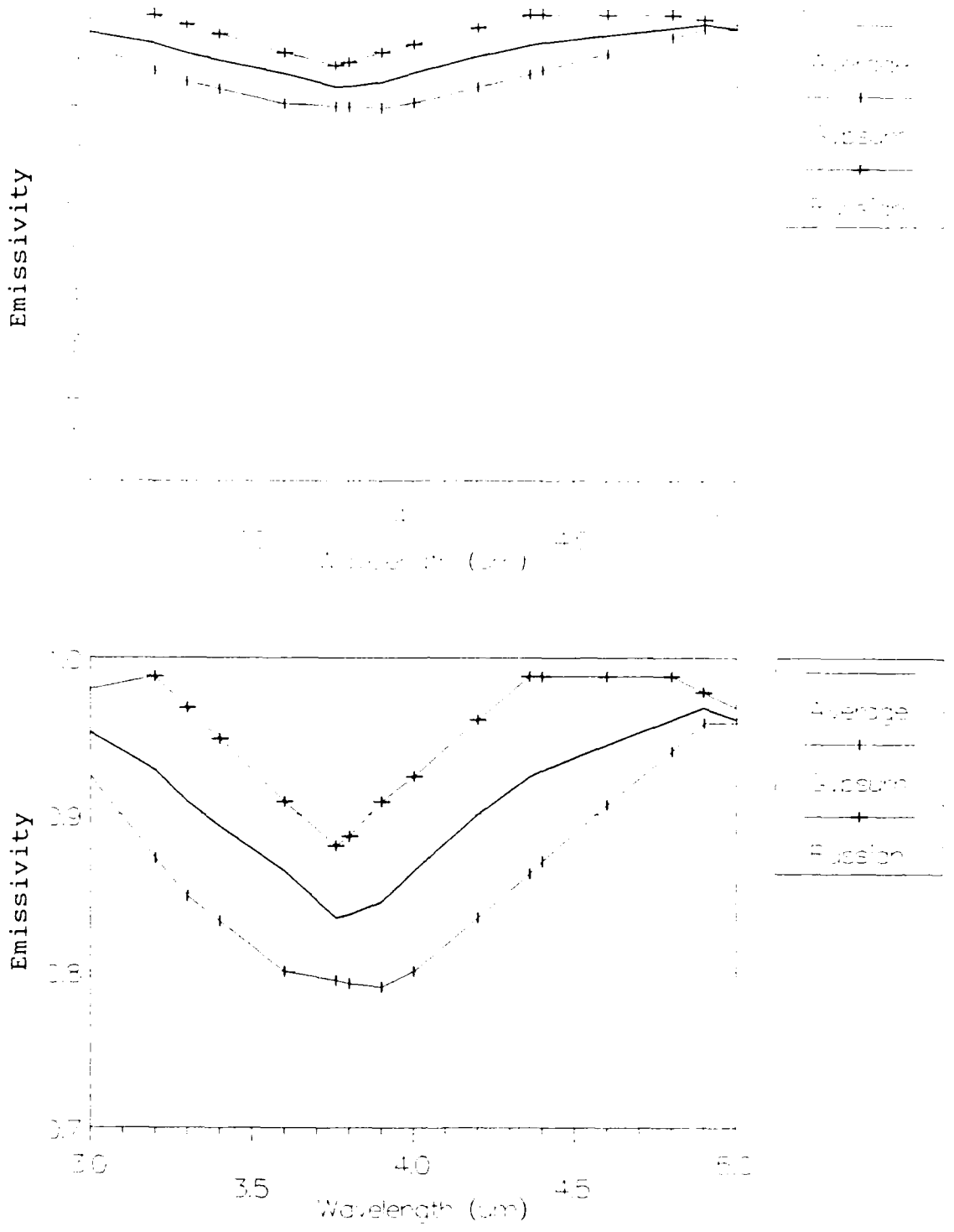

Figure 7. Spectral Emissivity of Sand
Adapted from (38:12)

made of pawnee grassland soil, topsoil, and russian soil (38:11). These emissivities are plotted in Figure 8.

Atmospheric Transmission

The atmospheric transmission, τ_{ATM}, for this investigation was obtained from the LOWTRAN 6 computer program for predicting atmospheric transmittance for different atmospheric conditions (18). Previous studies of PtSi and InSb as detector materials showed that of the several atmospheric models considered, only two provided dramatically different results; hence, they were selected for use in this thesis (32). The first model is for a rural setting and uses the LOWTRAN 6 1962 Standard Atmosphere density profiles for air, water vapor (humidity), and ozone. The second model is for a tropical setting and uses the LOWTRAN 6 tropical atmosphere, which increases the humidity profile over that of the first model. The standard and tropical humidity profiles are provided in Table II. Both atmospheric models have no cloud cover, are for spring-summer time, and use aerosol models which provide a visibility of 23 km. Plots of the atmospheric transmission calculated for a vertical path from ground to space (above 100 km) using each of the models are shown in Figure 9.

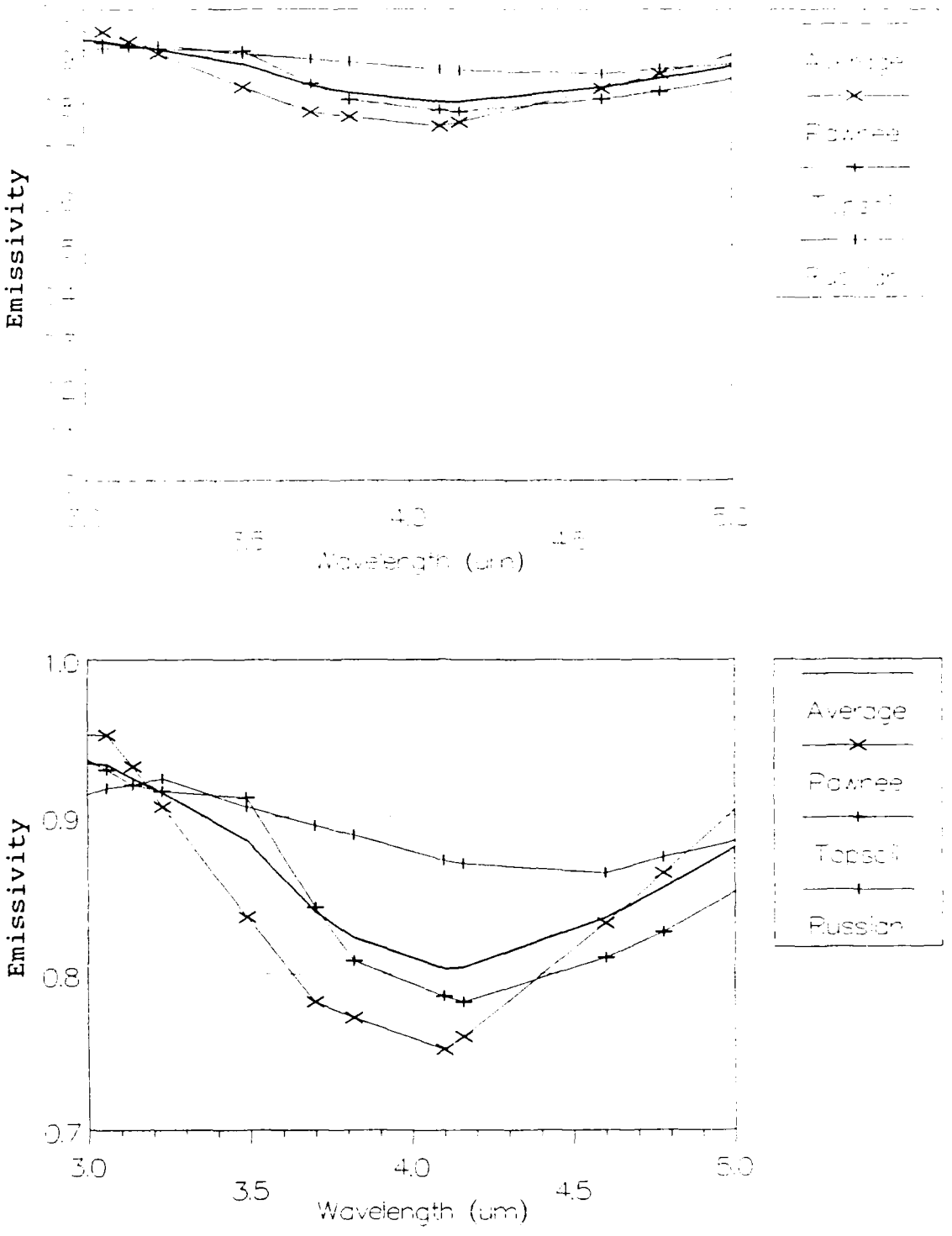

Figure 8. Spectral Emissivity of Soil
Adapted from (38:11)

Table II. Humidity Profiles

Altitude (km)	Standard Humidity (g/cm^3)	Tropical Humidity (g/cm^3)
0.0	5.758×10^{-6}	1.822×10^{-5}
1.0	3.719×10^{-6}	1.135×10^{-5}
2.0	2.323×10^{-6}	7.386×10^{-6}
3.0	1.302×10^{-6}	3.376×10^{-6}
4.0	7.166×10^{-7}	1.432×10^{-6}
5.0	3.745×10^{-7}	8.824×10^{-7}
6.0	1.992×10^{-7}	4.508×10^{-7}
7.0	9.834×10^{-8}	2.243×10^{-7}
8.0	5.004×10^{-8}	1.071×10^{-7}
9.0	1.703×10^{-8}	4.591×10^{-8}
10.0	5.894×10^{-9}	1.707×10^{-8}

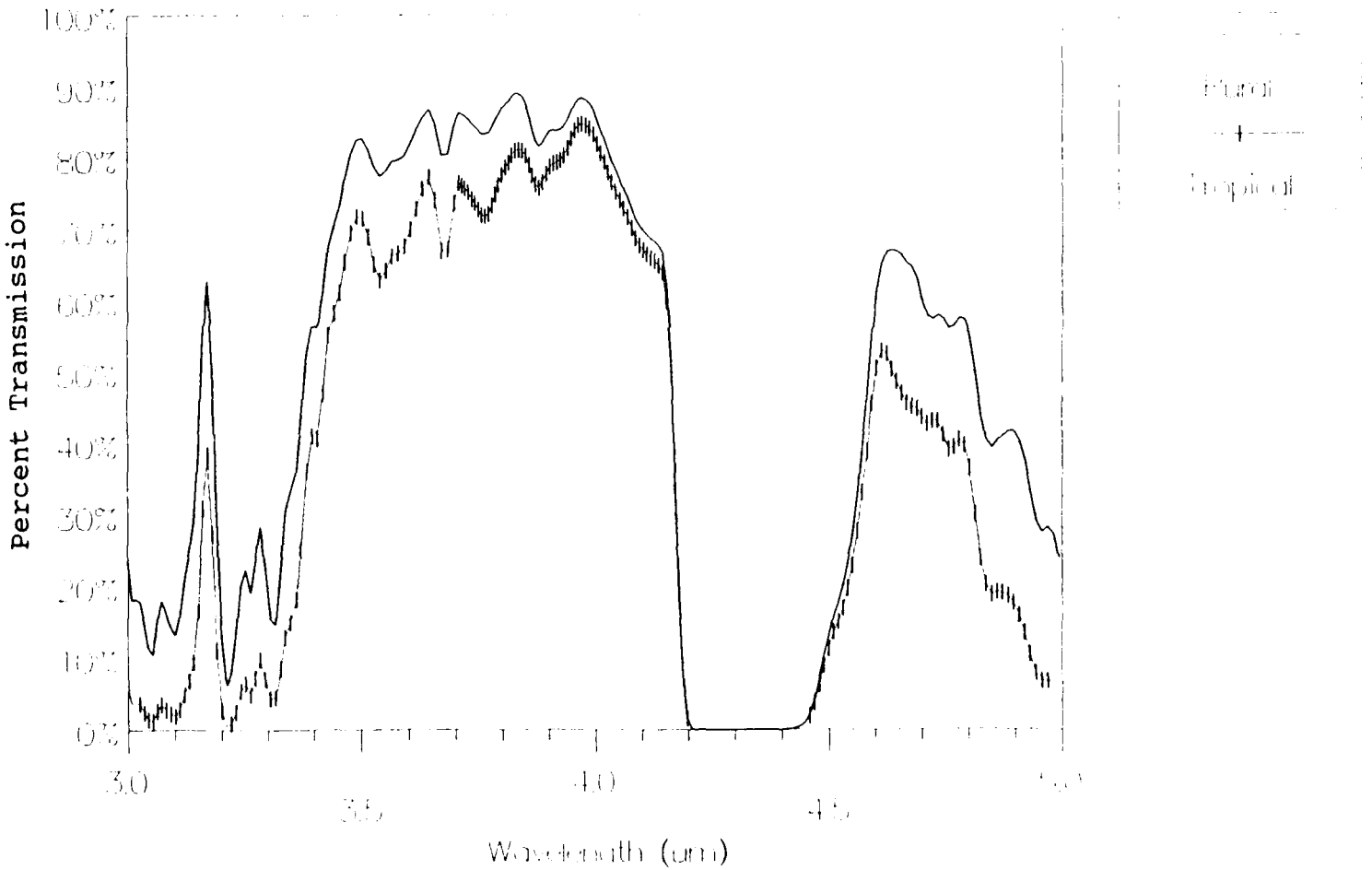

Figure 9. Atmospheric Transmission for Rural and Tropical Settings

Spectral Scaled Count Rate Plots

Using Equations 3, 4, 6, 7, and 8 and the appropriate emissivity, reflectivity, and atmospheric transmission data, sensor outputs for PtSi and InSb in the form of scaled count rates (SCR) and spectral scaled count rates (SCR_λ) were calculated. To visually depict the sensor output, plots of the SCR_λ versus λ were made for several different cases showing both the target and a particular background.

Scaled Count Rate Calculations

This part of the investigation involved determining whether discrimination of the target from the four backgrounds is possible using single and/or multiband remote sensing. Since the radiation from both the target and the backgrounds varies with wavelength, investigating sub-bands within the 3.0-to-5.0 μm band may reveal certain bands in which the target SCR is substantially higher than the background SCR or vice versa. Discrimination of the target from the background can best be done within one of these bands or possibly a combination of two of them.

Inspection of the SCR_λ versus λ plots indicated which bands to investigate. Calculation of the SCR using Equation 3 was accomplished for each of these bands for both the target and the backgrounds. Contrast for this thesis is defined as the difference between the target SCR and a background SCR within a particular band. The larger the

absolute difference, and therefore contrast, the easier the discrimination between target and background.

The evaluation of two-band remote sensing involved the calculation of the vector distance between the target and each background for each two-band combination. For example, the SCR value for the first sub-band is the X coordinate, while the SCR value for the second sub-band is the Y coordinate. Using the target as the first point and a background as the second point, the vector distance was calculated. The longer the distance between target and background, the better the discrimination for the particular combination of bands. This concept is illustrated in Figure 10.

Cases

Several cases were investigated using the sensor output calculations. These cases, listed in Table III, primarily focused on varying the temperature of the target and the background in order to determine each detector material's sensitivity to temperature. Background temperatures included 298°K (77°F), a typical warm earth surface temperature; 288°K (59°F), a moderate temperature; and 258°K (5°F), a cold temperature. Because the target spectral reflectivity can be adjusted to give a variety of values, two cases, one examining an increase and one examining a decrease in target reflectivity, were also investigated.

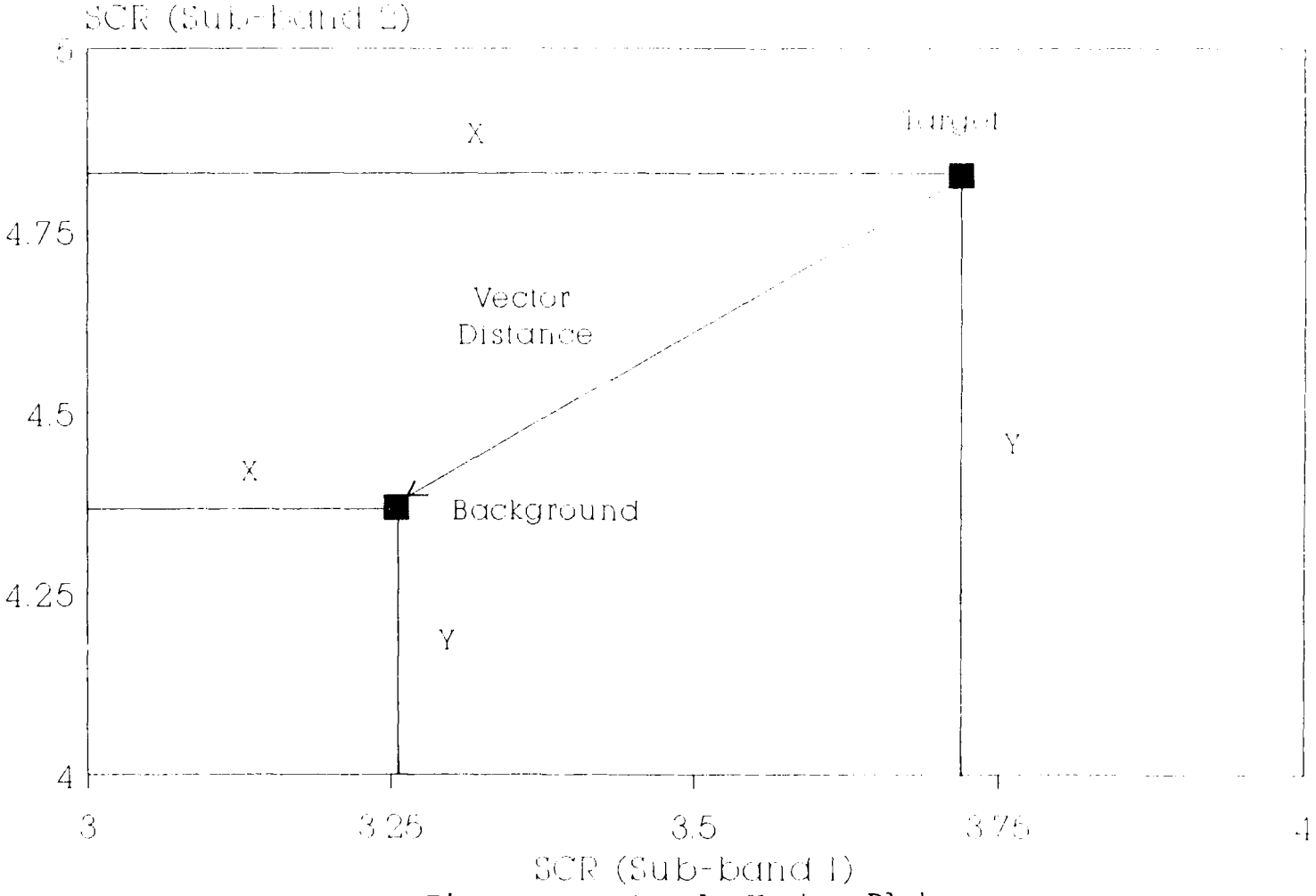

Figure 10. Sample Vector Plot

Table III. Cases Investigated

Case	Description (Atmospheric Setting, Temperatures)
Baseline	Rural, Target = 298°K, Background = 298°K
Case 1	Rural, Target = 300°K, Background = 298°K
Case 2	Rural, Target = 308°K, Background = 298°K
Case 3	Rural, Target = 288°K, Background = 288°K
Case 4	Rural, Target = 290°K, Background = 288°K
Case 5	Rural, Target = 258°K, Background = 258°K
Case 6	Rural, Target = 260°K, Background = 258°K
Case 7	Tropical, Target = 298°K, Background = 298°K
Case 8	Baseline, Target Reflectivity Decreased by 0.2
Case 9	Baseline, Target Reflectivity Increased by 0.2

This increase and decrease use the approximation to the standard deviation previously discussed.

Snow backgrounds are probably not consistent with some of the warmer temperatures in the matrix. Nevertheless, these cases are still included for completeness, especially since the reflectivity of snow is quite different from that of other common backgrounds.

IV. Results

Introduction

This chapter is divided into three parts. The first part discusses the results of the 10 cases examined on a case-by-case basis for PtSi. The second part does the same for InSb. The third part discusses the multiband possibilities within the 3.0-to-5.0 μm band for both PtSi and InSb.

Each case discussion has a day section and a night section. Within the day section the differences between target and background scaled count rates (SCR) are discussed with respect to the baseline case and with respect to each other. The night section discusses the same aspects as the day section, as well as, the differences between the nighttime SCRs and the daytime SCRs.

Platinum Silicide

Baseline: Rural, Target = 298°K, Background = 298°K

Day. Figures 11 and 12 contain plots of SCR_λ versus λ for the target against backgrounds of vegetation and snow, respectively, for the day baseline case. SCR_λ versus λ plots of the target against sand and soil backgrounds are very similar to that of the target against vegetation, hence, they are not included in this thesis. As can be seen in Figures 11 and 12, the target SCR dominates the background SCR in the 3.3-to-4.2 μm band. The

Rural Setting, 23 km Visibility

Target = 298 K, Background = 298 K

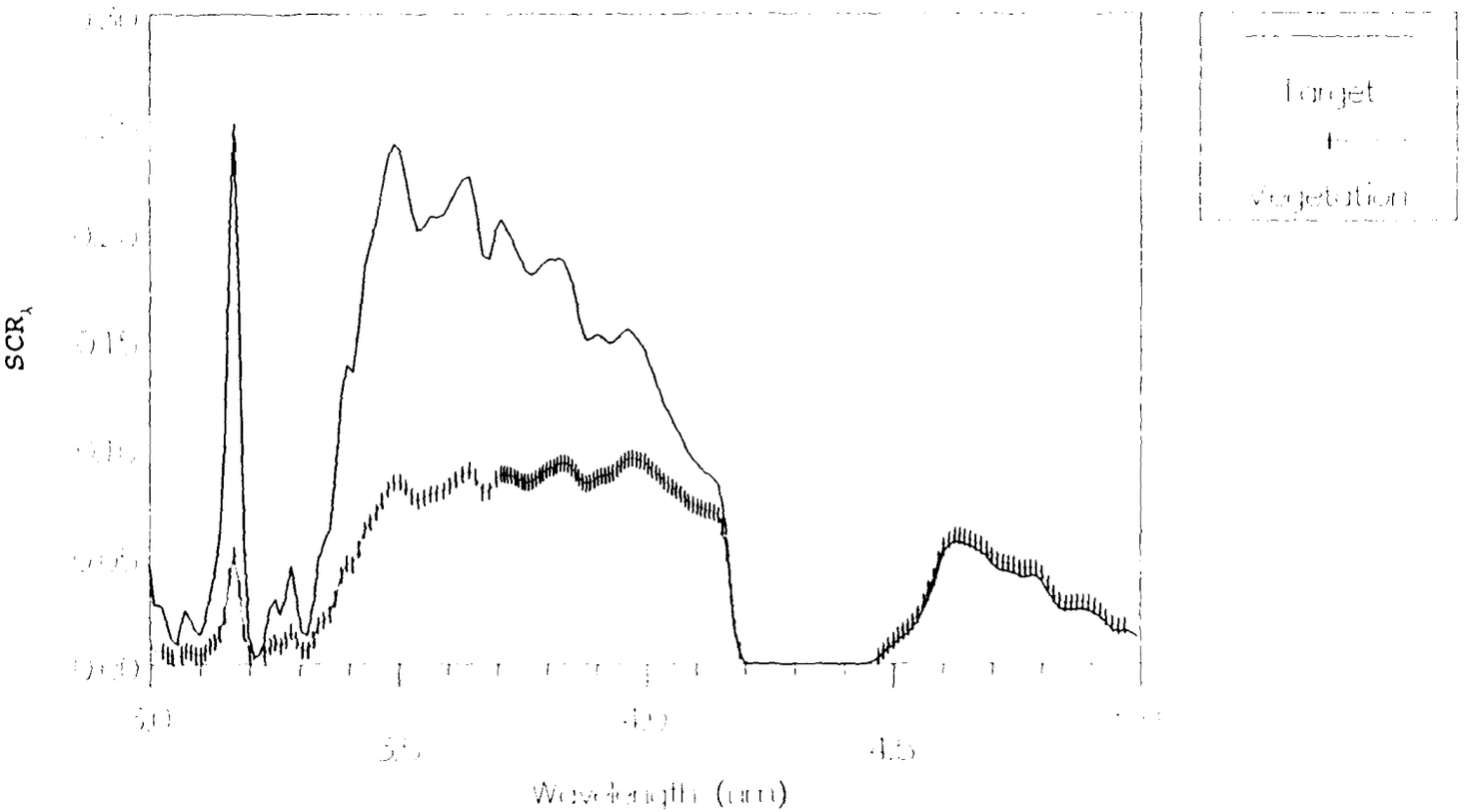

Figure 11. PtSi Baseline Case, Vegetation, Day

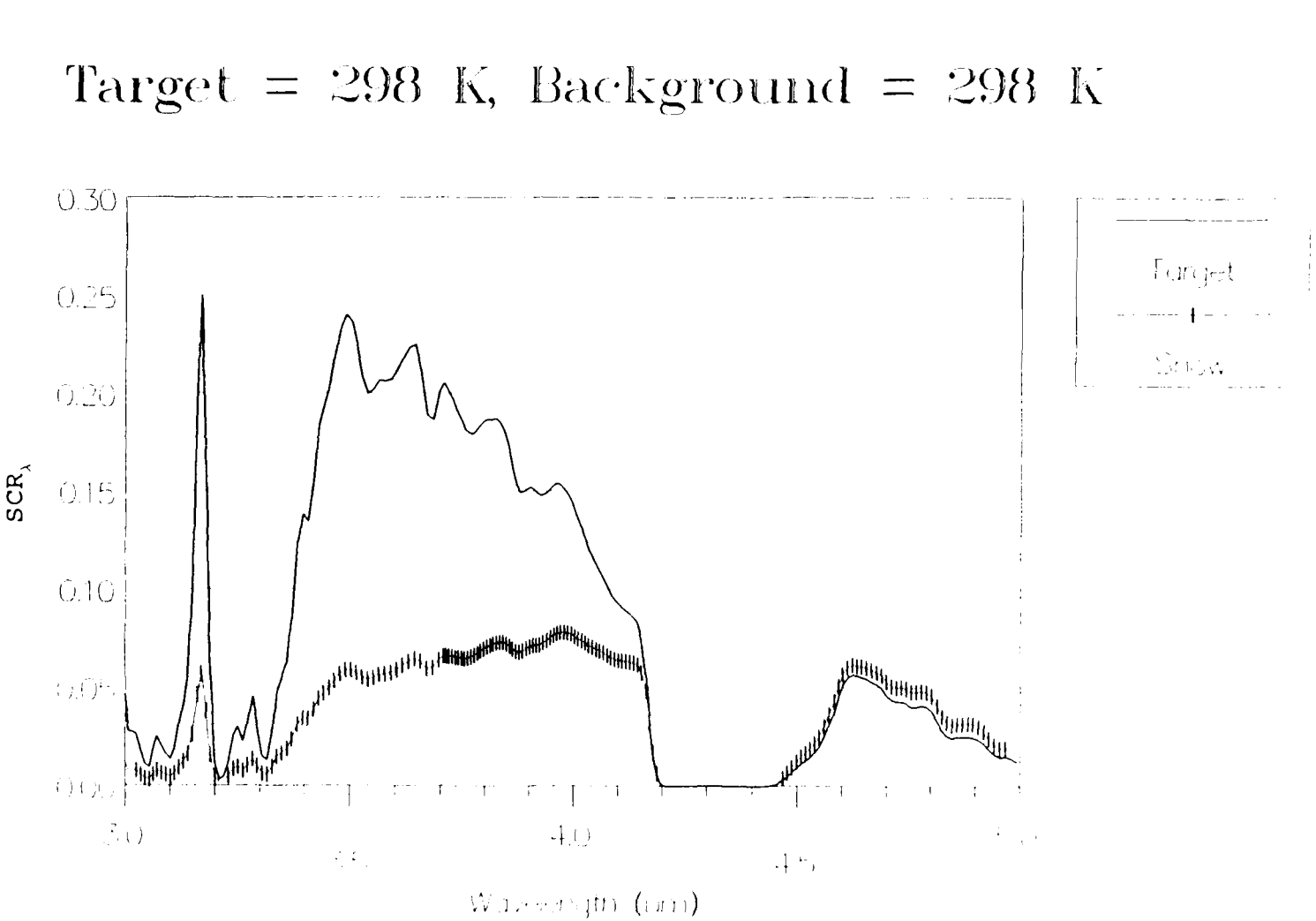

Figure 12. PtSi Baseline Case, Snow, Day

average background SCR, which is the average SCR of all four backgrounds, is 48.24% lower than the target SCR. This is primarily due to the higher reflectivity of the target. However, in the 4.5-to-5.0 μm band, the average background SCR is 13.98% higher than the target SCR. Although the thermal contribution to the SCR is increasing in this region, the atmospheric transmission as well as the quantum efficiency of PtSi reduces all the SCRs far more rapidly. With this relatively small difference in SCRs, the 4.5-to-5.0 μm band may be unsuitable for daytime remote sensing. Of the four backgrounds, snow provides the best contrast between target and background in both bands.

Night. Figures 13 and 14 contain plots of SCR_λ versus λ for the target against backgrounds of vegetation and snow, respectively, for the night baseline case. At night, the loss of the reflected portion of the SCR causes the target SCR to drop 79.17% in the 3.3-to-4.2 μm band, but only 18.51% in the 4.5-to-5.0 μm band. The average background SCR drops 43.08% in the 3.3-to-4.2 μm band, but only 5.07% in the 4.5-to-5.0 μm band. With only the thermal contribution of the source, the average background SCR is higher than the target SCR in both bands of the 3.0-to-5.0 μm region. This is due to the backgrounds having higher emissivities than the target. In the 3.3-to-4.2 μm band, the average background SCR is 34.17% higher, and in the 4.5-to-5.0 μm band, it is 32.93% higher.

Rural Setting, 23 km Visibility

Target = 298 K, Background = 298 K

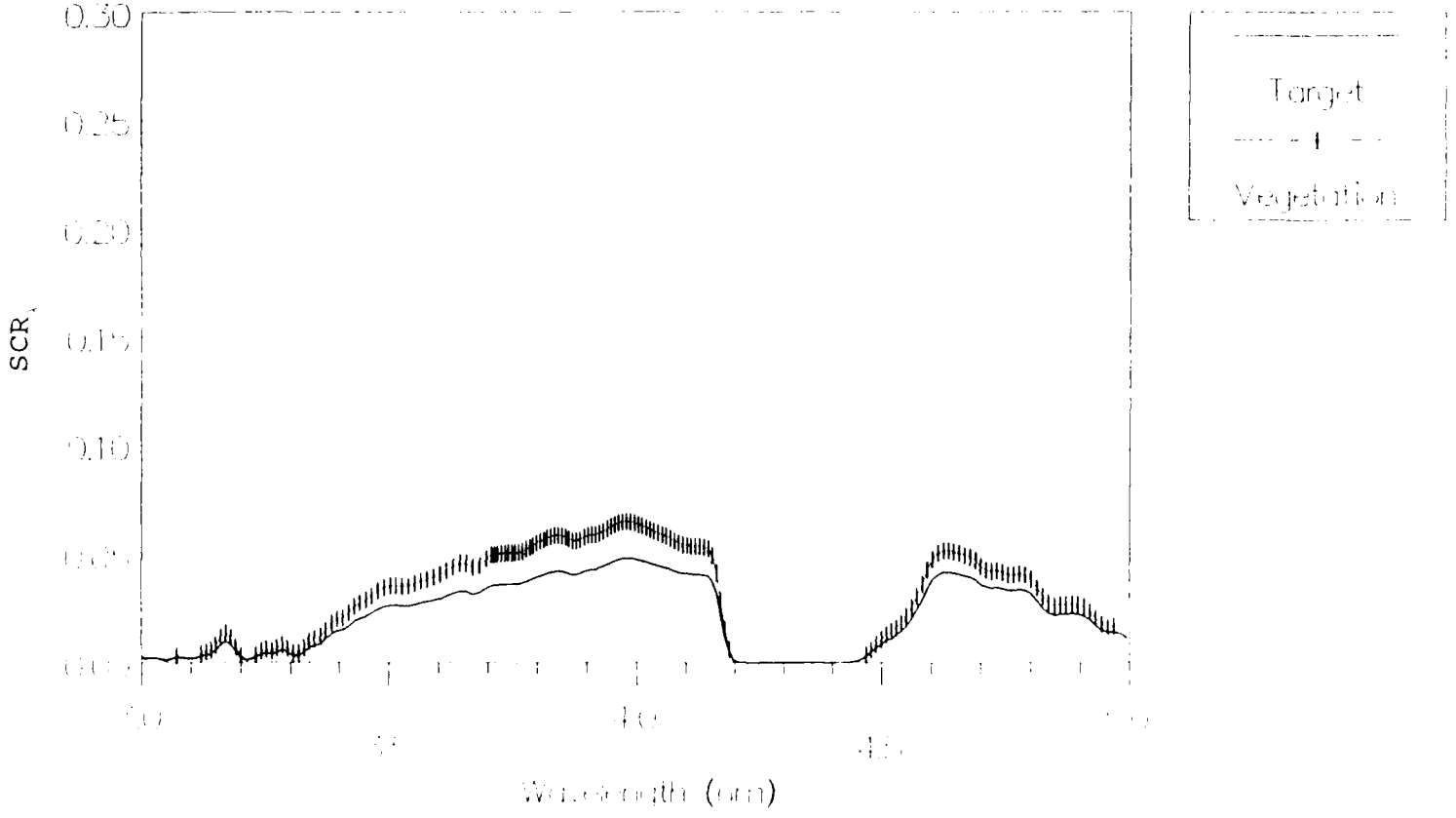

Figure 13. PtSi Baseline Case, Vegetation, Night

Rural Setting, 23 km Visibility

Target = 298 K, Background = 298 K

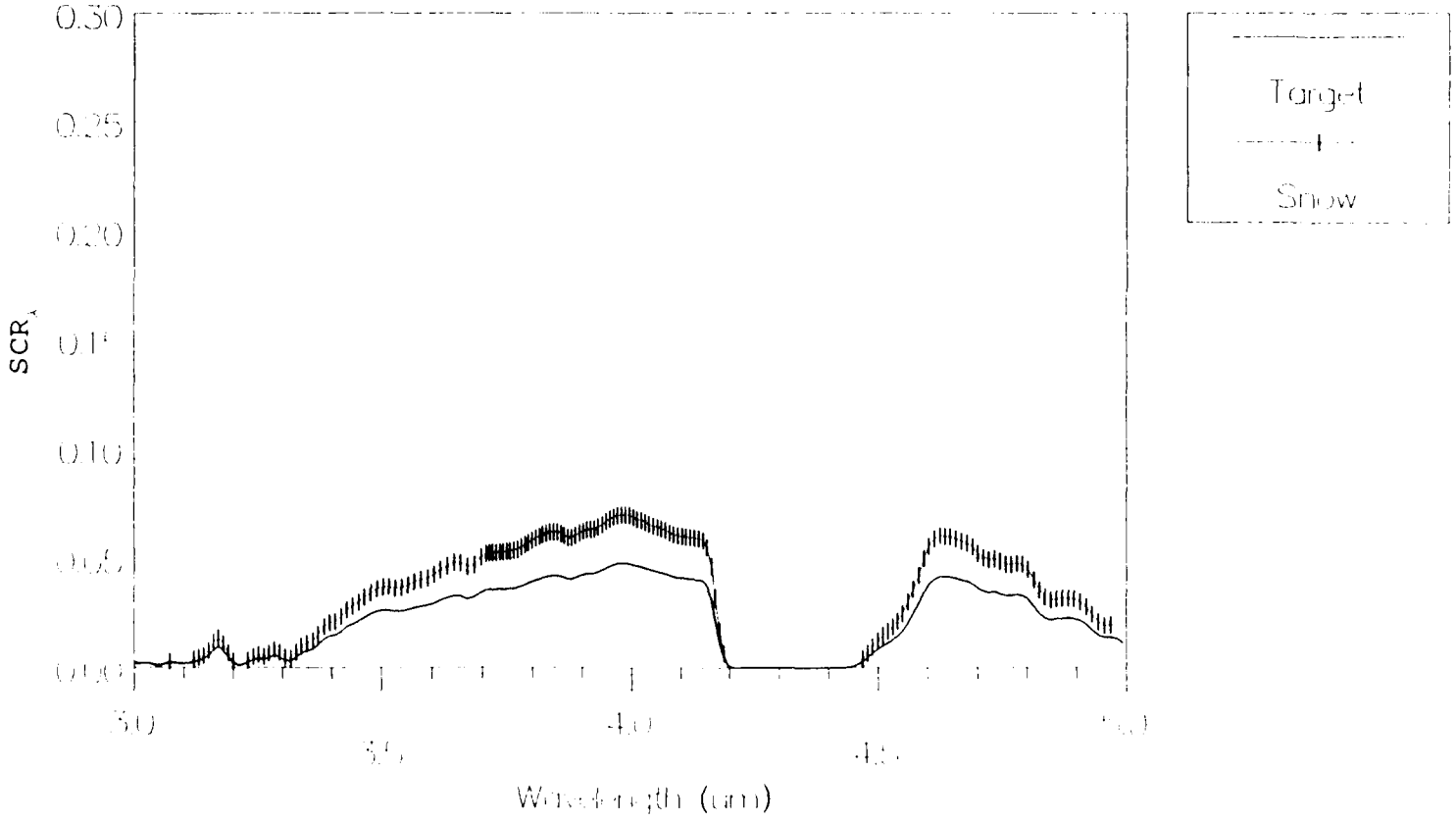

Figure 14. PtSi Baseline Case, Snow, Night

As with the day, snow provides the best contrast in both bands.

The above results seem to confirm previous findings that PtSi may be better suited for detecting targets during the day than at night (32). However, there appears to be sufficient contrast between the various backgrounds and the target to suggest that nighttime detection is still possible. In fact, the nighttime contrast in the 4.5-to-5.0 μm band is better than it is during the day.

Table IV contains the PtSi daytime SCR values for each band for all 10 cases as various parameters of the daytime baseline case are individually varied, while Table V contains the PtSi daytime SCR differences between the target and the backgrounds for all 10 cases. Similarly, Table VI contains the PtSi nighttime SCR values for each band for all 10 cases, while Table VII contains the PtSi nighttime SCR differences between the target and the backgrounds for all 10 cases. Finally, Table VIII contains the PtSi SCR differences between day and night for all 10 cases.

Case 1: Rural, Target = 300°K, Background = 298°K

Day. This case is very similar to the baseline case with the target SCR significantly higher than the background SCRs in the 3.3-to-4.2 μm band and slightly lower in the 4.5-to-5.0 μm band. The 2°K increase in target temperature increases the thermal contribution to the target SCR which, in turn, raises the target SCR 1.84% in the

Table IV. PtSi Daytime SCR Vector Distances for the 3.3-to-4.2 μm and 4.5-to-5.0 μm Bands

Case	Source	SCR 3.3-4.2 μm Band	SCR 4.5-5.0 μm Band	SCR Vector Distance	Average Vector Distance	Std Dev
Baseline	Target	0.1365	0.0163	******	0.0659	0.0156
Rural	Vegetation	0.0651	0.0179	0.0714		
T=298°K	Snow	0.0512	0.0194	0.0854		
B=298°K	Sand	0.0817	0.0191	0.0549		
	Soil	0.0847	0.0181	0.0519		
Case 1	Target	0.1390	0.0173	******	0.0684	0.0156
Rural	Vegetation	0.0651	0.0179	0.0739		
T=300°K	Snow	0.0512	0.0194	0.0879		
B=298°K	Sand	0.0817	0.0191	0.0574		
	Soil	0.0847	0.0181	0.0544		
Case 2	Target	0.1511	0.0216	******	0.0804	0.0156
Rural	Vegetation	0.0651	0.0179	0.0860		
T=308°K	Snow	0.0512	0.0194	0.0999		
B=298°K	Sand	0.0817	0.0191	0.0694		
	Soil	0.0847	0.0181	0.0664		
Case 3	Target	0.1264	0.0124	******	0.0693	0.0165
Rural	Vegetation	0.0512	0.0130	0.0752		
T=288°K	Snow	0.0364	0.0136	0.0900		
B=288°K	Sand	0.0686	0.0136	0.0578		
	Soil	0.0720	0.0131	0.0544		
Case 4	Target	0.1281	0.0131	******	0.0711	0.0165
Rural	Vegetation	0.0512	0.0130	0.0769		
T=290°K	Snow	0.0364	0.0136	0.0917		
B=288°K	Sand	0.0686	0.0136	0.0595		
	Soil	0.0720	0.0131	0.0561		
Case 5	Target	0.1121	0.0058	******	0.0742	0.0178
Rural	Vegetation	0.0317	0.0049	0.0804		
T=258°K	Snow	0.0155	0.0042	0.0966		
B=258°K	Sand	0.0501	0.0043	0.0620		
	Soil	0.0542	0.0049	0.0580		
Case 6	Target	0.1126	0.0060	******	0.0747	0.0178
Rural	Vegetation	0.0317	0.0049	0.0809		
T=260°K	Snow	0.0155	0.0042	0.0970		
B=258°K	Sand	0.0501	0.0043	0.0625		
	Soil	0.0542	0.0049	0.0584		

Table IV. Continued

Case	Source	SCR 3.3-4.2 μm Band	SCR 4.5-5.0 μm Band	SCR Vector Distance	Average Vector Distance	Std Dev
Case 7	Target	0.1071	0.0103	******	0.0480	0.0118
Tropical	Vegetation	0.0550	0.0116	0.0521		
T=298°K	Snow	0.0444	0.0127	0.0627		
B=298°K	Sand	0.0673	0.0125	0.0399		
	Soil	0.0699	0.0117	0.0372		
Case 8	Target	0.0795	0.0184	******	0.0126	0.0117
$\rho(\lambda)$-0.2	Vegetation	0.0651	0.0179	0.0144		
T=298°K	Snow	0.0512	0.0194	0.0283		
B=298°K	Sand	0.0817	0.0191	0.0023		
	Soil	0.0847	0.0181	0.0052		
Case 9	Target	0.1936	0.0143	******	0.1230	0.0156
$\rho(\lambda)$+0.2	Vegetation	0.0651	0.0179	0.1285		
T=298°K	Snow	0.0512	0.0194	0.1425		
B=298°K	Sand	0.0817	0.0191	0.1120		
	Soil	0.0847	0.0181	0.1089		
			Overall SCR Average		0.0688	

T = Target Temperature.

B = Background Temperature.

Table V. PtSi Daytime SCR Differences Between Target and Background for the 3.3-to-4.2 μm and 4.5-to-5.0 μm Bands

Case	Source	Diff 3.3-4.2 μm Band	Diff 4.5-5.0 μm Band	% Diff 3.3-4.2 μm Band	% Diff 4.5-5.0 μm Band
Baseline	Vegetation	-0.0714	0.0015	-52.32	9.47
Rural	Snow	-0.0853	0.0030	-62.51	18.48
T=298°K	Sand	-0.0548	0.0028	-40.17	17.19
B=298°K	Soil	-0.0518	0.0018	-37.97	10.78
	Average	-0.0659	0.0023	-48.24	13.98
Case 1	Vegetation	-0.0739	0.0006	-53.18	3.52
Rural	Snow	-0.0879	0.0021	-63.18	12.04
T=300°K	Sand	-0.0574	0.0019	-41.25	10.83
B=298°K	Soil	-0.0543	0.0008	-39.09	4.76
	Average	-0.0684	0.0013	-49.17	7.79
Case 2	Vegetation	-0.0860	-0.0037	-56.90	-17.11
Rural	Snow	-0.0999	-0.0022	-66.11	-10.29
T=308°K	Sand	-0.0694	-0.0024	-45.92	-11.26
B=298°K	Soil	-0.0664	-0.0035	-43.93	-16.12
	Average	-0.0804	-0.0030	-53.21	-13.70
Case 3	Vegetation	-0.0752	0.0006	-59.46	5.25
Rural	Snow	-0.0900	0.0013	-71.19	10.37
T=288°K	Sand	-0.0578	0.0012	-45.72	9.72
B=288°K	Soil	-0.0544	0.0008	-43.02	6.16
	Average	-0.0693	0.0010	-54.85	7.88
Case 4	Vegetation	-0.0769	-0.0001	-60.00	-0.43
Rural	Snow	-0.0917	0.0006	-71.58	4.40
T=290°K	Sand	-0.0595	0.0005	-46.46	3.79
B=288°K	Soil	-0.0561	0.0001	-43.79	0.42
	Average	-0.0711	0.0003	-55.46	2.05
Case 5	Vegetation	-0.0804	-0.0008	-71.73	-14.58
Rural	Snow	-0.0966	-0.0016	-86.14	-27.83
T=258°K	Sand	-0.0620	-0.0015	-55.28	-25.47
B=258°K	Soil	-0.0579	-0.0009	-51.69	-15.62
	Average	-0.0742	-0.0012	-66.21	-20.87
Case 6	Vegetation	-0.0809	-0.0011	-71.85	-18.26
Rural	Snow	-0.0970	-0.0019	-86.20	-30.94
T=260°K	Sand	-0.0624	-0.0017	-55.47	-28.69
B=258°K	Soil	-0.0584	-0.0012	-51.89	-19.26
	Average	-0.0747	-0.0015	-66.35	-24.29

Table V. Continued

Case	Source	Diff 3.3-4.2 μm Band	Diff 4.5-5.0 μm Band	% Diff 3.3-4.2 μm Band	% Diff 4.5-5.0 μm Band
Case 7	Vegetation	-0.0521	0.0013	-48.62	12.15
Tropical	Snow	-0.0626	0.0024	-58.50	23.44
T=298°K	Sand	-0.0398	0.0022	-37.18	21.65
B=298°K	Soil	-0.0372	0.0014	-34.71	13.44
	Average	-0.0479	0.0018	-44.75	17.67
Case 8	Vegetation	-0.0144	-0.0005	-18.11	-2.74
$\rho(\lambda)$-0.2	Snow	-0.0283	0.0010	-35.61	5.26
T=298°K	Sand	0.0022	0.0008	2.76	4.12
B=298°K	Soil	0.0052	-0.0003	6.54	-1.57
	Average	-0.0088	0.0002	-11.10	1.27
Case 9	Vegetation	-0.1285	0.0036	-66.37	25.18
$\rho(\lambda)$+0.2	Snow	-0.1424	0.0051	-73.56	35.48
T=298°K	Sand	-0.1119	0.0049	-57.80	34.02
B=298°K	Soil	-0.1089	0.0038	-56.25	26.68
	Average	-0.1229	0.0043	-63.49	30.34

T = Target Temperature

B = Background Temperature.

Difference calculations use the target SCR in each case as the reference point. Therefore, positive values are above the target SCR and negative values are below.

Table VI. PtSi Nighttime SCR Vector Distances for the 3.3-to-4.2 μm and 4.5-to-5.0 μm Bands

Case	Source	SCR 3.3-4.2 μm Band	SCR 4.5-5.0 μm Band	SCR Vector Distance	Average Vector Distance	Std Dev
Baseline	Target	0.0284	0.0133	******	0.0107	0.0027
Rural	Vegetation	0.0389	0.0163	0.0109		
T=298°K	Snow	0.0415	0.0191	0.0143		
B=298°K	Sand	0.0367	0.0187	0.0099		
	Soil	0.0355	0.0167	0.0078		
Case 1	Target	0.0310	0.0143	******	0.0081	0.0027
Rural	Vegetation	0.0389	0.0163	0.0082		
T=300°K	Snow	0.0415	0.0191	0.0116		
B=298°K	Sand	0.0367	0.0187	0.0073		
	Soil	0.0355	0.0167	0.0052		
Case 2	Target	0.0430	0.0186	******	0.0050	0.0026
Rural	Vegetation	0.0389	0.0163	0.0047		
T=308°K	Snow	0.0415	0.0191	0.0016		
B=298°K	Sand	0.0367	0.0187	0.0062		
	Soil	0.0355	0.0167	0.0077		
Case 3	Target	0.0183	0.0093	******	0.0070	0.0018
Rural	Vegetation	0.0250	0.0114	0.0070		
T=288°K	Snow	0.0267	0.0134	0.0093		
B=288°K	Sand	0.0237	0.0131	0.0065		
	Soil	0.0229	0.0117	0.0051		
Case 4	Target	0.0200	0.0100	******	0.0052	0.0017
Rural	Vegetation	0.0250	0.0114	0.0052		
T=290°K	Snow	0.0267	0.0134	0.0075		
B=288°K	Sand	0.0237	0.0131	0.0047		
	Soil	0.0229	0.0117	0.0033		
Case 5	Target	0.0040	0.0027	******	0.0016	0.0004
Rural	Vegetation	0.0055	0.0033	0.0016		
T=258°K	Snow	0.0058	0.0039	0.0022		
B=258°K	Sand	0.0052	0.0038	0.0016		
	Soil	0.0050	0.0034	0.0012		
Case 6	Target	0.0045	0.0030	******	0.0011	0.0004
Rural	Vegetation	0.0055	0.0033	0.0010		
T=260°K	Snow	0.0058	0.0039	0.0017		
B=258°K	Sand	0.0052	0.0038	0.0011		
	Soil	0.0050	0.0034	0.0007		

Table VI. Continued

Case	Source	SCR 3.3-4.2 μm Band	SCR 4.5-5.0 μm Band	SCR Vector Distance	Average Vector Distance	Std Dev
Case 7	Target	0.0255	0.0087	******	0.0092	0.0024
Tropical	Vegetation	0.0349	0.0108	0.0095		
T=298°K	Snow	0.0373	0.0126	0.0124		
B=298°K	Sand	0.0330	0.0123	0.0082		
	Soil	0.0318	0.0109	0.0067		
Case 8	Target	0.0370	0.0172	******	0.0025	0.0016
$\rho(\lambda)$-0.2	Vegetation	0.0389	0.0163	0.0021		
T=298°K	Snow	0.0415	0.0191	0.0049		
B=298°K	Sand	0.0367	0.0187	0.0015		
	Soil	0.0355	0.0167	0.0016		
Case 9	Target	0.0199	0.0094	******	0.0201	0.0027
$\rho(\lambda)$+0.2	Vegetation	0.0389	0.0163	0.0202		
T=298°K	Snow	0.0415	0.0191	0.0237		
B=298°K	Sand	0.0367	0.0187	0.0192		
	Soil	0.0355	0.0167	0.0172		
		Overall SCR Average			0.0071	

T = Target Temperature.

B = Background Temperature.

Table VII. PtSi Nighttime SCR Differences Between Target and Background for the 3.3-to-4.2 μm and 4.5-to-5.0 μm Bands

Case	Source	Diff 3.3-4.2 μm Band	Diff 4.5-5.0 μm Band	% Diff 3.3-4.2 μm Band	% Diff 4.5-5.0 μm Band
Baseline	Vegetation	0.0104	0.0030	36.68	22.53
Rural	Snow	0.0131	0.0058	45.90	43.65
T=298°K	Sand	0.0083	0.0054	29.17	40.40
B=298°K	Soil	0.0071	0.0033	24.92	25.15
	Average	0.0097	0.0044	34.17	32.93
Case 1	Vegetation	0.0079	0.0021	25.58	14.46
Rural	Snow	0.0105	0.0049	34.06	34.19
T=300°K	Sand	0.0058	0.0044	18.69	31.15
B=298°K	Soil	0.0046	0.0024	14.79	16.91
	Average	0.0072	0.0034	23.28	24.18
Case 2	Vegetation	-0.0041	-0.0022	-9.52	-12.07
Rural	Snow	-0.0015	0.0006	-3.41	3.09
T=308°K	Sand	-0.0062	0.0001	-14.49	0.75
B=298°K	Soil	-0.0074	-0.0019	-17.30	-10.19
	Average	-0.0048	-0.0009	-11.18	-4.61
Case 3	Vegetation	0.0067	0.0021	36.64	22.51
Rural	Snow	0.0084	0.0041	45.94	43.63
T=288°K	Sand	0.0053	0.0038	29.19	40.39
B=288°K	Soil	0.0045	0.0023	24.84	25.15
	Average	0.0063	0.0031	34.15	32.92
Case 4	Vegetation	0.0050	0.0014	24.82	13.90
Rural	Snow	0.0067	0.0034	33.32	33.53
T=290°K	Sand	0.0036	0.0031	18.02	30.52
B=288°K	Soil	0.0028	0.0016	14.04	16.35
	Average	0.0045	0.0024	22.55	23.58
Case 5	Vegetation	0.0015	0.0006	36.51	22.46
Rural	Snow	0.0018	0.0012	46.07	43.57
T=258°K	Sand	0.0012	0.0011	29.26	40.37
B=258°K	Soil	0.0010	0.0007	24.56	25.16
	Average	0.0014	0.0009	34.10	32.89
Case 6	Vegetation	0.0010	0.0004	22.04	11.84
Rural	Snow	0.0014	0.0009	30.59	31.12
T=260°K	Sand	0.0007	0.0008	15.56	28.20
B=258°K	Soil	0.0005	0.0004	11.36	14.30
	Average	0.0009	0.0006	19.89	21.37

Table VII. Continued

Case	Source	Diff 3.3-4.2 μm Band	Diff 4.5-5.0 μm Band	% Diff 3.3-4.2 μm Band	% Diff 4.5-5.0 μm Band
Case 7	Vegetation	0.0093	0.0020	36.57	22.97
Tropical	Snow	0.0117	0.0039	46.01	44.12
T=298°K	Sand	0.0074	0.0036	29.16	40.60
B=298°K	Soil	0.0063	0.0022	24.65	25.10
	Average	0.0087	0.0029	34.10	33.20
Case 8	Vegetation	0.0019	-0.0009	5.12	-5.35
$\rho(\lambda)$-0.2	Snow	0.0045	0.0019	12.22	10.97
T=298°K	Sand	-0.0002	0.0015	-0.65	8.46
B=298°K	Soil	-0.0014	-0.0006	-3.92	-3.33
	Average	0.0012	0.0005	3.19	2.69
Case 9	Vegetation	0.0190	0.0069	95.30	73.69
$\rho(\lambda)$+0.2	Snow	0.0216	0.0097	108.49	103.63
T=298°K	Sand	0.0168	0.0093	84.57	99.02
B=298°K	Soil	0.0156	0.0073	78.51	77.40
	Average	0.0183	0.0083	91.72	88.43

T = Target Temperature.

B = Background Temperature.

Difference calculations use the target SCR in each case as the reference point. Therefore, positive values are above the target SCR and negative values are below.

Table VIII. PtSi Differences Between Day and Night SCRs for the 3.3-to-4.2 μm and 4.5-to-5.0 μm Bands

Case	Source	Diff 3.3-4.2 μm Band	Diff 4.5-5.0 μm Band	% Diff 3.3-4.2 μm Band	% Diff 4.5-5.0 μm Band
Baseline	Target	-0.1081	-0.0030	-79.17	-18.51
Rural	Vegetation	-0.0262	-0.0016	-40.29	-8.79
T=298°K	Snow	-0.0097	-0.0002	-18.94	-1.20
B=298°K	Sand	-0.0450	-0.0005	-55.03	-2.37
	Soil	-0.0492	-0.0014	-58.05	-7.94
Background	Average	-0.0325	-0.0009	-43.08	-5.07
Case 1	Target	-0.1081	-0.0030	-77.74	-17.50
Rural	Vegetation	-0.0262	-0.0016	-40.29	-8.79
T=300°K	Snow	-0.0097	-0.0002	-18.94	-1.20
B=298°K	Sand	-0.0450	-0.0005	-55.03	-2.37
	Soil	-0.0492	-0.0014	-58.05	-7.94
Background	Average	-0.0325	-0.0009	-43.08	-5.07
Case 2	Target	-0.1081	-0.0030	-71.56	-14.02
Rural	Vegetation	-0.0262	-0.0016	-40.29	-8.79
T=308°K	Snow	-0.0097	-0.0002	-18.94	-1.20
B=298°K	Sand	-0.0450	-0.0005	-55.03	-2.37
	Soil	-0.0492	-0.0014	-58.05	-7.94
Background	Average	-0.0325	-0.0009	-43.08	-5.07
Case 3	Target	-0.1081	-0.0030	-85.52	-24.46
Rural	Vegetation	-0.0262	-0.0016	-51.19	-12.08
T=288°K	Snow	-0.0097	-0.0002	-26.63	-1.70
B=288°K	Sand	-0.0450	-0.0005	-65.53	-3.35
	Soil	-0.0492	-0.0014	-68.27	-10.95
Background	Average	-0.0325	-0.0009	-52.90	-7.02
Case 4	Target	-0.1081	-0.0030	-84.36	-23.14
Rural	Vegetation	-0.0262	-0.0016	-51.19	-12.08
T=290°K	Snow	-0.0097	-0.0002	-26.63	-1.70
B=288°K	Sand	-0.0450	-0.0005	-65.53	-3.35
	Soil	-0.0492	-0.0014	-68.27	-10.95
Background	Average	-0.0325	-0.0009	-52.90	-7.02
Case 5	Target	-0.1081	-0.0030	-96.43	-52.53
Rural	Vegetation	-0.0262	-0.0016	-82.77	-31.95
T=258°K	Snow	-0.0097	-0.0002	-62.40	-5.57
B=258°K	Sand	-0.0450	-0.0005	-89.69	-10.59
	Soil	-0.0492	-0.0014	-90.80	-29.59
Background	Average	-0.0325	-0.0009	-81.41	-19.43

Table VIII. Continued

Case	Source	Diff 3.3-4.2 μm Band	Diff 4.5-5.0 μm Band	% Diff 3.3-4.2 μm Band	% Diff 4.5-5.0 μm Band
Case 6	Target	-0.1081	-0.0030	-96.03	-50.26
Rural	Vegetation	-0.0262	-0.0016	-82.77	-31.95
T=260°K	Snow	-0.0097	-0.0002	-62.40	-5.57
B=258°K	Sand	-0.0450	-0.0005	-89.69	-10.59
	Soil	-0.0492	-0.0014	-90.80	-29.59
Background	Average	-0.0325	-0.0009	-81.41	-19.43
Case 7	Target	-0.0815	-0.0016	-76.16	-15.15
Tropical	Vegetation	-0.0201	-0.0008	-36.63	-6.96
T=298°K	Snow	-0.0072	-0.0001	-16.12	-0.94
B=298°K	Sand	-0.0343	-0.0002	-50.99	-1.94
	Soil	-0.0381	-0.0008	-54.49	-6.43
Background	Average	-0.0249	-0.0005	-39.56	-4.07
Case 8	Target	-0.0425	-0.0012	-53.49	-6.27
$\rho(\lambda)$-0.2	Vegetation	-0.0262	-0.0016	-40.29	-8.79
T=298°K	Snow	-0.0097	-0.0002	-18.94	-1.20
B=298°K	Sand	-0.0450	-0.0005	-55.03	-2.37
	Soil	-0.0492	-0.0014	-58.05	-7.94
Background	Average	-0.0325	-0.0009	-43.08	-5.07
Case 9	Target	-0.1737	-0.0049	-89.72	-34.26
$\rho(\lambda)$+0.2	Vegetation	-0.0262	-0.0016	-40.29	-8.79
T=298°K	Snow	-0.0097	-0.0002	-18.94	-1.20
B=298°K	Sand	-0.0450	-0.0005	-55.03	-2.37
	Soil	-0.0492	-0.0014	-58.05	-7.94
Background	Average	-0.0325	-0.0009	-43.08	-5.07

T = Target Temperature.

B = Background Temperature.

Difference calculations use the Daytime SCR for each source as the reference point. Therefore, positive values are above each source SCR and negative values are below.

3.3-to-4.2 μm band and 5.75% in the 4.5-to-5.0 μm band, compared to the baseline case. The background SCRs remain unchanged from the baseline case. The average background SCR for this case is 49.17% lower than the target SCR, compared to 48.24% for the baseline case, thus improving discrimination in this band. However, in the 4.5-to-5.0 μm band, the thermal increase actually decreases the difference between target and background SCRs from 13.98% for the baseline case, to 7.79%, thereby degrading discrimination. As with the baseline case, snow provides the best contrast. For warm conditions (298°K), any target temperature increase below 5°K over the background temperature makes discrimination in the 4.5-to-5.0 μm band ever more difficult due to the large decrease in contrast. However, in the 3.3-to-4.2 μm band, any increase in target temperature above the background temperature increases the contrast, thereby improving target detection.

Night. At night the target SCR drops 77.74% in the 3.3-to-4.2 μm band and 17.5% in the 4.5-to-5.0 μm band compared to the day. The background SCRs remain unchanged from the baseline case. Compared to the baseline case, the target SCR increases 8.83% in the 3.3-to-4.2 μm band and 7.05% in the 4.5-to-5.0 μm band. As with the baseline case, the average background SCR in both bands is higher than the target SCR. However, the increased thermal contribution reduces the difference between their SCRs, with the 3.3-to-4.2 μm band having a

24.18% difference. As with the baseline case, snow provides the best contrast for target discrimination. However, under such warm conditions (298°K), any target temperature increase below 7°K above the background temperature reduces the contrast between target and background in both bands, thereby making target detection more difficult.

Tables IX and X summarize the SCR changes for each case from the baseline case for day and night, respectively.

Case 2: Rural, Target = 308°K, Background = 298°K

Day. A relatively large increase in target temperature (10°K) increases its SCR over the baseline case, thus, improving the contrast in both bands. The background SCRs remain unchanged from the two previous cases. Like the baseline case and Case 1, the target SCR is considerably higher than the average background SCR in the 3.3-to-4.2 μm band. Unlike the two previous cases, the target SCR is now higher than the background SCRs in the 4.5-to-5.0 μm band as shown in Figure 15. Moreover, the contrast in the 4.5-to-5.0 μm band has improved over that for Case 1. Like the two previous cases, snow provides the best contrast in the 3.3-to-4.2 μm band. On the other hand, it has the worst contrast in the 4.5-to-5.0 μm band, where vegetation has the best. For warm conditions (298°K), any target temperature increase above 5°K over the background temperature increases the contrast in both bands, thereby improving target detection.

Table IX. PtSi Daytime SCR Changes From the Baseline for the 3.3-to-4.2 μm and 4.5-to-5.0 μm Bands

Case	Source	Diff 3.3-4.2 μm Band	Diff 4.5-5.0 μm Band	% Diff 3.3-4.2 μm Band	% Diff 4.5-5.0 μm Band
Case 1	Target	0.0025	0.0009	1.84	5.75
Rural	Vegetation	0.0000	0.0000	0.00	0.00
T=300°K	Snow	0.0000	0.0000	0.00	0.00
B=298°K	Sand	0.0000	0.0000	0.00	0.00
	Soil	0.0000	0.0000	0.00	0.00
Background	Average	0.0000	0.0000	0.00	0.00
Case 2	Target	0.0145	0.0052	10.63	32.07
Rural	Vegetation	0.0000	0.0000	0.00	0.00
T=308°K	Snow	0.0000	0.0000	0.00	0.00
B=298°K	Sand	0.0000	0.0000	0.00	0.00
	Soil	0.0000	0.0000	0.00	0.00
Background	Average	0.0000	0.0000	0.00	0.00
Case 3	Target	-0.0101	-0.0040	-7.42	-24.34
Rural	Vegetation	-0.0139	-0.0049	-21.28	-27.25
T=288°K	Snow	-0.0148	-0.0057	-28.86	-29.52
B=288°K	Sand	-0.0131	-0.0056	-16.02	-29.16
	Soil	-0.0127	-0.0050	-14.96	-27.49
Background	Average	-0.0136	-0.0053	-20.28	-28.36
Case 4	Target	-0.0084	-0.0033	-6.15	-20.02
Rural	Vegetation	-0.0139	-0.0049	-21.28	-27.25
T=290°K	Snow	-0.0148	-0.0057	-28.86	-29.52
B=288°K	Sand	-0.0131	-0.0056	-16.02	-29.16
	Soil	-0.0127	-0.0050	-14.96	-27.49
Background	Average	-0.0136	-0.0053	-20.28	-28.36
Case 5	Target	-0.0244	-0.0106	-17.90	-64.76
Rural	Vegetation	-0.0334	-0.0130	-51.32	-72.50
T=258°K	Snow	-0.0357	-0.0152	-69.65	-78.53
B=258°K	Sand	-0.0316	-0.0149	-38.64	-77.59
	Soil	-0.0305	-0.0132	-36.06	-73.16
Background	Average	-0.0328	-0.0141	-48.92	-75.45
Case 6	Target	-0.0240	-0.0103	-17.55	-63.18
Rural	Vegetation	-0.0334	-0.0130	-51.32	-72.50
T=260°K	Snow	-0.0357	-0.0152	-69.65	-78.53
B=258°K	Sand	-0.0316	-0.0149	-38.64	-77.59
	Soil	-0.0305	-0.0132	-36.06	-73.16
Background	Average	-0.0328	-0.0141	-48.92	-75.45

Table IX. Continued

Case	Source	Diff 3.3-4.2 μm Band	Diff 4.5-5.0 μm Band	% Diff 3.3-4.2 μm Band	% Diff 4.5-5.0 μm Band
Case 7	Target	-0.0295	-0.0060	-21.59	-36.89
Tropical	Vegetation	-0.0101	-0.0063	-15.51	-35.35
T=298°K	Snow	-0.0068	-0.0066	-13.21	-34.25
B=298°K	Sand	-0.0144	-0.0066	-17.67	-34.49
	Soil	-0.0148	-0.0064	-17.47	-35.38
Background	Average	-0.0115	-0.0065	-15.97	-34.87
Case 8	Target	-0.0570	0.0021	-41.78	12.55
$\rho(\lambda)$-0.2	Vegetation	0.0000	0.0000	0.00	0.00
T=298°K	Snow	0.0000	0.0000	0.00	0.00
B=298°K	Sand	0.0000	0.0000	0.00	0.00
	Soil	0.0000	0.0000	0.00	0.00
Background	Average	0.0000	0.0000	0.00	0.00
Case 9	Target	0.0570	-0.0021	41.78	-12.55
$\rho(\lambda)$+0.2	Vegetation	0.0000	0.0000	0.00	0.00
T=298°K	Snow	0.0000	0.0000	0.00	0.00
B=298°K	Sand	0.0000	0.0000	0.00	0.00
	Soil	0.0000	0.0000	0.00	0.00
Background	Average	0.0000	0.0000	0.00	0.00

T = Target Temperature.

B = Background Temperature.

Difference calculations use the Baseline case SCR in each case as the reference point. Therefore, positive values are above each source SCR and negative values are below.

Table X. PtSi Nighttime SCR Changes From the Baseline for the 3.3-to-4.2 μm and 4.5-to-5.0 μm Bands

Case	Source	Diff 3.3-4.2 μm Band	Diff 4.5-5.0 μm Band	% Diff 3.3-4.2 μm Band	% Diff 4.5-5.0 μm Band
Case 1	Target	0.0025	0.0009	8.83	7.05
Rural	Vegetation	0.0000	0.0000	0.00	0.00
T=300°K	Snow	0.0000	0.0000	0.00	0.00
B=298°K	Sand	0.0000	0.0000	0.00	0.00
	Soil	0.0000	0.0000	0.00	0.00
Background	Average	0.0000	0.0000	0.00	0.00
Case 2	Target	0.0145	0.0052	51.05	39.35
Rural	Vegetation	0.0000	0.0000	0.00	0.00
T=308°K	Snow	0.0000	0.0000	0.00	0.00
B=298°K	Sand	0.0000	0.0000	0.00	0.00
	Soil	0.0000	0.0000	0.00	0.00
Background	Average	0.0000	0.0000	0.00	0.00
Case 3	Target	-0.0101	-0.0040	-35.63	-29.87
Rural	Vegetation	-0.0139	-0.0049	-35.64	-29.88
T=288°K	Snow	-0.0148	-0.0057	-35.61	-29.88
B=288°K	Sand	-0.0131	-0.0056	-35.62	-29.87
	Soil	-0.0127	-0.0050	-35.67	-29.87
Background	Average	-0.0136	-0.0053	-35.63	-29.87
Case 4	Target	-0.0084	-0.0033	-29.53	-24.56
Rural	Vegetation	-0.0139	-0.0049	-35.64	-29.88
T=290°K	Snow	-0.0148	-0.0057	-35.61	-29.88
B=288°K	Sand	-0.0131	-0.0056	-35.62	-29.87
	Soil	-0.0127	-0.0050	-35.67	-29.87
Background	Average	-0.0136	-0.0053	-35.63	-29.87
Case 5	Target	-0.0244	-0.0106	-85.94	-79.47
Rural	Vegetation	-0.0334	-0.0130	-85.95	-79.49
T=258°K	Snow	-0.0357	-0.0152	-85.92	-79.49
B=258°K	Sand	-0.0316	-0.0149	-85.93	-79.48
	Soil	-0.0305	-0.0132	-85.98	-79.47
Background	Average	-0.0328	-0.0141	-85.94	-79.48
Case 6	Target	-0.0240	-0.0103	-84.27	-77.52
Rural	Vegetation	-0.0334	-0.0130	-85.95	-79.49
T=260°K	Snow	-0.0357	-0.0152	-85.92	-79.49
B=258°K	Sand	-0.0316	-0.0149	-85.93	-79.48
	Soil	-0.0305	-0.0132	-85.98	-79.47
Background	Average	-0.0328	-0.0141	-85.94	-79.48

Table X. Continued

Case	Source	Diff 3.3-4.2 μm Band	Diff 4.5-5.0 μm Band	% Diff 3.3-4.2 μm Band	% Diff 4.5-5.0 μm Band
Case 7	Target	-0.0029	-0.0046	-10.26	-34.29
Tropical	Vegetation	-0.0040	-0.0056	-10.33	-34.05
T=298°K	Snow	-0.0042	-0.0065	-10.20	-34.08
B=298°K	Sand	-0.0038	-0.0064	-10.27	-34.20
	Soil	-0.0037	-0.0057	-10.46	-34.32
Background	Average	-0.0039	-0.0060	-10.31	-34.16
Case 8	Target	0.0085	0.0039	30.02	29.45
$\rho(\lambda)$-0.2	Vegetation	0.0000	0.0000	0.00	0.00
T=298°K	Snow	0.0000	0.0000	0.00	0.00
B=298°K	Sand	0.0000	0.0000	0.00	0.00
	Soil	0.0000	0.0000	0.00	0.00
Background	Average	0.0000	0.0000	0.00	0.00
Case 9	Target	-0.0085	-0.0039	-30.02	-29.45
$\rho(\lambda)$+0.2	Vegetation	0.0000	0.0000	0.00	0.00
T=298°K	Snow	0.0000	0.0000	0.00	0.00
B=298°K	Sand	0.0000	0.0000	0.00	0.00
	Soil	0.0000	0.0000	0.00	0.00
Background	Average	0.0000	0.0000	0.00	0.00

T = Target Temperature.

B = Background Temperature.

Difference calculations use the Baseline case SCR in each case as the reference point. Therefore, positive values are above each source SCR and negative values are below.

Baseline

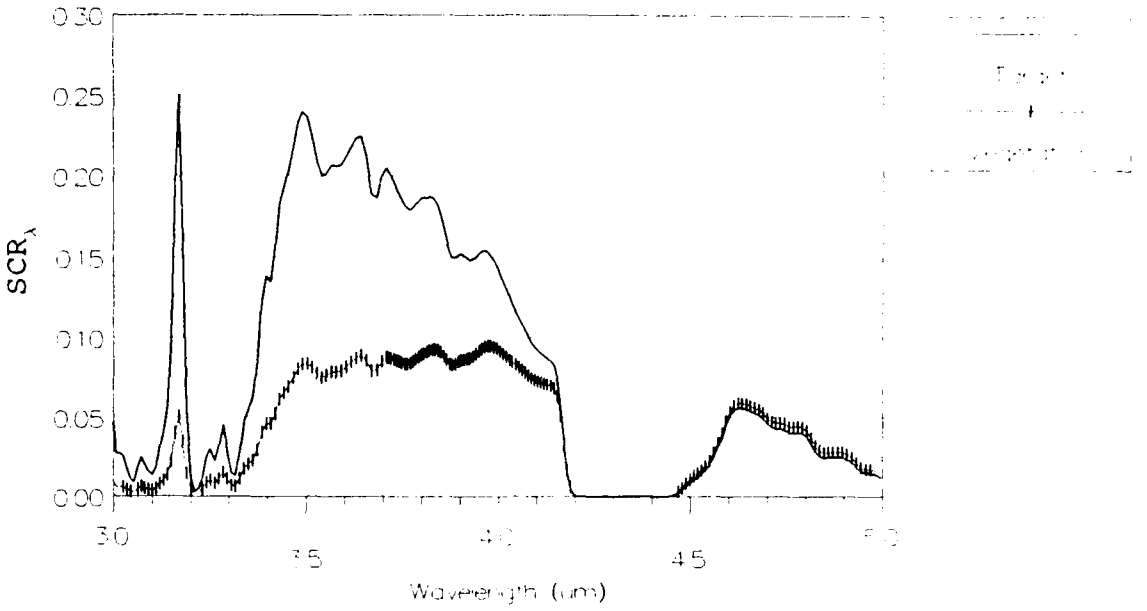

Case 2

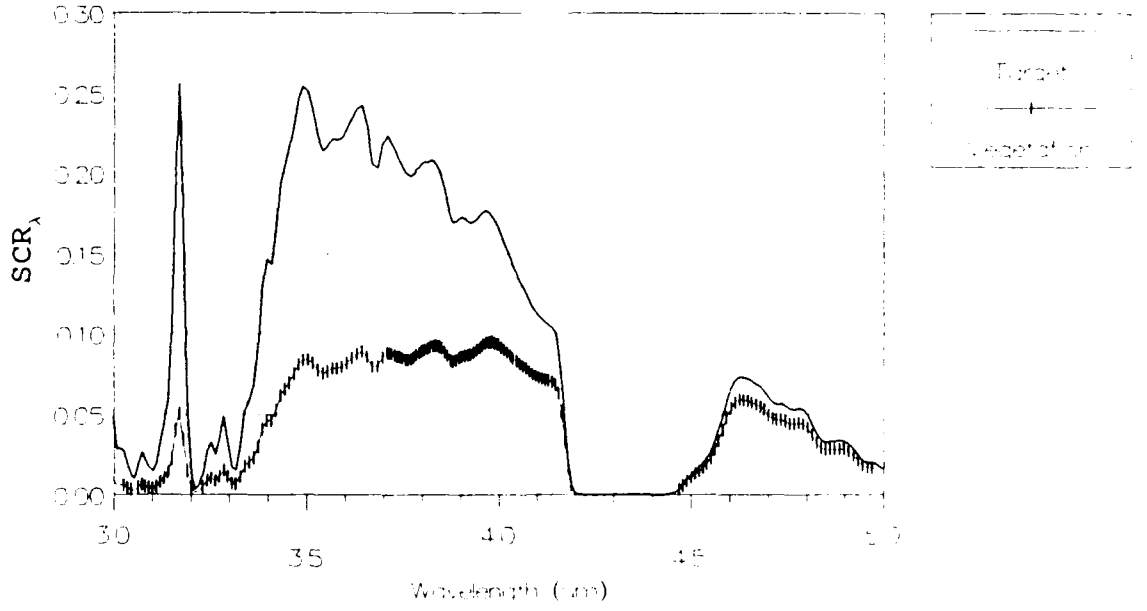

Figure 15. Baseline vs Case 2, PtSi, Day

Night. At night the target SCR drops in both bands compared to the day. The background SCRs remain unchanged from the previous two cases. The large thermal increase makes the target SCR higher in both bands compared to the baseline case. Unlike the previous cases, the average background SCR is lower than the target SCR in the 3.3-to-4.2 μm band as shown in Figure 16. In the 4.5-to-5.0 μm band, the SCRs for both vegetation and soil are below the target SCR, while the SCRs for both snow and sand are above. Furthermore, the average background SCR is lower than the target SCR. This implies that as the target temperature increases, eventually all the background SCRs will be below the target. Unlike previous cases, soil provides the best contrast in the 3.3-to-4.2 μm band, while snow has the worst. In the 4.5-to-5.0 μm band, vegetation provides the best contrast, while sand has the worst. However, the low contrast in the 4.5-to-5.0 μm band may make target detection more difficult. For warm conditions (298°K), any target increase above 7°K over the background temperature increases the contrast in both bands, thereby improving target detection.

Case 3: Rural, Target = 288°K, Background = 288°K

Day. In this case both the background and the target temperatures are reduced by 10°K, thereby reducing the thermal contribution to the SCR. As a result, the target and the background SCRs are reduced somewhat in both

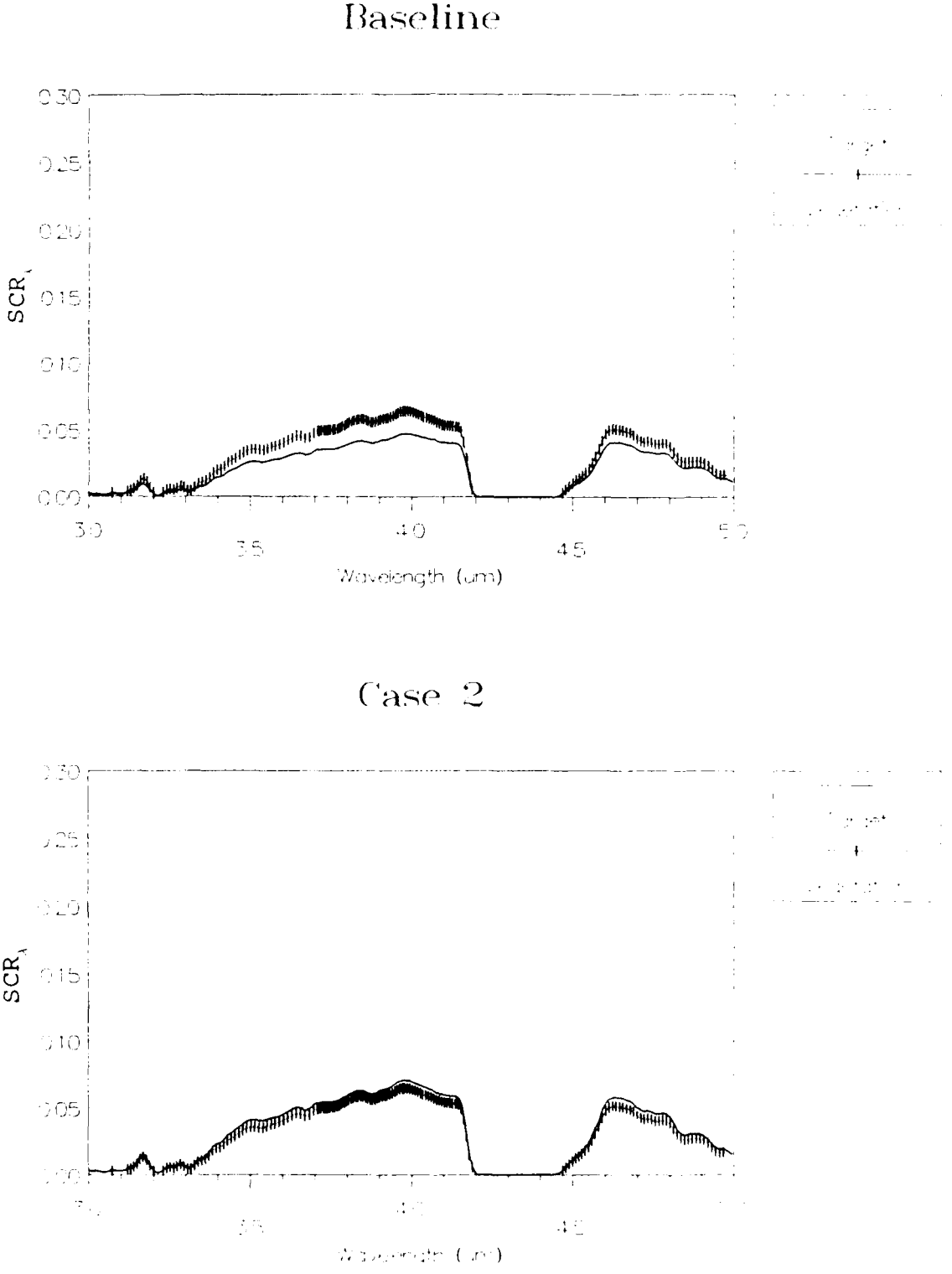

Figure 16. Baseline vs Case 2, PtSi, Night

bands compared to the baseline case. As with the baseline case, the background SCRs are much lower than the target SCR in the 3.3-to-4.2 μm band and somewhat higher in the 4.5-to-5.0 μm band. In addition, snow provides the best contrast in both bands. At these moderate temperatures (288°K), the contrast in the 4.5-to-5.0 μm band may not be good enough for target detection. On the other hand, the contrast in the 3.3-to-4.2 μm band is not only sufficient for target detection, but is slightly better than that for the baseline case and Case 1.

Night. At night the target and background SCRs drop significantly in both bands compared to the day and baseline case. As with the baseline case and Case 1, the background SCRs are higher than the target SCR in both bands. In addition, snow provides the best contrast for target detection in both bands. As with the baseline case and Case 1, the contrast in the 4.5-to-5.0 μm band actually improves slightly over that during the day.

Case 4: Rural, Target = 290°K, Background = 288°K

Day. A 2°K increase in target temperature increases the thermal portion of its SCR. Compared to the baseline case, the target SCR is lower in both bands. The background SCRs remain unchanged from Case 3. As with the baseline case, Case 1, and Case 2, the background SCRs are much lower than the target SCR in the 3.3-to-4.2 μm band. With the exception of vegetation, all of the background SCRs

are slightly higher than the target SCR in the 4.5-to-5.0 μm band. However, the contrast between target and background in this band is so small that target detection may be impossible. For moderate conditions (288°K), target temperature increases below 5°K over the background temperature reduce the contrast in the 4.5-to-5.0 μm band, thereby making target detection more difficult. However, in the 3.3-to-4.2 μm band, any target temperature increase over the background temperature increases the contrast between target and background. As with most of the previous cases, snow provides the best contrast in both bands.

Night. At night the target SCR drops in both bands compared to the day and baseline case. The background SCRs remain unchanged from Case 3. As with the baseline case, Case 1, and Case 3, the background SCRs are higher than the target SCR in both bands. However, with the slight increase in target temperature, the differences between the target and background SCRs in both bands are smaller compared to Case 3, thus reducing discrimination. Again, as with most of the other cases, snow provides the best contrast in both bands. A target temperature increase below 7°K over the background temperature reduces the contrast in both bands, thereby making target detection difficult, while an increase above 7°K increases the contrast, thereby improving target detection. As with the baseline case,

Case 1, and Case 3, contrast in the 4.5-to-5.0 μm band improves at night.

Case 5: Rural, Target = 258°K, Background = 258°K

Day. In this case both the target and the backgrounds are reduced 40°K in temperature from the baseline case. This reduction in thermal radiation reduces the target and the background SCRs somewhat in the 3.3-to-4.2 μm band and dramatically by a factor of 65-to-75% in the 4.5-to-5.0 μm band compared to the baseline case. Like the baseline case, the target SCR dominates in the 3.3-to-4.2 μm band. Unlike the baseline case, but similar to Case 2, the target SCR is somewhat higher than the background SCR in the 4.5-to-5.0 μm band. This effect, shown in Figure 17, results from the fact that at such cold temperatures, the thermal contribution to the SCR becomes small compared to the reflected contribution and, therefore, the target, having a higher reflectivity than the backgrounds, has a higher SCR. As with most of the other cases, snow provides the best contrast. However, the low contrast in the 4.5-to-5.0 μm band may not allow for target detection. At such cold temperatures (258°K), the contrast between target and background in the 3.3-to-4.2 μm band is actually slightly better than at warmer temperatures.

Night. At night the target and background SCRs drop dramatically in both bands compared to the day and baseline case. The average background SCR is higher than

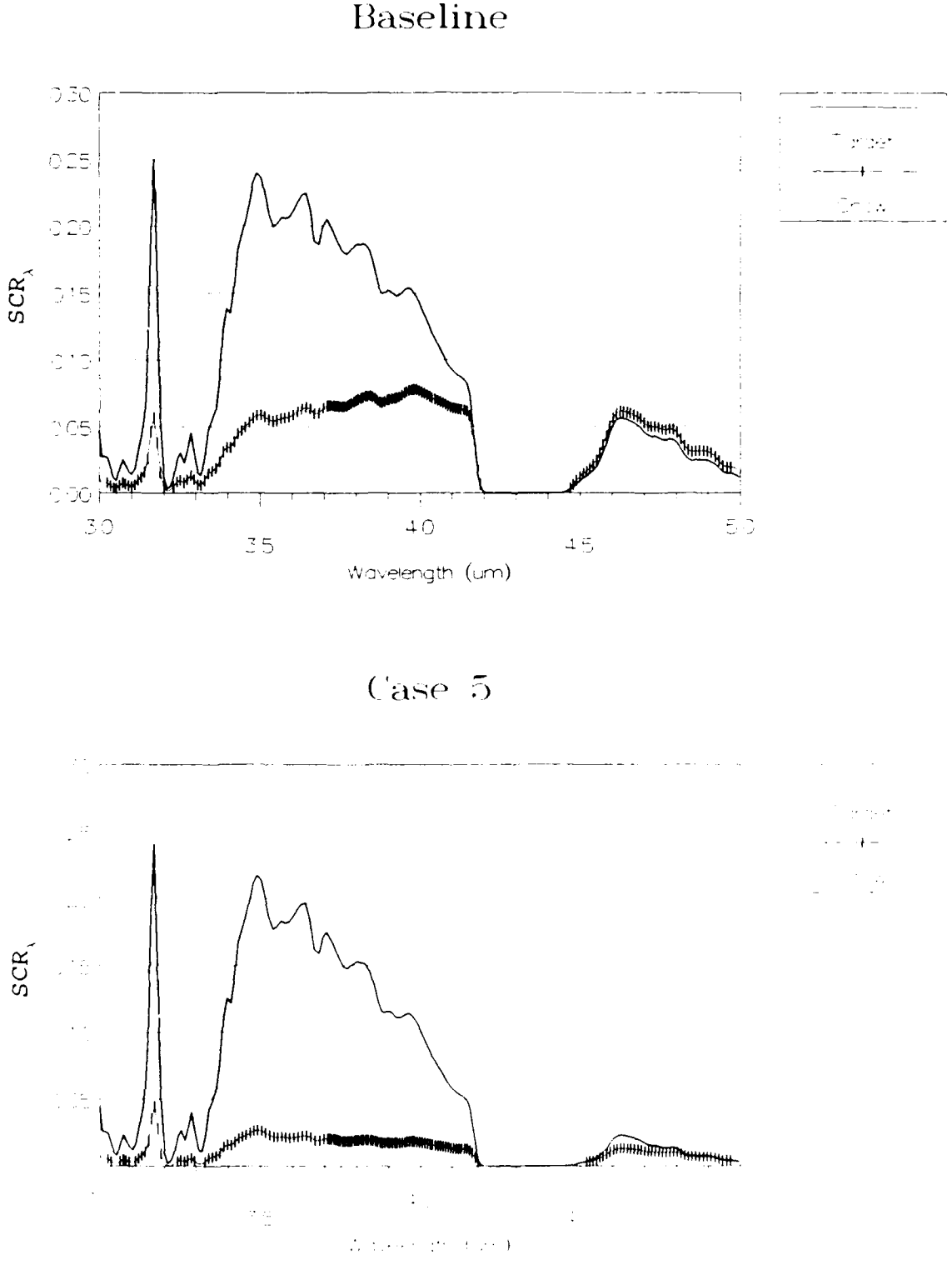

Figure 17. Baseline Case vs Case 5, PtSi, Day

the target SCR in both bands. As with most of the previous cases, snow provides the best contrast. However, the low contrast in both bands may make target detection very difficult.

Case 6: Rural, Target = 260°K, Background = 258°K

Day. A small temperature increase of 2°K in the target over Case 5 slightly increases the contrast in both bands. Compared to the baseline case, the target SCR is reduced in both bands. The background SCRs remain as they were in Case 5. Again, snow provides the best contrast. However, the contrast in the 4.5-to-5.0 μm band may not be sufficient for target detection. For cold conditions (258°K), any increase in target temperature over the background temperature will improve the contrast between target and background in both bands.

Night. The increase in target temperature decreases the contrast with respect to Case 5. Compared to the day and the baseline case, the target SCR is smaller in both bands. The background SCRs remain unchanged from Case 5. The background SCRs are higher than the target SCR in both bands. As before, snow provides the best contrast for target detection. However, the low contrast in both bands may make remote sensing difficult. For cold conditions (258°K), any increase in target temperature below 7°K over the background temperature reduces the contrast in both bands, while an increase above 7°K in target

temperature increases the contrast, thereby improving target detection in both bands.

Case 7: Tropical, Target = 298°K, Background = 298°K

Day. The tropical atmosphere used in this case reduces the atmospheric transmission compared to the rural setting, with the larger effect in the 4.5-to-5.0 μm band as shown in Figure 9. This, in turn, reduces the SCR for the target and the backgrounds. Although the SCRs are smaller, the basic results seen for the baseline case remain the same. Compared to the baseline case, the target and the background SCRs are lower in both bands. As with most of the rural setting cases, the target SCR dominates in the 3.3-to-4.2 μm band, but is slightly lower than the background SCRs in the 4.5-to-5.0 μm band. Like most of the rural cases, snow provides the best contrast in both bands. However, the low contrast in the 4.5-to-5.0 μm band may make target discrimination difficult.

Night. At night the target and background SCRs drop in both bands compared to the day and baseline case. As with most of the rural setting cases, the background SCRs are higher than the target SCR in both bands. Snow provides the best contrast. As with the baseline case, Case 1, Case 3, and Case 4, the contrast in the 4.5-to-5.0 μm band improves at night compared to the day.

Case 8: Baseline, Target Reflectivity Decreased by 0.2

Day. Figure 18 shows that when the target reflectivity is uniformly decreased by 0.2 (from ≈ 0.3 to ≈ 0.1) across the 3.0-to-5.0 μm band, the target SCR is lower in the 3.3-to-4.2 μm band and higher in the 4.5-to-5.0 μm band compared to the baseline case. The increase in target SCR in the 4.5-to-5.0 μm band results from the increase in target emissivity that occurs with the decrease in target reflectivity. This uniform decrease in reflectivity reduces the contrast between the target and background in both bands compared to the baseline case. The background SCRs are somewhat lower than the target SCR in the 3.3-to-4.2 μm band and slightly higher in the 4.5-to-5.0 μm band. Snow still provides the best contrast. However, the extremely low contrast in the 4.5-to-5.0 μm band makes target detection difficult. This case indicates that target reflectivities lower than the baseline target reflectivity value of ≈ 0.3 decrease the contrast between target and background in both bands, especially in the 4.5-to-5.0 μm band. As a result, target detection becomes more difficult.

Night. As with the day and shown in Figure 19, the contrast in both bands has been considerably reduced compared to the baseline case. This contrast reduction is due to the increase in target SCR resulting from the increase in target emissivity. Nevertheless, as with the baseline case, Case 1, Case 3, Case 4, and Case 7, the

Baseline

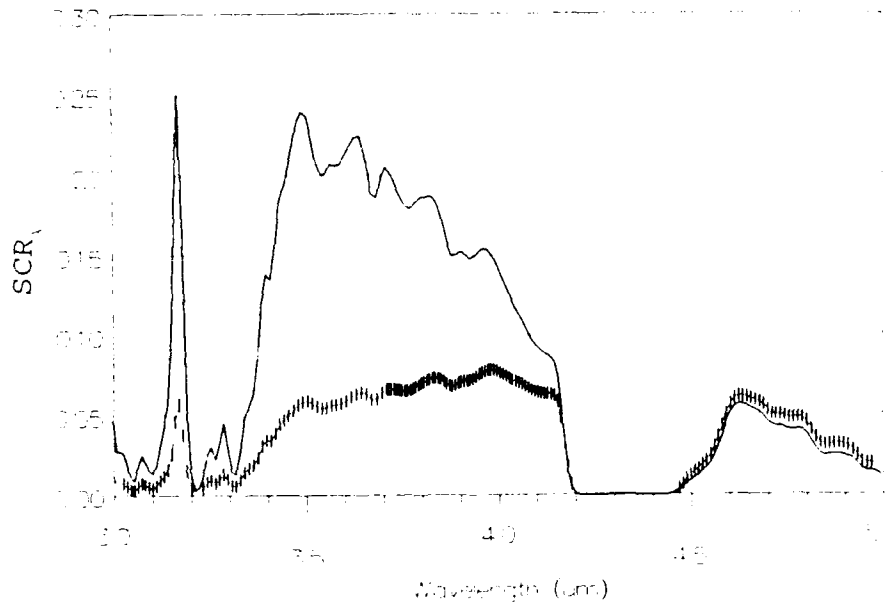

Case 8

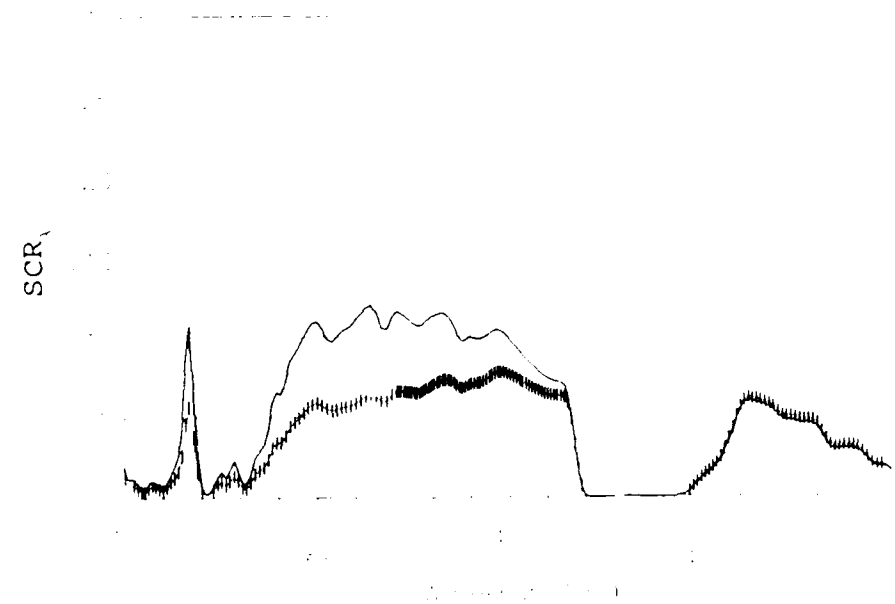

Figure 18. Baseline Case vs Case 8, PtSi, Day

Baseline

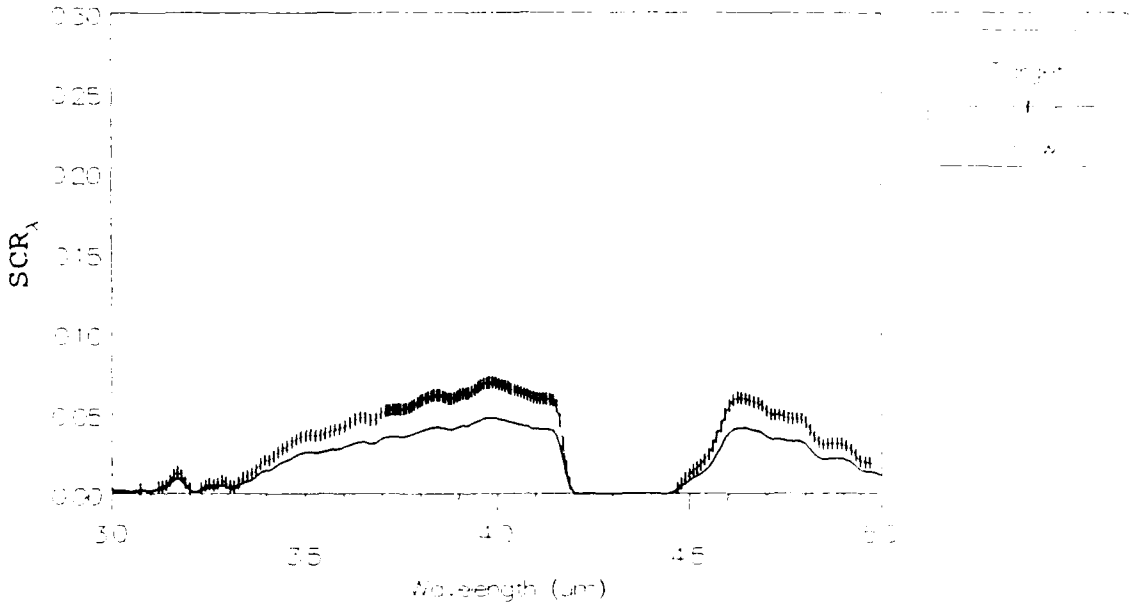

Case 8

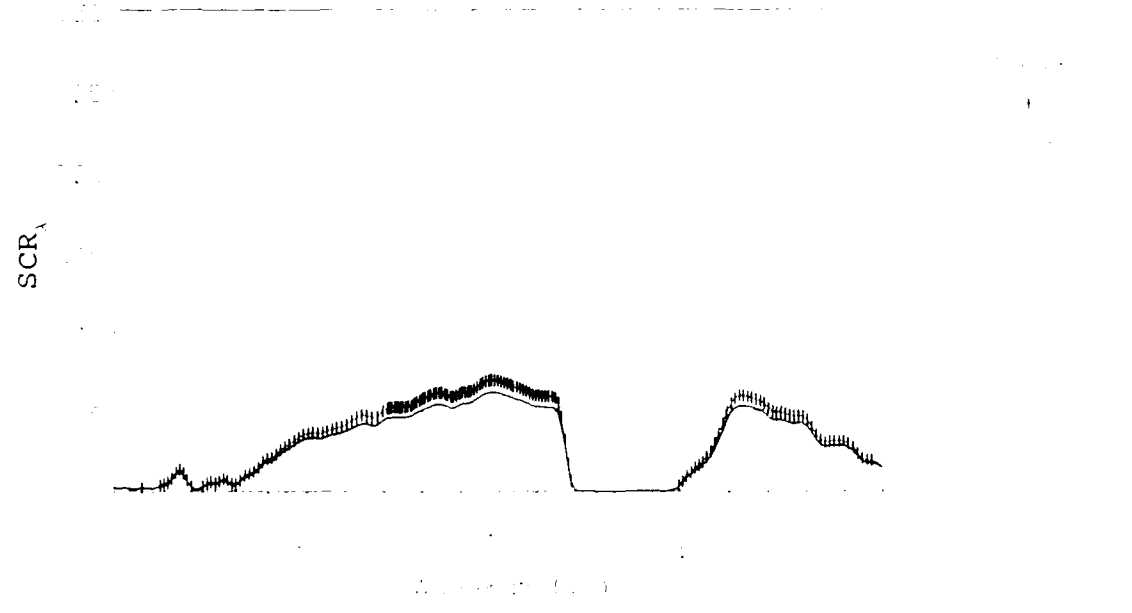

Figure 1.. Baseline Case vs Case 8, PtSi, Night

4.5-to-5.0 μm band nighttime contrast is slightly better than it is during the day. Compared to the day, the target SCR is lower in both bands. The background SCRs are slightly higher than the target SCR in both bands. Although snow provides the best contrast, like most of the previous cases, the extremely low contrast in both bands makes target detection very difficult. Target reflectivities lower than the baseline target reflectivity of $\approx$ 0.3 reduce the contrast between target and background in both bands, thereby making target detection more difficult.

Case 9: Baseline, Target Reflectivity Increased by 0.2

Day. In this case, the target reflectivity is uniformly increased by 0.2 (from $\approx$ 0.3 to $\approx$ 0.5) across the 3.0-to-5.0 μm band, while keeping all other parameters the same as the baseline case. Compared to the baseline case, the target SCR is higher in the 3.3-to-4.2 μm band and lower in the 4.5-to-5.0 μm band. The 0.2 increase in target reflectivity substantially improves the contrast in the 3.3-to-4.2 μm band, while slightly improving it in the 4.5-to-5.0 μm band. As with the baseline case, the target SCR overwhelms the background SCRs in the 3.3-to-4.2 μm band. Unlike the baseline case, the target SCR is now slightly lower than the background SCR in the 4.5-to-5.0 μm band as shown in Figure 20. This drop in target SCR results from the decrease in target emissivity that occurs with the increase in target reflectivity. Like the baseline case,

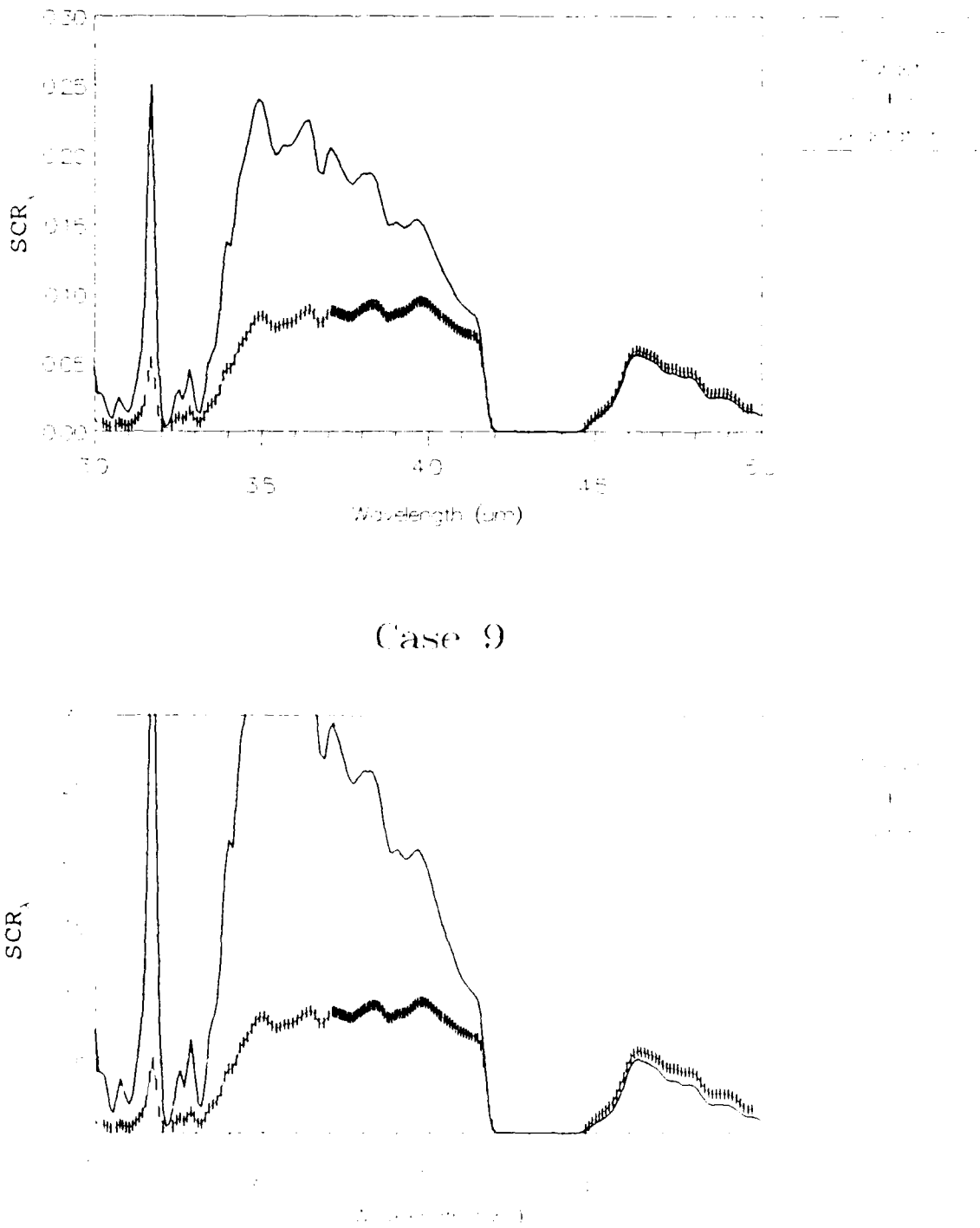

Figure 20. Baseline Case vs Case 9, PtSi, Day

snow provides the best contrast. This case shows that target reflectivities greater than the baseline target reflectivity of ≈ 0.3 increase the contrast between target and background in both bands, thereby making target detection easier.

Night. At night the target SCR is lower in both bands compared to the day. Compared to the baseline case, the target SCR is lower in both bands, which results from the lower target emissivity that occurs with the increase in target reflectivity. As with the day and shown in Figure 21, the contrast between target and background has improved over that of the baseline. The background SCRs are considerably higher than the target SCR in both bands. As before, snow provides the best contrast. This case indicates that target reflectivities greater than the baseline target reflectivity of ≈ 0.3 increase the contrast between target and background in both bands, thereby making target detection easier.

Indium Antimonide

Baseline: Rural, Target = 298°K, Background = 298°K

Day. Figures 22 and 23 contain plots of SCR_λ versus λ for the target against backgrounds of vegetation and snow, respectively, for the day baseline case. SCR_λ versus λ plots of target against sand and soil backgrounds are very similar to that of the target against

Baseline

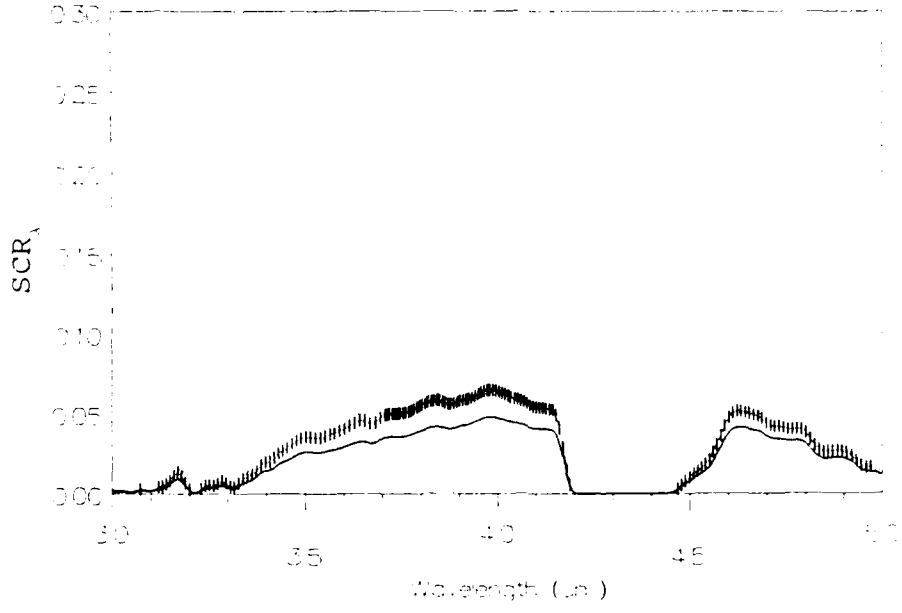

Case 9

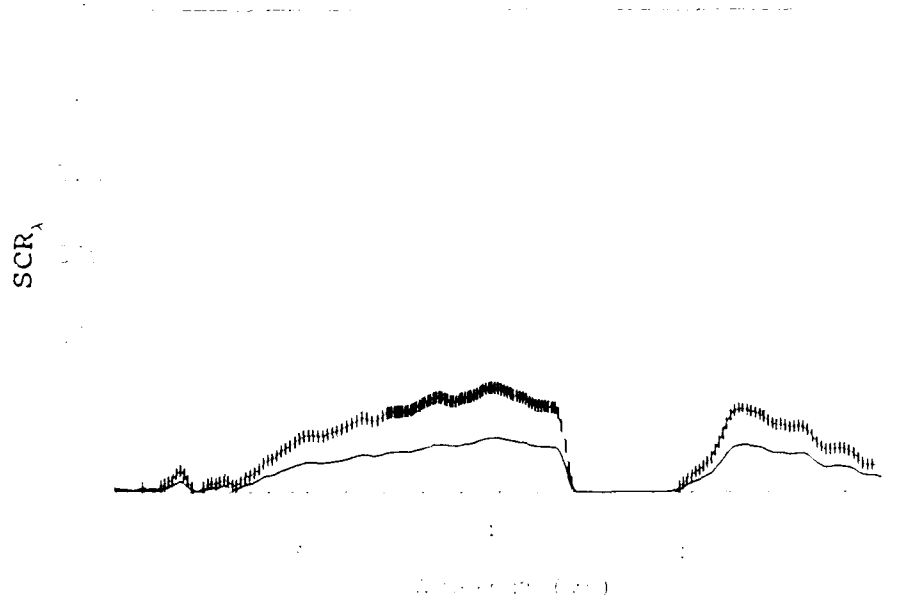

Figure 21. Baseline vs Case 9, PtSi, Night

Rural Setting, 23 km Visibility

Target = 298 K, Background = 298 K

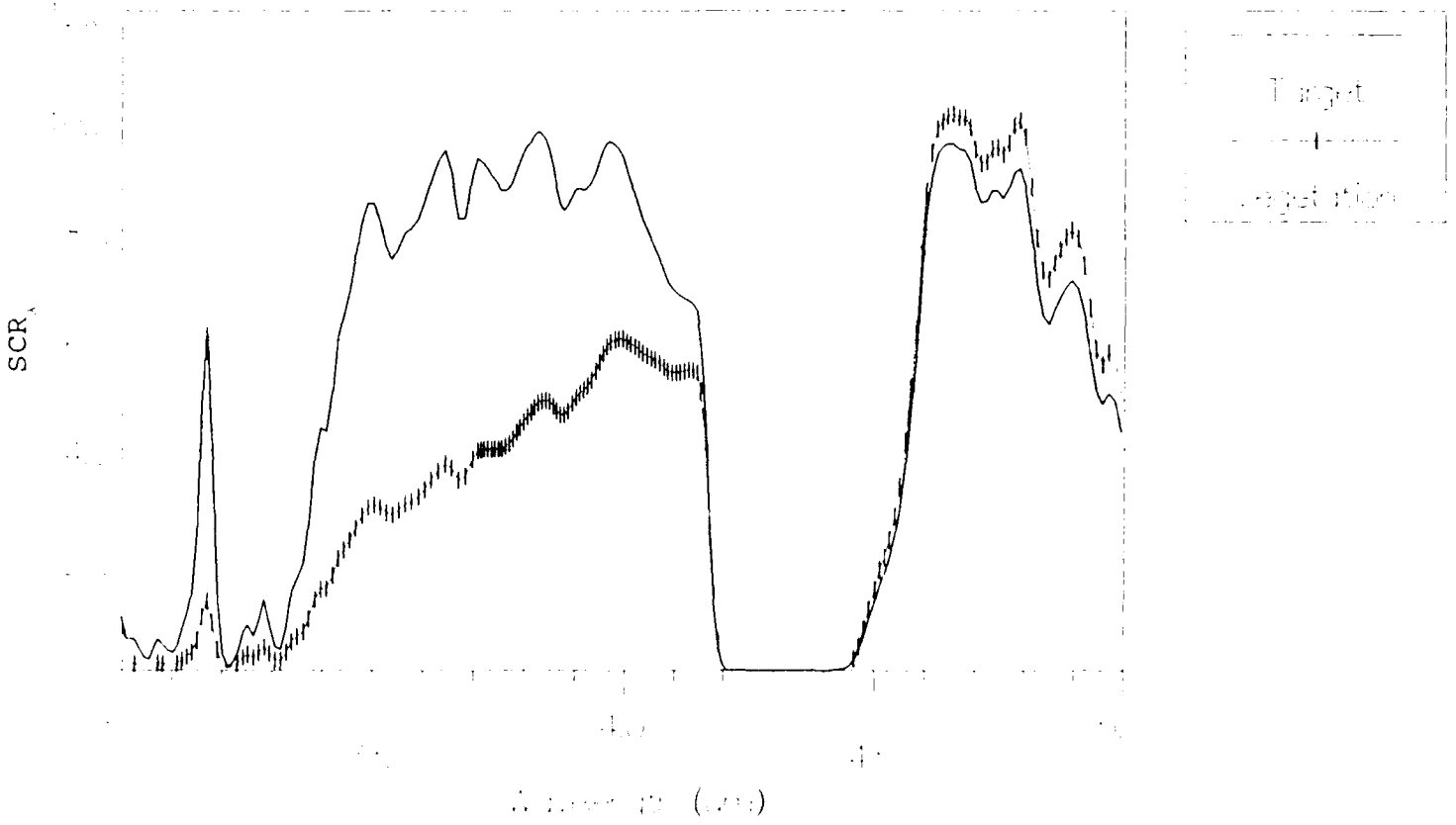

Figure 22. InSb Baseline Case, Vegetation, Day

Rural Setting, 23 km Visibility

Target = 298 K, Background = 298 K

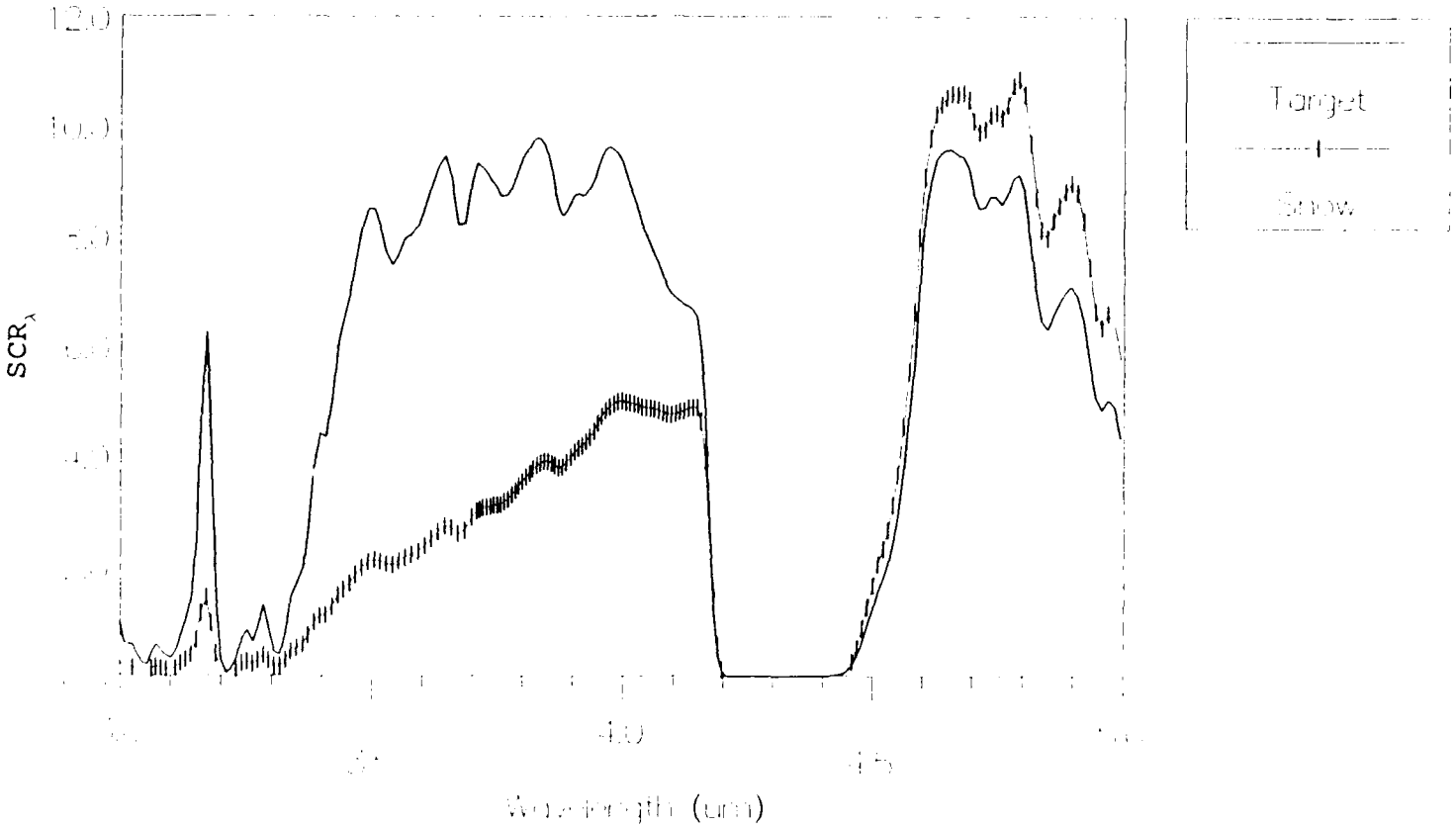

Figure 23. InSb Baseline Case, Snow, Day

vegetation, hence, they are not included in this thesis. As can be seen in these figures, the target SCR dominates the background SCRs in the 3.3-to-4.2 μm band. This is primarily due to the higher reflectivity of the target. The average background SCR is 44.85% lower than the target SCR in this band. In the 4.5-to-5.0 μm band the background SCRs are somewhat higher than the target SCR. The average background SCR is 14.94% higher than the target SCR. Snow provides the best contrast for target discrimination.

Night. Figures 24 and 25 contain plots of SCR_λ versus λ for the target against backgrounds of vegetation and snow, respectively, for the night baseline case. At night, without the reflected radiation contributing to the SCR, the target SCR drops 76.42% in the 3.3-to-4.2 μm band and 17.34% in the 4.5-to-5.0 μm band, compared to the day. The average background SCR is 40.04% lower in the 3.3-to-4.2 μm band, but only 4.7% lower in the 4.5-to-5.0 μm band. These results demonstrate the heavy influence of reflected radiation in the 3.3-to-4.2 μm band and the heavy influence of the thermal radiation in the 4.5-to-5.0 μm band. In both bands the background SCRs are higher than the target SCR. The average background SCR is 34.0% and 32.66% higher than the target SCR in the 3.3-to-4.2 μm and 4.5-to-5.0 μm bands, respectively. Moreover, the contrast in the 4.5-to-5.0 μm band is considerably better than that during the day. As with the

Rural Setting, 23 km Visibility

Target = 298 K, Background = 298 K

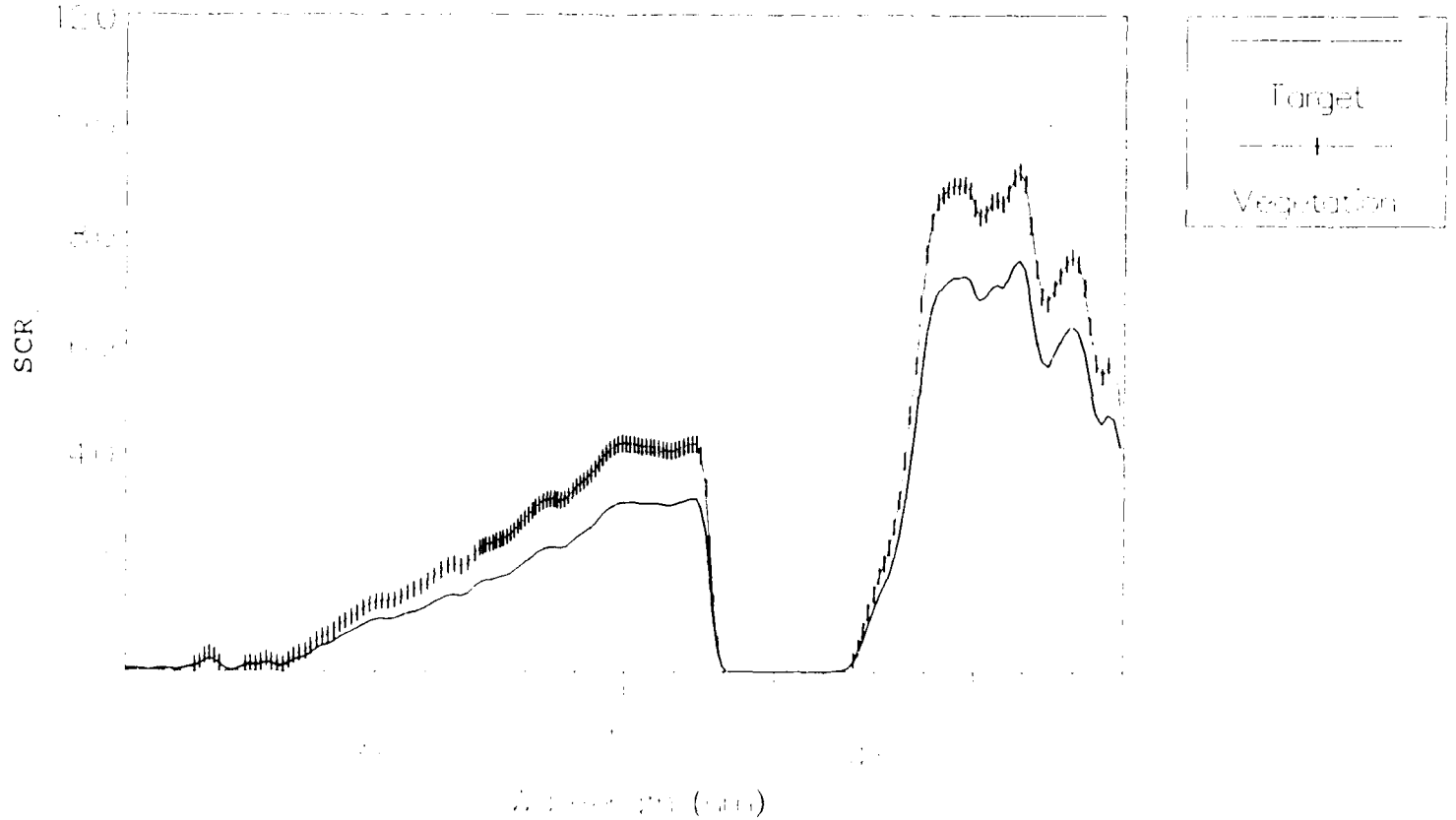

Figure 24. InSb Baseline Case, Vegetation, Night

Rural Setting, 23 km Visibility

Target = 298 K, Background = 298 K

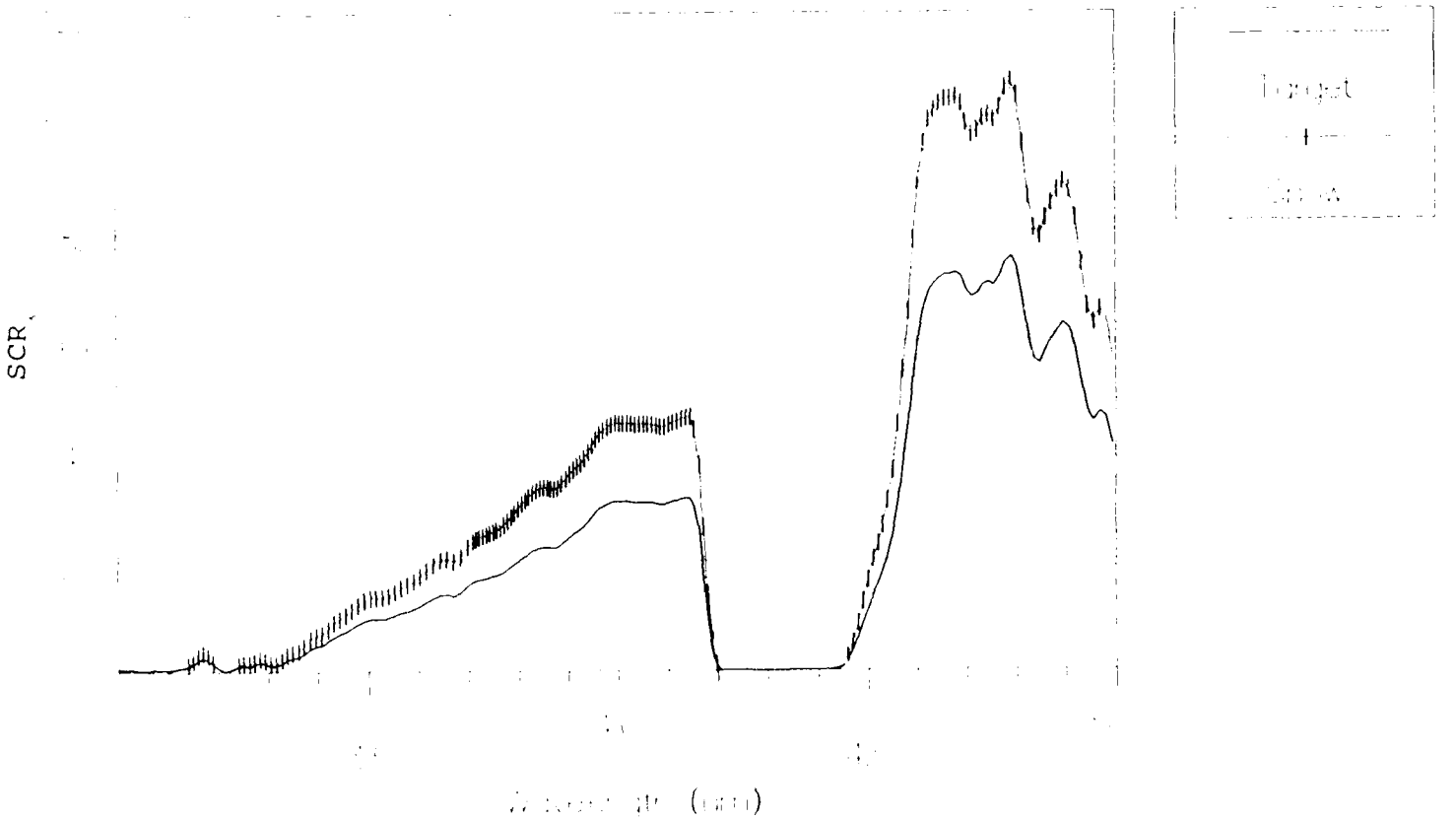

Figure 25. InSb Baseline Case, Snow, Night

day, snow provides the best contrast.

Table XI contains the InSb daytime SCR values for each band for all 10 cases as various parameters of the daytime baseline case are individually varied, while Table XII contains the InSb daytime SCR differences between the target and the backgrounds for all 10 cases. Similarly, Table XIII contains the InSb nighttime SCR values for each band for all 10 cases, while Table XIV contains the InSb nighttime SCR differences between the target and the backgrounds for all 10 cases. Finally, Table XV contains the InSb SCR differences between day and night for all 10 cases.

Case 1: Rural, Target = 300°K, Background = 298°K

Day. An increase in target temperature of 2°K slightly raises the target SCR. Compared to the baseline case, the target SCR increases 2.05% and 5.79% in the 3.3-to-4.2 μm and 4.5-to-5.0 μm bands, respectively. The background SCRs remain the same as the baseline case. The increase in target temperature slightly improves the contrast in the 3.3-to-4.2 μm band, but slightly decreases it in the 4.5-to-5.0 μm band, compared to the baseline case. The average background SCR is 45.96% lower than the target SCR in the 3.3-to-4.2 μm band and 8.65% higher in the 4.5-to-5.0 μm band. As with the baseline case, snow provides the best contrast. However, the low contrast in the 4.5-to-5.0 μm band may make target detection difficult. For warm conditions (298°K), any target temperature increase

Table XI. InSb Daytime SCR Vector Distances for the 3.3-to-4.2 μm and 4.5-to-5.0 μm Bands

Case	Source	SCR 3.3-4.2 μm Band	SCR 4.5-5.0 μm Band	SCR Vector Distance	Average Vector Distance	Std Dev
Baseline	Target	6.5480	3.4109	******	2.9842	0.7309
Rural	Vegetation	3.3599	3.7512	3.2061		
T=298°K	Snow	2.6928	4.0821	3.9131		
B=298°K	Sand	4.1002	4.0397	2.5272		
	Soil	4.2925	3.8083	2.2902		
Case 1	Target	6.6822	3.6084	******	3.0896	0.7342
Rural	Vegetation	3.3599	3.7512	3.3253		
T=300°K	Snow	2.6928	4.0821	4.0174		
B=298°K	Sand	4.1002	4.0397	2.6178		
	Soil	4.2925	3.8083	2.3980		
Case 2	Target	7.3218	4.5121	******	3.7623	0.7169
Rural	Vegetation	3.3599	3.7512	4.0342		
T=308°K	Snow	2.6928	4.0821	4.6489		
B=298°K	Sand	4.1002	4.0397	3.2560		
	Soil	4.2925	3.8083	3.1099		
Case 3	Target	6.0044	2.5733	******	3.1312	0.7831
Rural	Vegetation	2.6191	2.7283	3.3889		
T=288°K	Snow	1.8983	2.8825	4.1178		
B=288°K	Sand	3.3969	2.8652	2.6238		
	Soil	3.6172	2.7596	2.3945		
Case 4	Target	6.0977	2.7222	******	3.2166	0.7840
Rural	Vegetation	2.6191	2.7283	3.4786		
T=290°K	Snow	1.8983	2.8825	4.2025		
B=288°K	Sand	3.3969	2.8652	2.7046		
	Soil	3.6172	2.7596	2.4807		
Case 5	Target	5.2273	1.1760	******	3.3936	0.8573
Rural	Vegetation	1.5606	1.0224	3.6700		
T=258°K	Snow	0.7619	0.8819	4.4751		
B=258°K	Sand	2.3909	0.9061	2.8492		
	Soil	2.6528	1.0103	2.5798		
Case 6	Target	5.2534	1.2311	******	3.4237	0.8567
Rural	Vegetation	1.5606	1.0224	3.6988		
T=260°K	Snow	0.7619	0.8819	4.5051		
B=258°K	Sand	2.3909	0.9061	2.8809		
	Soil	2.6528	1.0103	2.6100		

Table XI. Continued

Case	Source	SCR 3.3-4.2 μm Band	SCR 4.5-5.0 μm Band	SCR Vector Distance	Average Vector Distance	Std Dev
Case 7	Target	5.3234	2.0222	******	3.8530	0.4133
Tropical	Vegetation	2.9220	2.2752	3.6130		
T=298°K	Snow	2.3984	2.5149	3.3946		
B=298°K	Sand	3.4810	2.4801	4.1813		
	Soil	3.6504	2.3079	4.2231		
Case 8	Target	3.9933	3.8709	******	0.6169	0.5041
$\rho(\lambda)$-0.2	Vegetation	3.3599	3.7512	0.6446		
T=298°K	Snow	2.6928	4.0821	1.3175		
B=298°K	Sand	4.1002	4.0397	0.1999		
	Soil	4.2925	3.8083	0.3057		
Case 9	Target	9.1026	2.9510	******	5.5781	0.7312
$\rho(\lambda)$+0.2	Vegetation	3.3599	3.7512	5.7982		
T=298°K	Snow	2.6928	4.0821	6.5088		
B=298°K	Sand	4.1002	4.0397	5.1195		
	Soil	4.2925	3.8083	4.8859		
			Overall SCR Average		3.3049	

T = Target Temperature.

B = Background Temperature.

Table XII. InSb Daytime SCR Differences Between Target and Background for the 3.3-to-4.2 μm and 4.5-to-5.0 μm Bands

Case	Source	Diff 3.3-4.2 μm Band	Diff 4.5-5.0 μm Band	% Diff 3.3-4.2 μm Band	% Diff 4.5-5.0 μm Band
Baseline	Vegetation	-3.1880	0.3403	-48.69	9.98
Rural	Snow	-3.8551	0.6712	-58.88	19.68
T=298°K	Sand	-2.4478	0.6288	-37.38	18.44
B=298°K	Soil	-2.2554	0.3974	-34.45	11.65
	Average	-2.9366	0.5094	-44.85	14.94
Case 1	Vegetation	-3.3223	0.1428	-49.72	3.96
Rural	Snow	-3.9894	0.4737	-59.70	13.13
T=300°K	Sand	-2.5820	0.4314	-38.64	11.95
B=298°K	Soil	-2.3897	0.1999	-35.76	5.54
	Average	-3.0708	0.3119	-45.96	8.65
Case 2	Vegetation	-3.9618	-0.7609	-54.11	-16.86
Rural	Snow	-4.6289	-0.4300	-63.22	-9.53
T=308°K	Sand	-3.2216	-0.4724	-44.00	-10.47
B=298°K	Soil	-3.0293	-0.7038	-41.37	-15.60
	Average	-3.7104	-0.5918	-50.68	-13.12
Case 3	Vegetation	-3.3853	0.1550	-56.38	6.02
Rural	Snow	-4.1062	0.3092	-68.39	12.02
T=288°K	Sand	-2.6076	0.2919	-43.43	11.34
B=288°K	Soil	-2.3872	0.1864	-39.76	7.24
	Average	-3.1216	0.2356	-51.99	9.16
Case 4	Vegetation	-3.4786	0.0061	-57.05	0.22
Rural	Snow	-4.1994	0.1603	-68.87	5.89
T=290°K	Sand	-2.7008	0.1430	-44.29	5.25
B=288°K	Soil	-2.4805	0.0375	-40.68	1.38
	Average	-3.2148	0.0867	-52.72	3.19
Case 5	Vegetation	-3.6668	-0.1536	-70.15	-13.06
Rural	Snow	-4.4655	-0.2942	-85.43	-25.01
T=258°K	Sand	-2.8364	-0.2700	-54.26	-22.95
B=258°K	Soil	-2.5745	-0.1657	-49.25	-14.09
	Average	-3.3858	-0.2209	-64.77	-18.78
Case 6	Vegetation	-3.6929	-0.2087	-70.29	-16.95
Rural	Snow	-4.4916	-0.3493	-85.50	-28.37
T=260°K	Sand	-2.8625	-0.3251	-54.49	-26.41
B=258°K	Soil	-2.6006	-0.2208	-49.50	-17.94
	Average	-3.4119	-0.2760	-64.95	-22.42

Table XII. Continued

Case	Source	Diff 3.3-4.2 μm Band	Diff 4.5-5.0 μm Band	% Diff 3.3-4.2 μm Band	% Diff 4.5-5.0 μm Band
Case 7	Vegetation	-2.4014	0.2531	-45.11	12.51
Tropical	Snow	-2.9250	0.4927	-54.95	24.37
T=298°K	Sand	-1.8424	0.4579	-34.61	22.65
B=298°K	Soil	-1.6730	0.2858	-31.43	14.13
	Average	-2.2105	0.3724	-41.52	18.41
Case 8	Vegetation	-0.6334	-0.1197	-15.86	-3.09
$\rho(\lambda)-0.2$	Snow	-1.3005	0.2112	-32.57	5.46
T=298°K	Sand	0.1069	0.1689	2.68	4.36
B=298°K	Soil	0.2992	-0.0625	7.49	-1.62
	Average	-0.3819	0.0495	-9.56	1.28
Case 9	Vegetation	-5.7427	0.8002	-63.09	27.12
$\rho(\lambda)+0.2$	Snow	-6.4098	1.1311	-70.42	38.33
T=298°K	Sand	-5.0024	1.0888	-54.96	36.90
B=298°K	Soil	-4.8101	0.8573	-52.84	29.05
	Average	-5.4913	0.9694	-60.33	32.85

T = Target Temperature.

B = Background Temperature.

Difference calculations use the target SCR in each case as the reference point. Therefore, positive values are above the target SCR and negative values are below.

Table XIII. InSb Nighttime SCR Vector Distances for the 3.3-to-4.2 μm and 4.5-to-5.0 μm Bands

Case	Source	SCR 3.3-4.2 μm Band	SCR 4.5-5.0 μm Band	SCR Vector Distance	Average Vector Distance	Std Dev
Baseline	Target	1.5441	2.8195	******	1.0679	0.2975
Rural	Vegetation	2.1034	3.4420	0.8368		
T=298°K	Snow	2.2581	4.0368	1.4112		
B=298°K	Sand	1.9989	3.9532	1.2215		
	Soil	1.9164	3.5300	0.8021		
Case 1	Target	1.6784	3.0170	******	0.8323	0.2975
Rural	Vegetation	2.1034	3.4420	0.6011		
T=300°K	Snow	2.2581	4.0368	1.1730		
B=298°K	Sand	1.9989	3.9532	0.9895		
	Soil	1.9164	3.5300	0.5655		
Case 2	Target	2.3179	3.9207	******	0.3840	0.1992
Rural	Vegetation	2.1034	3.4420	0.5246		
T=308°K	Snow	2.2581	4.0368	0.1306		
B=298°K	Sand	1.9989	3.9532	0.3207		
	Soil	1.9164	3.5300	0.5603		
Case 3	Target	1.0006	1.9819	******	0.7360	0.2083
Rural	Vegetation	1.3626	2.4191	0.5676		
T=288°K	Snow	1.4635	2.8371	0.9725		
B=288°K	Sand	1.2956	2.7786	0.8496		
	Soil	1.2411	2.4813	0.5543		
Case 4	Target	1.0939	2.1308	******	0.5625	0.2083
Rural	Vegetation	1.3626	2.4191	0.3941		
T=290°K	Snow	1.4635	2.8371	0.7972		
B=288°K	Sand	1.2956	2.7786	0.6785		
	Soil	1.2411	2.4813	0.3802		
Case 5	Target	0.2235	0.5846	******	0.2062	0.0612
Rural	Vegetation	0.3040	0.7132	0.1517		
T=258°K	Snow	0.3271	0.8365	0.2724		
B=258°K	Sand	0.2896	0.8195	0.2440		
	Soil	0.2767	0.7320	0.1567		
Case	Target	0.2496	0.6398	******	0.1458	0.0611
Rural	Vegetation	0.3040	0.7132	0.0914		
T=260°K	Snow	0.3271	0.8365	0.2115		
B=258°K	Sand	0.2896	0.8195	0.1841		
	Soil	0.2767	0.7320	0.0961		

Table XIII. Continued

Case	Source	SCR 3.3-4.2 μm Band	SCR 4.5-5.0 μm Band	SCR Vector Distance	Average Vector Distance	Std Dev
Case 7	Target	1.4112	1.7344	******	2.9607	0.2006
Tropical	Vegetation	1.9208	2.1263	2.8418		
T=298°K	Snow	2.0647	2.4929	3.2139		
B=298°K	Sand	1.8272	2.4362	3.0230		
	Soil	1.7485	2.1702	2.7641		
Case 8	Target	2.0084	3.6471	******	0.2860	0.1342
$\rho(\lambda)$-0.2	Vegetation	2.1034	3.4420	0.2260		
T=298°K	Snow	2.2581	4.0368	0.4628		
B=298°K	Sand	1.9989	3.9532	0.3062		
	Soil	1.9164	3.5300	0.1489		
Case 9	Target	1.0799	1.9919	******	2.0129	0.2995
$\rho(\lambda)$+0.2	Vegetation	2.1034	3.4420	1.7749		
T=298°K	Snow	2.2581	4.0368	2.3600		
B=298°K	Sand	1.9989	3.9532	2.1659		
	Soil	1.9164	3.5300	1.7508		
		Overall SCR Average			0.9194	

T = Target Temperature.

B = Background Temperature.

Table XIV. InSb Nighttime SCR Differences Between Target and Background for the 3.3-to-4.2 μm and 4.5-to-5.0 μm Bands

Case	Source	Diff 3.3-4.2 μm Band	Diff 4.5-5.0 μm Band	% Diff 3.3-4.2 μm Band	% Diff 4.5-5.0 μm Band
Baseline	Vegetation	0.5593	0.6225	36.22	22.08
Rural	Snow	0.7139	1.2172	46.23	43.17
T=298°K	Sand	0.4548	1.1336	29.45	40.21
B=298°K	Soil	0.3723	0.7105	24.11	25.20
	Average	0.5251	0.9210	34.00	32.66
Case 1	Vegetation	0.4250	0.4250	25.32	14.09
Rural	Snow	0.5797	1.0198	34.54	33.80
T=300°K	Sand	0.3205	0.9362	19.10	31.03
B=298°K	Soil	0.2380	0.5130	14.18	17.00
	Average	0.3908	0.7235	23.28	23.98
Case 2	Vegetation	-0.2145	-0.4787	-9.26	-12.21
Rural	Snow	-0.0599	0.1160	-2.58	2.96
T=308°K	Sand	-0.3190	0.0324	-13.76	0.83
B=298°K	Soil	-0.4015	-0.3908	-17.32	-9.97
	Average	-0.2488	-0.1803	-10.73	-4.60
Case 3	Vegetation	0.3620	0.4372	36.18	22.06
Rural	Snow	0.4629	0.8553	46.26	43.15
T=288°K	Sand	0.2950	0.7967	29.48	40.20
B=288°K	Soil	0.2405	0.4994	24.04	25.20
	Average	0.3401	0.6472	33.99	32.65
Case 4	Vegetation	0.2687	0.2883	24.57	13.53
Rural	Snow	0.3696	0.7064	33.79	33.15
T=290°K	Sand	0.2017	0.6478	18.44	30.40
B=288°K	Soil	0.1472	0.3505	13.46	16.45
	Average	0.2468	0.4983	22.56	23.38
Case 5	Vegetation	0.0805	0.1286	36.02	22.00
Rural	Snow	0.1036	0.2519	46.35	43.09
T=258°K	Sand	0.0661	0.2349	29.58	40.17
B=258°K	Soil	0.0532	0.1474	23.80	25.21
	Average	0.0759	0.1907	33.94	32.62
Case 6	Vegetation	0.0544	0.0735	21.80	11.49
Rural	Snow	0.0775	0.1968	31.05	30.76
T=260°K	Sand	0.0400	0.1797	16.03	28.09
B=258°K	Soil	0.0271	0.0922	10.85	14.42
	Average	0.0497	0.1356	19.93	21.19

Table XIV. Continued

Case	Source	Diff 3.3-4.2 μm Band	Diff 4.5-5.0 μm Band	% Diff 3.3-4.2 μm Band	% Diff 4.5-5.0 μm Band
Case 7	Vegetation	0.5096	0.3919	36.11	22.60
Tropical	Snow	0.6535	0.7585	46.30	43.74
T=298°K	Sand	0.4160	0.7018	29.48	40.47
B=298°K	Soil	0.3372	0.4359	23.90	25.13
	Average	0.4791	0.5720	33.95	32.98
Case 8	Vegetation	0.0950	-0.2051	4.73	-5.62
$\rho(\lambda)$-0.2	Snow	0.2497	0.3897	12.43	10.68
T=298°K	Sand	-0.0095	0.3061	-0.47	8.39
B=298°K	Soil	-0.0920	-0.1171	-4.58	-3.21
	Average	0.0608	0.0934	3.03	2.56
Case 9	Vegetation	1.0235	1.4501	94.78	72.80
$\rho(\lambda)$+0.2	Snow	1.1782	2.0448	109.10	102.66
T=298°K	Sand	0.9190	1.9612	85.10	98.46
B=298°K	Soil	0.8365	1.5380	77.46	77.21
	Average	0.9893	1.7486	91.61	87.78

T = Target Temperature.

B = Background Temperature.

Difference calculations use the target SCR in each case as the reference point. Therefore, positive values are above the target SCR and negative values are below.

Table XV. InSb Differences Between Day and Night SCRs for the 3.3-to-4.2 μm and 4.5-to-5.0 μm Bands

Case	Source	Diff 3.3-4.2 μm Band	Diff 4.5-5.0 μm Band	% Diff 3.3-4.2 μm Band	% Diff 4.5-5.0 μm Band
Basline	Target	-5.0038	-0.5914	-76.42	-17.34
Rural	Vegetation	-1.2566	-0.3092	-37.40	-8.24
T=298°K	Snow	-0.4348	-0.0453	-16.15	-1.11
B=298°K	Sand	-2.1013	-0.0866	-51.25	-2.14
	Soil	-2.3761	-0.2783	-55.36	-7.31
Background	Average	-1.5422	-0.1798	-40.04	-4.70
Case 1	Target	-5.0038	-0.5914	-74.88	-16.39
Rural	Vegetation	-1.2566	-0.3092	-37.40	-8.24
T=300°K	Snow	-0.4348	-0.0453	-16.15	-1.11
B=298°K	Sand	-2.1013	-0.0866	-51.25	-2.14
	Soil	-2.3761	-0.2783	-55.36	-7.31
Background	Average	-1.5422	-0.1798	-40.04	-4.70
Case 2	Target	-5.0038	-0.5914	-68.34	-13.11
Rural	Vegetation	-1.2566	-0.3092	-37.40	-8.24
T=308°K	Snow	-0.4348	-0.0453	-16.15	-1.11
B=298°K	Sand	-2.1013	-0.0866	-51.25	-2.14
	Soil	-2.3761	-0.2783	-55.36	-7.31
Background	Average	-1.5422	-0.1798	-40.04	-4.70
Case 3	Target	-5.0038	-0.5914	-83.34	-22.98
Rural	Vegetation	-1.2566	-0.3092	-47.98	-11.33
T=288°K	Snow	-0.4348	-0.0453	-22.90	-1.57
B=288°K	Sand	-2.1013	-0.0866	-61.86	-3.02
	Soil	-2.3761	-0.2783	-65.69	-10.09
Background	Average	-1.5422	-0.1798	-49.61	-6.50
Case 4	Target	-5.0038	-0.5914	-82.06	-21.72
Rural	Vegetation	-1.2566	-0.3092	-47.98	-11.33
T=290°K	Snow	-0.4348	-0.0453	-22.90	-1.57
B=288°K	Sand	-2.1013	-0.0866	-61.86	-3.02
	Soil	-2.3761	-0.2783	-65.69	-10.09
Background	Average	-1.5422	-0.1798	-49.61	-6.50
Case 5	Target	-5.0038	-0.5914	-95.72	-50.29
Rural	Vegetation	-1.2566	-0.3092	-80.52	-30.24
T=258°K	Snow	-0.4348	-0.0453	-57.07	-5.14
B=258°K	Sand	-2.1013	-0.0866	-87.89	-9.55
	Soil	-2.3761	-0.2783	-89.57	-27.55
Background	Average	-1.5422	-0.1798	-78.76	-18.12

Table XV. Continued

Case	Source	Diff 3.3-4.2 μm Band	Diff 4.5-5.0 μm Band	% Diff 3.3-4.2 μm Band	% Diff 4.5-5.0 μm Band
Case 6	Target	-5.0038	-0.5914	-95.25	-48.04
Rural	Vegetation	-1.2566	-0.3092	-80.52	-30.24
T=260°K	Snow	-0.4348	-0.0453	-57.07	-5.14
B=258°K	Sand	-2.1013	-0.0866	-87.89	-9.55
	Soil	-2.3761	-0.2783	-89.57	-27.55
Background	Average	-1.5422	-0.1798	-78.76	-18.12
Case 7	Target	-3.9122	-0.2878	-73.49	-14.23
Tropical	Vegetation	-1.0012	-0.1490	-34.26	-6.55
T=298°K	Snow	-0.3337	-0.0220	-13.91	-0.88
B=298°K	Sand	-1.6538	-0.0439	-47.51	-1.77
	Soil	-1.9019	-0.1377	-52.10	-5.97
Background	Average	-1.2227	-0.0882	-36.95	-3.79
Case 8	Target	-1.9849	-0.2237	-49.71	-5.78
$\rho(\lambda)$-0.2	Vegetation	-1.2566	-0.3092	-37.40	-8.24
T=298°K	Snow	-0.4348	-0.0453	-16.15	-1.11
B=298°K	Sand	-2.1013	-0.0866	-51.25	-2.14
	Soil	-2.3761	-0.2783	-55.36	-7.31
Background	Average	-1.5422	-0.1798	-40.04	-4.70
Case 9	Target	-8.0227	-0.9590	-88.14	-32.50
$\rho(\lambda)$+0.2	Vegetation	-1.2566	-0.3092	-37.40	-8.24
T=298°K	Snow	-0.4348	-0.0453	-16.15	-1.11
B=298°K	Sand	-2.1013	-0.0866	-51.25	-2.14
	Soil	-2.3761	-0.2783	-55.36	-7.31
Background	Average	-1.5422	-0.1798	-40.04	-4.70

T = Target Temperature.

B = Background Temperature.

Difference calculations use the Daytime SCR for each source as the reference point. Therefore, positive values are above each source SCR and negative values are below.

below 5°K over the background temperature reduces the contrast in the 4.5-to-5.0 μm band, thereby making target detection difficult. However, in the 3.3-to-4.2 μm band, any increase in target temperature over the background temperature increases the contrast, thereby improving target detection.

Night. At night, the target SCR is 74.88% and 16.39% lower in the 3.3-to-4.2 μm and 4.5-to-5.0 μm bands, respectively, compared to the day. The background SCRs are the same as in the baseline case. Compared to the baseline case, the target SCR is 8.69% higher in the 3.3-to-4.2 μm band and 7.0% higher in the 4.5-to-5.0 μm band. As with the baseline case, the target SCR is lower than the background SCRs. Furthermore, the increase in target temperature reduces the contrast in both bands. However, the contrast in the 4.5-to-5.0 μm band is better than that during the day. The average background SCR is 23.28% and 23.98% higher than the target SCR in the 3.3-to-4.2 μm and 4.5-to-5.0 μm bands, respectively. Again, snow provides the best contrast. For warm conditions (298°K), any target temperature increase below 7°K over the background temperature reduces the contrast between target and background in both bands.

Tables XVI and XVII summarize the SCR changes for each case from the baseline case for day and night, respectively.

Table XVI. InSb Daytime SCR Changes From the Baseline for the 3.3-to-4.2 μm and 4.5-to-5.0 μm Bands

Case	Source	Diff 3.3-4.2 μm Band	Diff 4.5-5.0 μm Band	% Diff 3.3-4.2 μm Band	% Diff 4.5-5.0 μm Band
Case 1	Target	0.1342	0.1975	2.05	5.79
Rural	Vegetation	0.0000	0.0000	0.00	0.00
T=300°K	Snow	0.0000	0.0000	0.00	0.00
B=298°K	Sand	0.0000	0.0000	0.00	0.00
	Soil	0.0000	0.0000	0.00	0.00
Background	Average	0.0000	0.0000	0.00	0.00
Case 2	Target	0.7738	1.1012	11.82	32.29
Rural	Vegetation	0.0000	0.0000	0.00	0.00
T=308°K	Snow	0.0000	0.0000	0.00	0.00
B=298°K	Sand	0.0000	0.0000	0.00	0.00
	Soil	0.0000	0.0000	0.00	0.00
Background	Average	0.0000	0.0000	0.00	0.00
Case 3	Target	-0.5435	-0.8376	-8.30	-24.56
Rural	Vegetation	-0.7408	-1.0229	-22.05	-27.27
T=288°K	Snow	-0.7945	-1.1996	-29.51	-29.39
B=288°K	Sand	-0.7033	-1.1746	-17.15	-29.08
	Soil	-0.6753	-1.0487	-15.73	-27.54
Background	Average	-0.7285	-1.1115	-21.11	-28.32
Case 4	Target	-0.4503	-0.6887	-6.88	-20.19
Rural	Vegetation	-0.7408	-1.0229	-22.05	-27.27
T=290°K	Snow	-0.7945	-1.1996	-29.51	-29.39
B=288°K	Sand	-0.7033	-1.1746	-17.15	-29.08
	Soil	-0.6753	-1.0487	-15.73	-27.54
Background	Average	-0.7285	-1.1115	-21.11	-28.32
Case 5	Target	-1.3206	-2.2349	-20.17	-65.52
Rural	Vegetation	-1.7994	-2.7288	-53.55	-72.74
T=258°K	Snow	-1.9310	-3.2002	-71.71	-78.40
B=258°K	Sand	-1.7093	-3.1337	-41.69	-77.57
	Soil	-1.6397	-2.7980	-38.20	-73.47
Background	Average	-1.7698	-2.9652	-51.29	-75.55
Case 6	Target	-1.2945	-2.1798	-19.77	-63.91
Rural	Vegetation	-1.7994	-2.7288	-53.55	-72.74
T=260°K	Snow	-1.9310	-3.2002	-71.71	-78.40
B=258°K	Sand	-1.7093	-3.1337	-41.69	-77.57
	Soil	-1.6397	-2.7980	-38.20	-73.47
Background	Average	-1.7698	-2.9652	-51.29	-75.55

Table XVI. Continued

Case	Source	Diff 3.3-4.2 μm Band	Diff 4.5-5.0 μm Band	% Diff 3.3-4.2 μm Band	% Diff 4.5-5.0 μm Band
Case 7	Target	-1.2246	-1.3837	-18.70	-40.71
Tropical	Vegetation	-0.4379	-1.4759	-13.03	-39.35
T=298°K	Snow	-0.2944	-1.5672	-10.93	-38.39
B=298°K	Sand	-0.6192	-1.5596	-15.10	-38.61
	Soil	-0.6421	-1.5004	-14.96	-39.40
Background	Average	-0.4984	-1.5258	-13.51	-38.94
Case 8	Target	-2.5547	0.4599	-39.01	13.48
$\rho(\lambda)$-0.2	Vegetation	0.0000	0.0000	0.00	0.00
T=298°K	Snow	0.0000	0.0000	0.00	0.00
B=298°K	Sand	0.0000	0.0000	0.00	0.00
	Soil	0.0000	0.0000	0.00	0.00
Background	Average	0.0000	0.0000	0.00	0.00
Case 9	Target	2.5547	-0.4599	39.01	-13.48
$\rho(\lambda)$+0.2	Vegetation	0.0000	0.0000	0.00	0.00
T=298°K	Snow	0.0000	0.0000	0.00	0.00
B=298°K	Sand	0.0000	0.0000	0.00	0.00
	Soil	0.0000	0.0000	0.00	0.00
Background	Average	0.0000	0.0000	0.00	0.00

T = Target Temperature.

B = Background Temperature.

Difference calculations use the Baseline case SCR in each case as the reference point. Therefore, positive values are above each source SCR and negative values are below.

Table XVII. InSb Nighttime SCR Changes From the Baseline for the 3.3-to-4.2 μm and 4.5-to-5.0 μm Bands

Case	Source	Diff 3.3-4.2 μm Band	Diff 4.5-5.0 μm Band	% Diff 3.3-4.2 μm Band	% Diff 4.5-5.0 μm Band
Case 1	Target	0.1342	0.1975	8.69	7.00
Rural	Vegetation	0.0000	0.0000	0.00	0.00
T=300°K	Snow	0.0000	0.0000	0.00	0.00
B=298°K	Sand	0.0000	0.0000	0.00	0.00
	Soil	0.0000	0.0000	0.00	0.00
Background	Average	0.0000	0.0000	0.00	0.00
Case 2	Target	0.7738	1.1012	50.11	39.06
Rural	Vegetation	0.0000	0.0000	0.00	0.00
T=308°K	Snow	0.0000	0.0000	0.00	0.00
B=298°K	Sand	0.0000	0.0000	0.00	0.00
	Soil	0.0000	0.0000	0.00	0.00
Background	Average	0.0000	0.0000	0.00	0.00
Case 3	Target	-0.5435	-0.8376	-35.20	-29.71
Rural	Vegetation	-0.7408	-1.0229	-35.22	-29.72
T=288°K	Snow	-0.7945	-1.1996	-35.19	-29.72
B=288°K	Sand	-0.7033	-1.1746	-35.19	-29.71
	Soil	-0.6753	-1.0487	-35.24	-29.71
Background	Average	-0.7285	-1.1115	-35.21	-29.71
Case 4	Target	-0.4503	-0.6887	-29.16	-24.43
Rural	Vegetation	-0.7408	-1.0229	-35.22	-29.72
T=290°K	Snow	-0.7945	-1.1996	-35.19	-29.72
B=288°K	Sand	-0.7033	-1.1746	-35.19	-29.71
	Soil	-0.6753	-1.0487	-35.24	-29.71
Background	Average	-0.7285	-1.1115	-35.21	-29.71
Case 5	Target	-1.3206	-2.2349	-85.53	-79.27
Rural	Vegetation	-1.7994	-2.7288	-85.55	-79.28
T=258°K	Snow	-1.9310	-3.2002	-85.51	-79.28
B=258°K	Sand	-1.7093	-3.1337	-85.51	-79.27
	Soil	-1.6397	-2.7980	-85.56	-79.26
Background	Average	-1.7698	-2.9652	-85.53	-79.27
Case 6	Target	-1.2945	-2.1798	-83.83	-77.31
Rural	Vegetation	-1.7994	-2.7288	-85.55	-79.28
T=260°K	Snow	-1.9310	-3.2002	-85.51	-79.28
B=258°K	Sand	-1.7093	-3.1337	-85.51	-79.27
	Soil	-1.6397	-2.7980	-85.56	-79.26
Background	Average	-1.7698	-2.9652	-85.53	-79.27

Table XVII. Continued

Case	Source	Diff 3.3-4.2 μm Band	Diff 4.5-5.0 μm Band	% Diff 3.3-4.2 μm Band	% Diff 4.5-5.0 μm Band
Case 7	Target	-0.1329	-1.0852	-8.61	-38.49
Tropical	Vegetation	-0.1826	-1.3158	-8.68	-38.23
T=298°K	Snow	-0.1934	-1.5439	-8.56	-38.24
B=298°K	Sand	-0.1717	-1.5170	-8.59	-38.37
	Soil	-0.1679	-1.3598	-8.76	-38.52
Background	Average	-0.1789	-1.4341	-8.65	-38.34
Case 8	Target	0.4642	0.8276	30.06	29.35
$\rho(\lambda)$-0.2	Vegetation	0.0000	0.0000	0.00	0.00
T=298°K	Snow	0.0000	0.0000	0.00	0.00
B=298°K	Sand	0.0000	0.0000	0.00	0.00
	Soil	0.0000	0.0000	0.00	0.00
Background	Average	0.0000	0.0000	0.00	0.00
Case 9	Target	-0.4642	-0.8276	-30.06	-29.35
$\rho(\lambda)$+0.2	Vegetation	0.0000	0.0000	0.00	0.00
T=298°K	Snow	0.0000	0.0000	0.00	0.00
B=298°K	Sand	0.0000	0.0000	0.00	0.00
	Soil	0.0000	0.0000	0.00	0.00
Background	Average	0.0000	0.0000	0.00	0.00

T = Target Temperature.

B = Background Temperature.

Difference calculations use the Baseline case SCR in each case as the reference point. Therefore, positive values are above each source SCR and negative values are below.

Case 2: Rural, Target = 308°K, Background = 298°K

Day. A 10°K increase in target temperature raises the target SCR. Compared to the baseline case, the target SCR is increased in both bands. The background SCRs remain unchanged from the previous two cases. As with the baseline case and Case 1, the target SCR is higher in the 3.3-to-4.2 μm band. Unlike these two cases, the target SCR is now higher than the background SCRs in the 4.5-to-5.0 μm band as shown in Figure 26. Snow still provides the best contrast in the 3.3-to-4.2 μm band, but has the worst in the 4.5-to-5.0 μm band, where vegetation has the best. For warm conditions (298°K), an increase in target temperature above 5°K over the background temperature improves the contrast in both bands, thereby improving target detection.

Night. Compared to the day, the target SCR drops in both bands. The background SCRs remain the same as in the baseline case and Case 1. As shown in Figure 27, this case differs from the baseline case and Case 1 in that the target SCR is now higher than all of the background SCRs in the 3.3-to-4.2 μm band and higher than the SCRs of vegetation and soil in the 4.5-to-5.0 μm band. In the 3.3-to-4.2 μm band, soil has the best contrast and snow has the worst. In the 4.5-to-5.0 μm band, vegetation has the best contrast and sand has the worst. The low contrast in both bands make target detection difficult. For warm conditions (298°K), any increase in target temperature above

Baseline

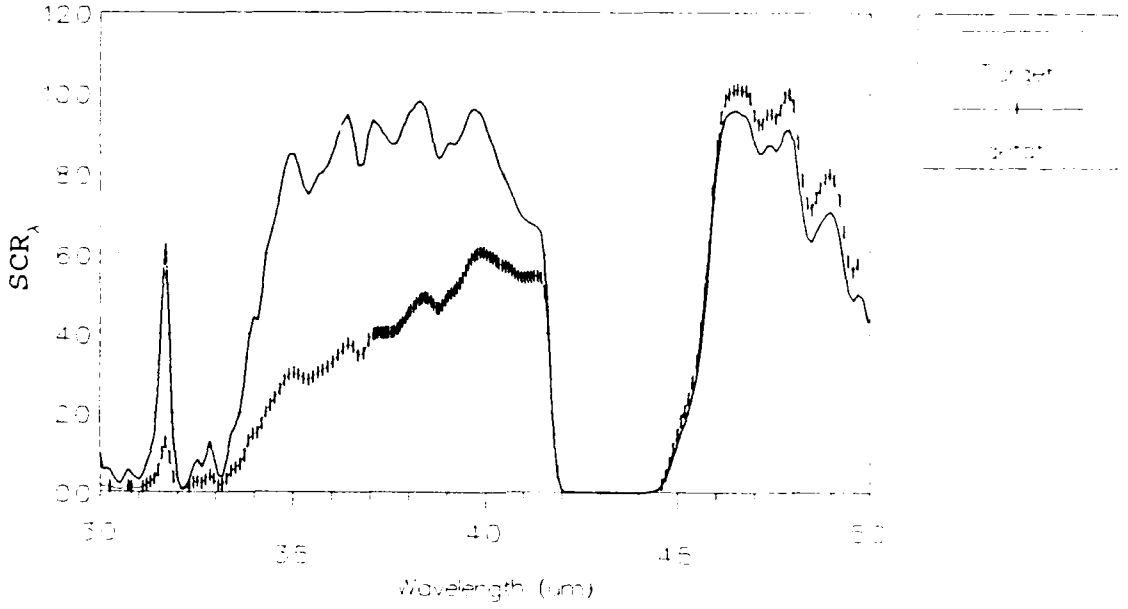

Case 2

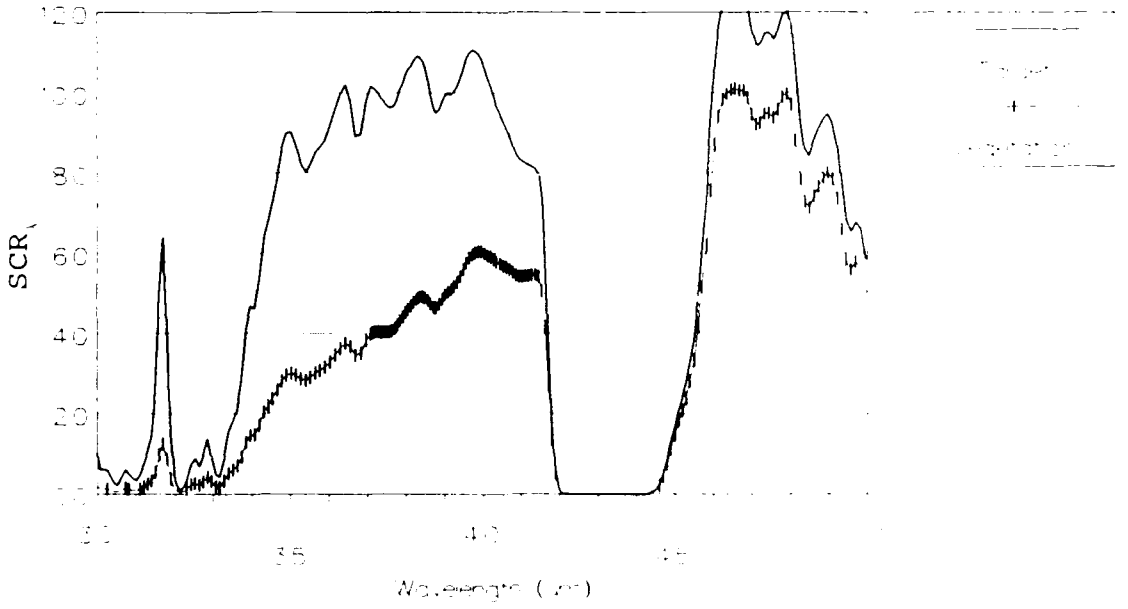

Figure 26. Baseline vs Case 2, InSb, Day

Baseline

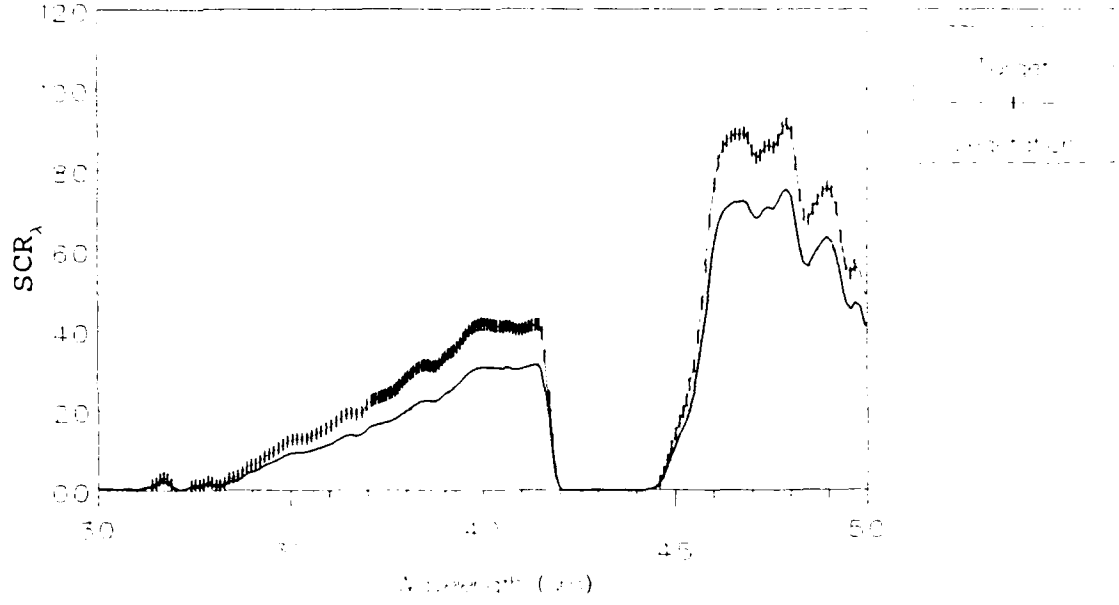

Case 2

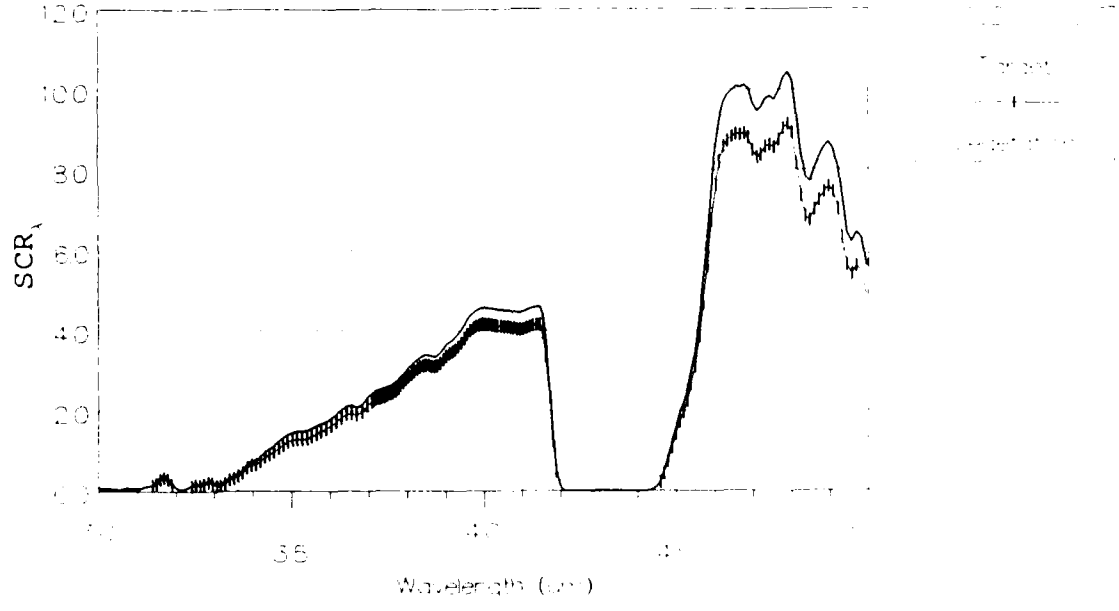

Figure 27. Baseline vs Case 2, InSb, Night

7°K over the background temperature increases the contrast in both bands, thereby improving target detection.

Case 3: Rural, Target = 288°K, Background = 288°K

Day. In this case both the background and the target temperatures are reduced by 10°K. This reduces the thermal radiation, which in turn somewhat reduces the SCRs of the target and background, compared to the baseline case. Like the baseline case and Case 1, the target SCR dominates in the 3.3-to-4.2 μm band, while the background SCRs are only slightly higher in the 4.5-to-5.0 μm band. As with the baseline case and Case 1, snow provides the best contrast. However, the low contrast in the 4.5-to-5.0 μm band may make target detection in this band difficult.

Night. At night the target and background SCRs drop in both bands compared to the day and baseline case. As with the baseline case and Case 1, the background SCRs are higher than the target SCR in both bands. Like the baseline case and Case 1, snow provides the best contrast. Furthermore, the contrast in the 4.5-to-5.0 μm band is better than that during the day.

Case 4: Rural, Target = 290°K, Background = 288°K

Day. In this case the target temperature is raised 2°K over its value in Case 3. This increase in thermal radiation increases the target SCR. The background SCRs remain unchanged from Case 3. Compared to the baseline case, the target SCR is reduced both bands. As with the

baseline case, Case 1, and Case 3, the target SCR overwhelms the background SCRs in the 3.3-to-4.2 μm band, but is slightly lower in the 4.5-to-5.0 μm band. In the 3.3-to-4.2 μm band the contrast improves over that in Case 3. However, in the 4.5-to-5.0 μm band the contrast is worse. Again, snow provides the best contrast in both bands. However, the low contrast in the 4.5-to-5.0 μm band may make target discrimination difficult. For moderate temperatures (288°K), any target temperature increase below 5°K over the background temperature lowers the contrast in the 4.5-to-5.0 μm band, while an increase higher than 5°K in target temperature increases the contrast. On the other hand, any increase in target temperature improves the contrast in the 3.3-to-4.2 μm band.

Night. An increase in target temperature of 2°K does very little to change the results from Case 3. Compared to the day and the baseline case, the target SCR is lower in both bands. The background SCRs remain unchanged from Case 3. As with Case 3, the background SCRs are higher than the target SCR in both bands, however, the contrast is reduced. In addition, the contrast in the 4.5-to-5.0 μm band is better than it is during the day. As before, snow provides the best contrast. For moderate temperatures (288°K), any target temperature increase below 7°K over the background temperature reduces the contrast in both bands, thereby making target detection more difficult, while an

increase in target temperature above 7°K increases the contrast in both bands, thereby improving target detection.

Case 5: Rural, Target = 258°K, Background = 258°K

Day. In this case both the target and the background temperatures are reduced by 40°K. This significant reduction in thermal radiation reduces their SCRs considerably compared to the baseline case. Like all of the previous cases, the target SCR dominates in the 3.3-to-4.2 μm band. On the other hand, in the 4.5-to-5.0 μm band, the target SCR is now higher than the background SCRs as shown in Figure 28. This results from the fact that at such cold temperatures the thermal contribution to the SCR becomes small compared to the reflected contribution and, therefore, the target, having a higher reflectivity than the backgrounds, has a higher SCR. Like most other cases, snow provides the best contrast in both bands.

Night. The large decrease in thermal radiation for this case is especially evident at night. Compared to the day and the baseline case, the target and background SCRs are reduced. As with the baseline case, Case 1, Case 3, and Case 4, the background SCRs are higher than the target SCR in both bands. Like the majority of the previous cases, snow provides the best contrast. However, the low contrast in both bands may make target detection difficult.

Baseline

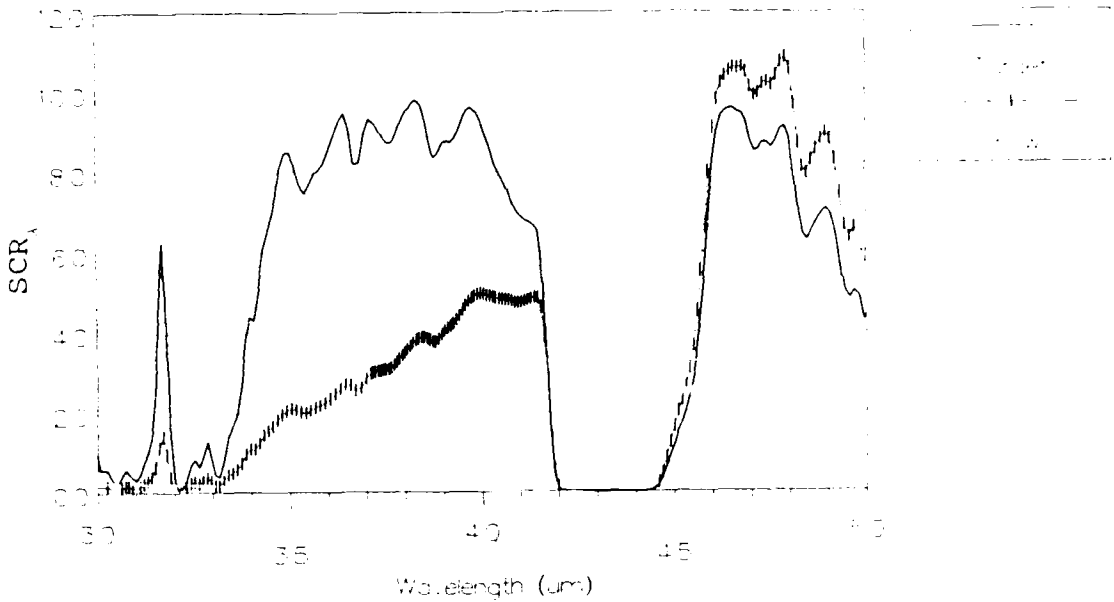

Case 5

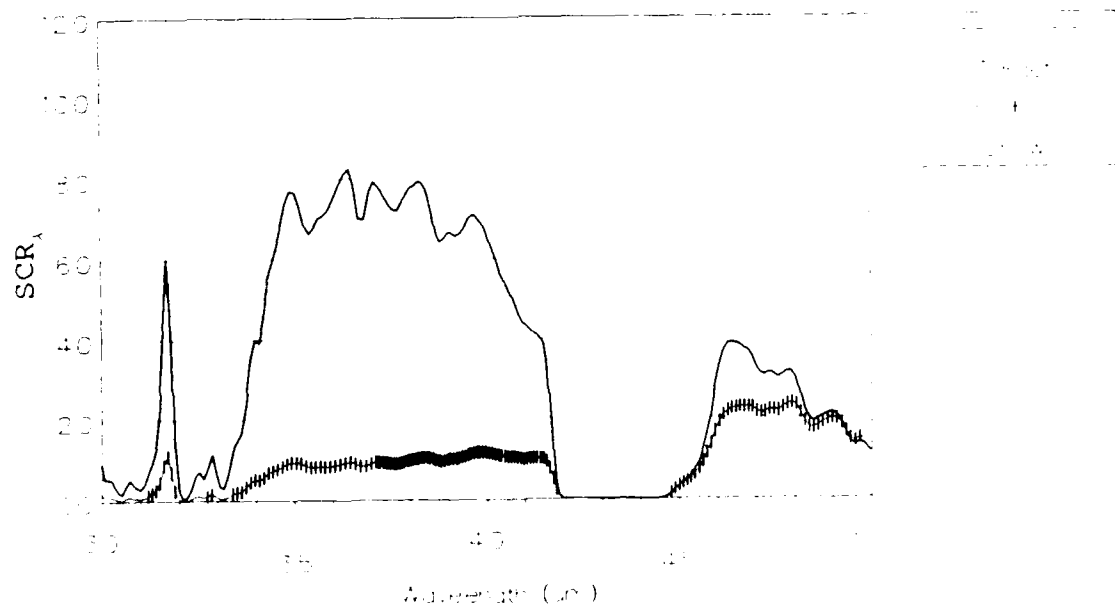

Figure 28. Baseline vs Case 5, InSb, Day

Case 6: Rural, Target = 260°K, Background = 258°K

Day. A 2°K target temperature increase over that in Case 5 increases the target SCR. Compared to the baseline case, the target SCR is smaller in both bands. The background SCRs remain unchanged from Case 5. Like Case 5, the target SCR is larger in both bands. Moreover, the increase in target temperature improves the contrast in both bands. As before, snow provides the best contrast. Under cold conditions (258°K), for both bands, any increase in target temperature over the background temperature increases the contrast, which improves the possibility of target detection.

Night. At night the target SCR drops in both bands compared to the day and the baseline case. The background SCRs remain unchanged from Case 5. As with all of the previous cases, except Case 2, the background SCRs are higher than the target SCR in both bands. However, the increase in target temperature reduces the contrast in both bands. Again, snow provides the best contrast. However, the low contrast in both bands may make target detection difficult. For cold conditions (258°K), any target temperature increase below 7°K over the background temperature reduces the contrast between target and background in both bands, while an increase in target temperature above 7°K increases the contrast in both bands, thereby improving target detection.

Case 7: Tropical, Target = 298°K, Background = 298 K

Day. In this case, the tropical atmosphere, previously shown in Figure 9, reduces the atmospheric transmission, which in turn reduces the SCRs of the target and backgrounds in both bands compared to the baseline case. Like the baseline case, the target SCR is considerably higher than the background SCRs in the 3.3-to-4.2 μm band and somewhat lower in the 4.5-to-5.0 μm band. Like the baseline case, Case 1, Case 3, and Case 4, all of which have rural settings, snow provides the best contrast.

Night. At night the target and background SCRs are reduced compared to the day and the baseline case. Like all of the previous cases, except for Case 2, the background SCRs are higher than the target SCR in both bands. Again, as with the majority of the rural setting cases, snow provides the best contrast. In addition, the 4.5-to-5.0 μm band contrast improves over that during the day.

Case 8: Baseline, Target Reflectivity Decreased by 0.2

Day. Figure 29 shows that when the target reflectivity is uniformly decreased by 0.2 (from $\approx$ 0.3 to $\approx$ 0.1) across the 3.0-to-5.0 μm band, the target SCR is lower in the 3.3-to-4.2 μm band and higher in the 4.5-to-5.0 μm band compared to the baseline case. The target SCR increase in the 4.5-to-5.0 μm band results from the increase in

Baseline

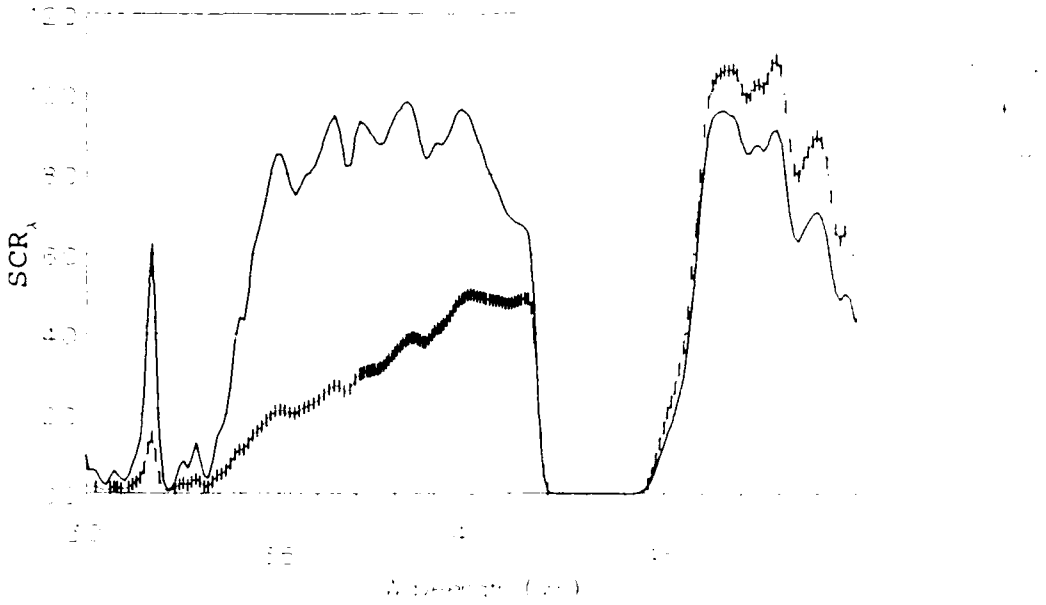

Case 8

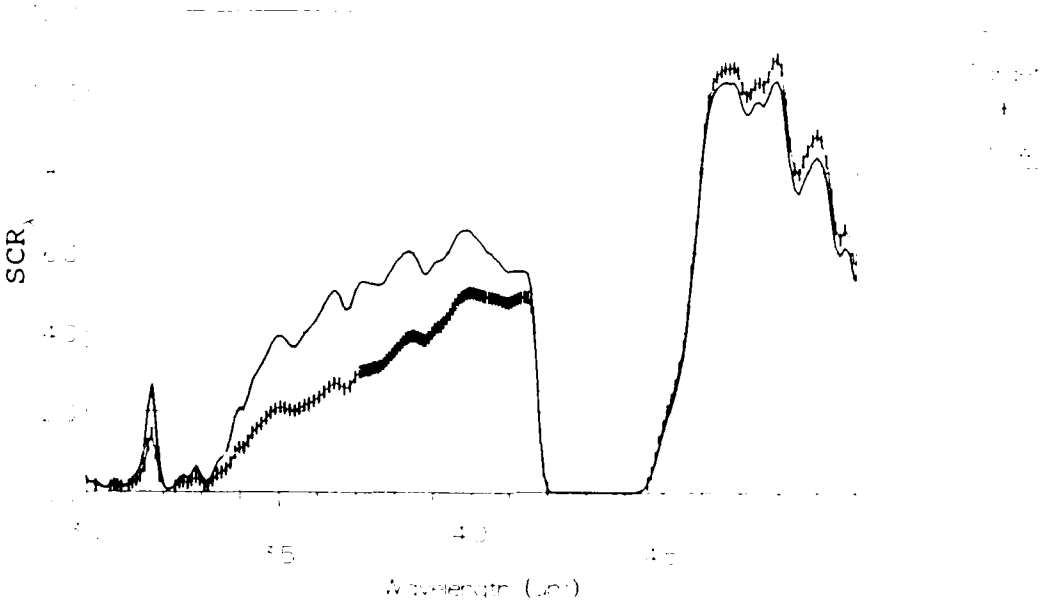

Figure 29. Baseline vs Case 8, InSb, Day

target emissivity that occurs with the decrease in target reflectivity. The contrast in both bands is worse than in the baseline case. While snow provides the best contrast in both bands, target detection in the 4.5-to-5.0 μm band may be difficult due to the low contrast. This case indicates that target reflectivities below the baseline target reflectivity value of $\approx$ 0.3 decrease the contrast between target and background in both bands, thereby making target detection more difficult.

Night. At night the target SCR drops compared to the day. Compared to the baseline case, the target SCR is larger due to the increase in target emissivity. Figure 30 shows that while the background SCRs are slightly higher than the target SCR in both bands, the contrast in both bands is degraded compared to the baseline case. Like most of the other cases, snow gives the best contrast. However, target detection may be difficult in both bands, particularly in the 3.3-to-4.2 μm band. As with the day, target reflectivities below the baseline target reflectivity value of $\approx$ 0.3 decrease the contrast between target and background in both bands, thereby making target detection more difficult.

Case 9: Baseline, Target Reflectivity Increased by 0.2

Day. Figure 31 shows that when the target reflectivity is uniformly increased by 0.2 (from $\approx$ 0.3 to $\approx$ 0.5) across the 3.0-to-5.0 μm band, both bands show a

Baseline

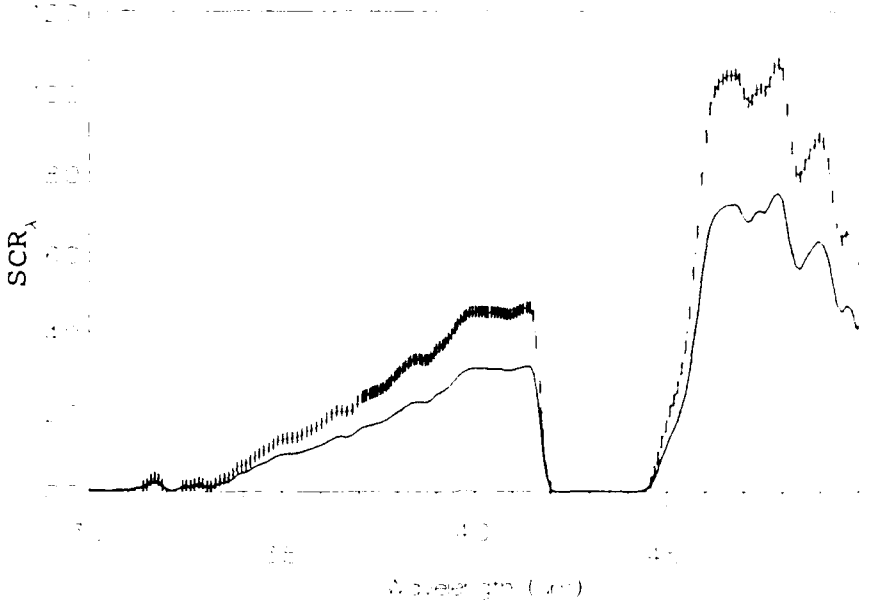

Case 8

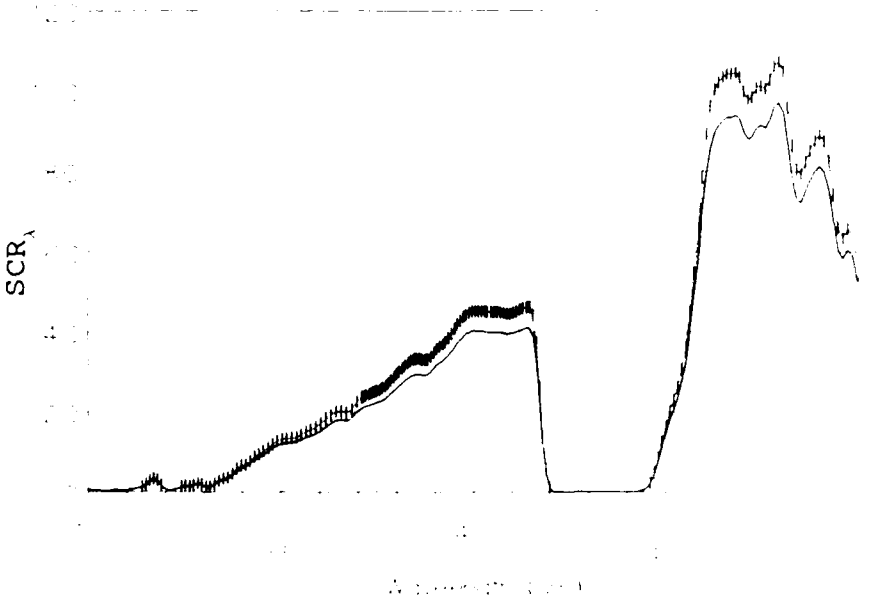

Figure 30. Baseline vs Case 8, InSb, Night

Baseline

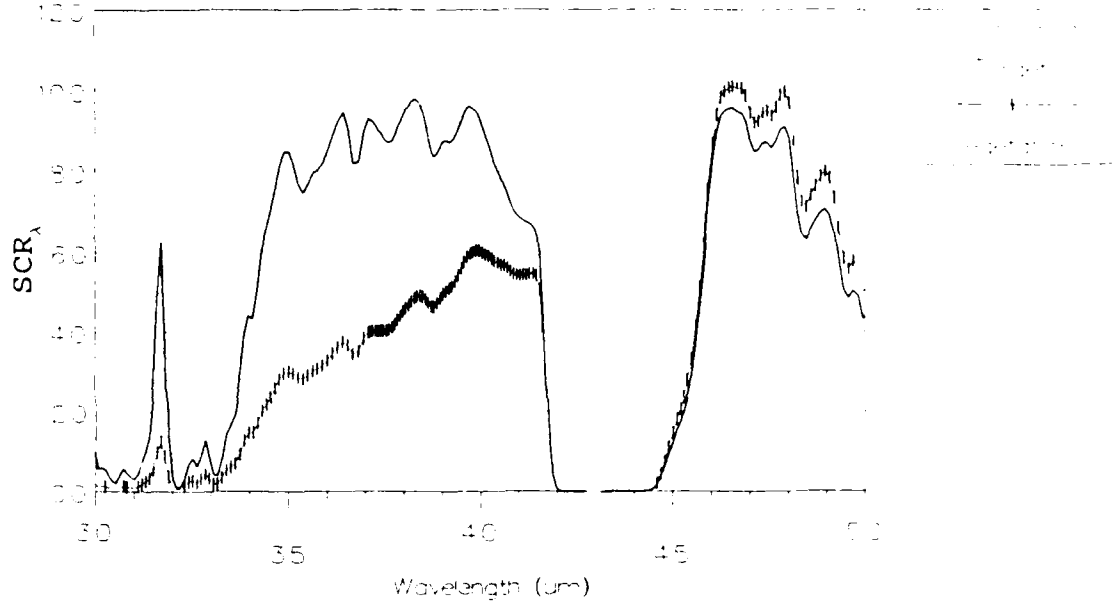

Case 9

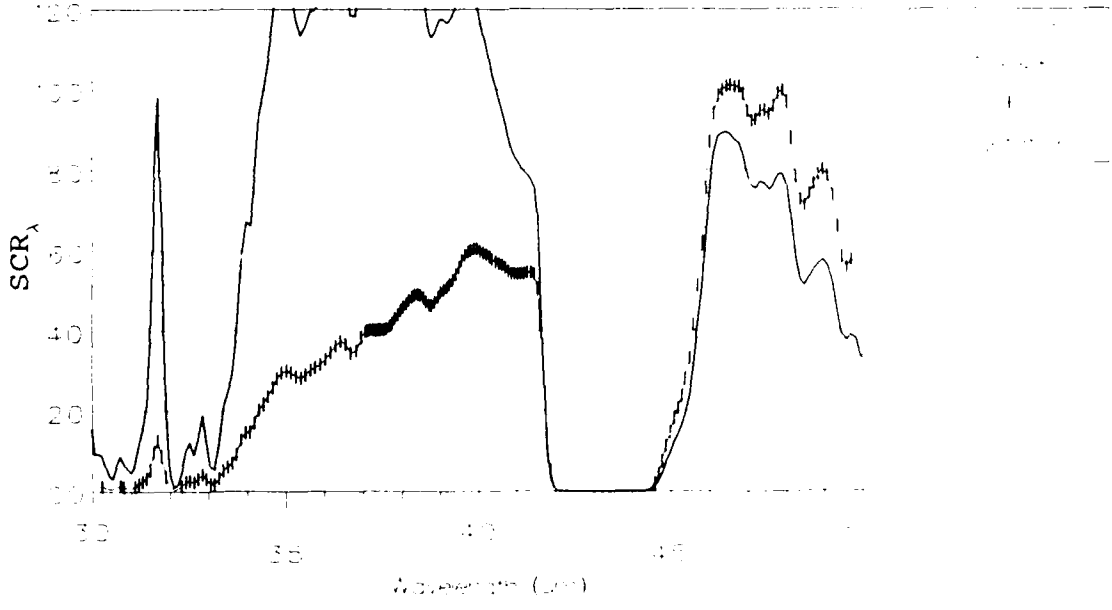

Figure 31. Baseline vs Case 9, InSb, Day

dramatic improvement in contrast over the baseline case, with the target SCR being higher in the 3.3-to-4.2 μm band and lower in the 4.5-to-5.0 μm band. The drop in target SCR in the 4.5-to-5.0 μm band results from the decrease in target emissivity that occurs with the increase in target reflectivity. Snow still provides the best contrast. This case shows that target reflectivities greater than the baseline target reflectivity value of $\approx$ 0.3 increase the contrast between target and background in both bands, thereby making target detection easier.

Night. At night the target SCR drops compared to the day and the baseline case. The target SCR reduction from the baseline case results from the decrease in target emissivity. As with the day and shown in Figure 32, the contrast in both bands is improved over the baseline case, with the background SCRs being higher than the target SCR in both bands. Snow provides the best contrast. Like the day, target reflectivities higher than the baseline target reflectivity value of $\approx$ 0.3 increase the contrast between target and background in both bands, thereby making target detection easier.

Multiband

As was discussed in Chapter II and shown in Figure 2, the 3.0-to-5.0 μm band is unique in that both reflected and thermal radiation are present. In an effort to make use of

Baseline

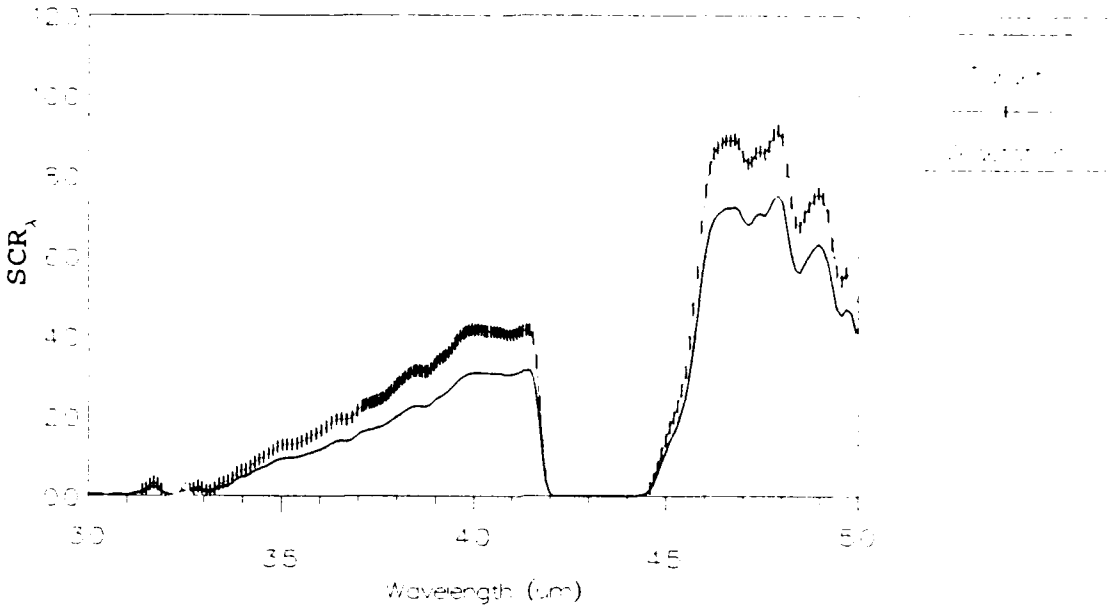

Case 9

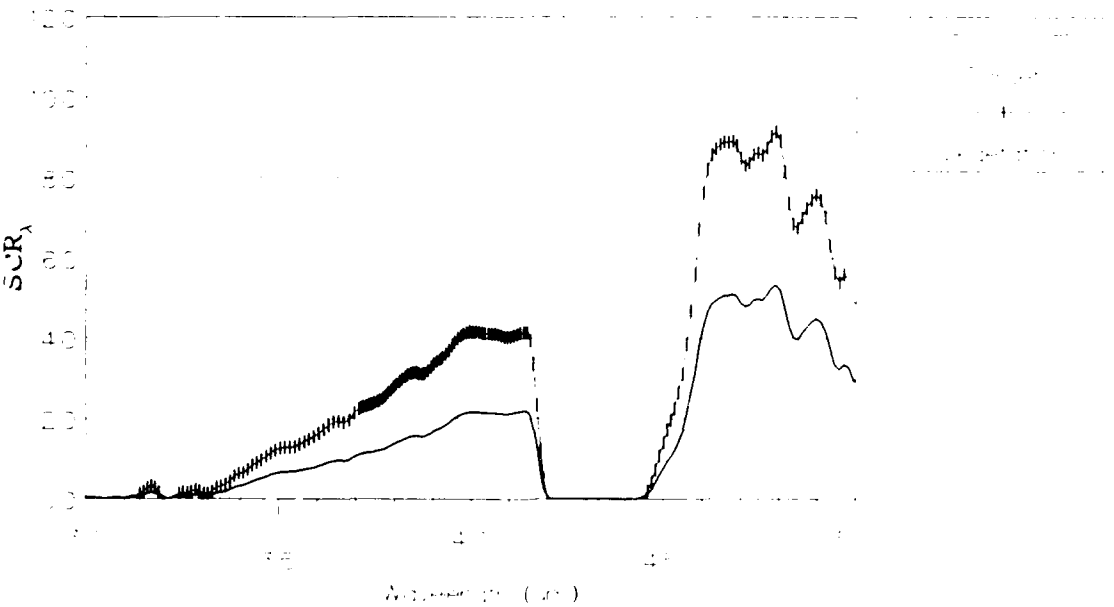

Figure 32. Baseline vs Case 9, InSb, Night

both types of radiation, an investigation of the multiband possibilities was accomplished as discussed in Chapter III.

Platinum Silicide. Examination of the previous results (Tables IV through VII) indicated that for PtSi there are essentially two sets of bands that could work for multiband remote sensing. The first and most obvious combination is that of the 3.3-to-4.2 μm and 4.5-to-5.0 μm bands. Examination of the 4.5-to-5.0 μm band indicated this band may not be useful, due to the low contrast between the target SCR and background SCR in many cases. Therefore, the second combination of bands results from dividing the 3.3-to-4.2 μm band into two bands, the 3.3-to-3.8 μm band and the 3.8-to-4.2 μm band. Computation of the distance between the target and the background, as explained in Chapter III, was accomplished for all of the cases previously discussed. For the 3.3-to-4.2 μm and 4.5-to-5.0 μm band combination the overall average distance between target and background is 0.0688 during the day and 0.0071 at night. Tables IV and VI, previously shown, contain all of the detailed data for day and night, respectively.

For the 3.3-to-3.8 μm and 3.8-to-4.2 μm band combination, the overall average distance between target and background is 0.0535 during the day and 0.0046 at night. Tables XVIII and XIX contain all of the detailed data for day and night, respectively. Comparing the two combinations

Table XVIII. PtSi Daytime SCR Vector Distances for the 3.3-to-3.8 μm and 3.8-to-4.2 μm Bands

Case	Source	SCR 3.3-3.8 μm Band	SCR 3.8-4.2 μm Band	SCR Vector Distance	Average Vector Distance	Std Dev
Baseline	Target	0.0874	0.0504	******	0.0521	0.0117
Rural	Vegetation	0.0342	0.0316	0.0565		
T=298°K	Snow	0.0253	0.0264	0.0666		
B=298°K	Sand	0.0467	0.0358	0.0432		
	Soil	0.0469	0.0386	0.0422		
Case 1	Target	0.0886	0.0518	******	0.0537	0.0117
Rural	Vegetation	0.0342	0.0316	0.0581		
T=300°K	Snow	0.0253	0.0264	0.0682		
B=298°K	Sand	0.0467	0.0358	0.0448		
	Soil	0.0469	0.0386	0.0437		
Case 2	Target	0.0943	0.0582	******	0.0614	0.0117
Rural	Vegetation	0.0342	0.0316	0.0658		
T=308°K	Snow	0.0253	0.0264	0.0760		
B=298°K	Sand	0.0467	0.0358	0.0526		
	Soil	0.0469	0.0386	0.0512		
Case 3	Target	0.0828	0.0448	******	0.0543	0.0122
Rural	Vegetation	0.0277	0.0240	0.0588		
T=288°K	Snow	0.0185	0.0182	0.0695		
B=288°K	Sand	0.0407	0.0286	0.0451		
	Soil	0.0410	0.0318	0.0438		
Case 4	Target	0.0836	0.0458	******	0.0554	0.0122
Rural	Vegetation	0.0277	0.0240	0.0599		
T=290°K	Snow	0.0185	0.0182	0.0706		
B=288°K	Sand	0.0407	0.0286	0.0462		
	Soil	0.0410	0.0318	0.0448		
Case 5	Target	0.0765	0.0367	******	0.0574	0.0130
Rural	Vegetation	0.0190	0.0130	0.0621		
T=258°K	Snow	0.0094	0.0063	0.0736		
B=258°K	Sand	0.0326	0.0180	0.0476		
	Soil	0.0329	0.0218	0.0460		
Case 6	Target	0.0767	0.0370	******	0.0577	0.0131
Rural	Vegetation	0.0190	0.0130	0.0624		
T=260°K	Snow	0.0094	0.0063	0.0739		
B=258°K	Sand	0.0326	0.0180	0.0479		
	Soil	0.0329	0.0218	0.0463		

Table XVIII. Continued

Case	Source	SCR 3.3-3.8 μm Band	SCR 3.8-4.2 μm Band	SCR Vector Distance	Average Vector Distance	Std Dev
Case 7	Target	0.0625	0.0456	******	0.0366	0.0086
Tropical	Vegetation	0.0262	0.0293	0.0398		
T=298°K	Snow	0.0200	0.0249	0.0473		
B=298°K	Sand	0.0350	0.0330	0.0303		
	Soil	0.0352	0.0355	0.0292		
Case 8	Target	0.0453	0.0350	******	0.0098	0.0091
$\rho(\lambda)$-0.2	Vegetation	0.0342	0.0316	0.0116		
T=298°K	Snow	0.0253	0.0264	0.0218		
B=298°K	Sand	0.0467	0.0358	0.0017		
	Soil	0.0469	0.0386	0.0040		
Case 9	Target	0.1296	0.0658	******	0.0970	0.0117
$\rho(\lambda)$+0.2	Vegetation	0.0342	0.0316	0.1014		
T=298°K	Snow	0.0253	0.0264	0.1115		
B=298°K	Sand	0.0467	0.0358	0.0881		
	Soil	0.0469	0.0386	0.0870		
			Overall SCR Average		0.0535	

T = Target Temperature.

B = Background Temperature.

Table XIX. PtSi Nighttime SCR Vector Distances for the 3.3-to-3.8 μm and 3.8-to-4.2 μm Bands

Case	Source	SCR 3.3-3.8 μm Band	SCR 3.8-4.2 μm Band	SCR Vector Distance	Average Vector Distance	Std Dev
Baseline	Target	0.0125	0.0162	******	0.0070	0.0019
Rural	Vegetation	0.0173	0.0219	0.0075		
T=298°K	Snow	0.0181	0.0238	0.0094		
B=298°K	Sand	0.0161	0.0210	0.0060		
	Soil	0.0161	0.0198	0.0051		
Case 1	Target	0.0137	0.0175	******	0.0052	0.0019
Rural	Vegetation	0.0173	0.0219	0.0057		
T=300°K	Snow	0.0181	0.0238	0.0076		
B=298°K	Sand	0.0161	0.0210	0.0042		
	Soil	0.0161	0.0198	0.0033		
Case 2	Target	0.0194	0.0240	******	0.0035	0.0018
Rural	Vegetation	0.0173	0.0219	0.0029		
T=308°K	Snow	0.0181	0.0238	0.0013		
B=298°K	Sand	0.0161	0.0210	0.0044		
	Soil	0.0161	0.0198	0.0053		
Case 3	Target	0.0079	0.0106	******	0.0045	0.0012
Rural	Vegetation	0.0109	0.0144	0.0048		
T=288°K	Snow	0.0114	0.0156	0.0061		
B=288°K	Sand	0.0101	0.0138	0.0039		
	Soil	0.0101	0.0130	0.0033		
Case 4	Target	0.0087	0.0116	******	0.0033	0.0012
Rural	Vegetation	0.0109	0.0144	0.0036		
T=290°K	Snow	0.0114	0.0156	0.0049		
B=288°K	Sand	0.0101	0.0138	0.0026		
	Soil	0.0101	0.0130	0.0020		
Case 5	Target	0.0016	0.0025	******	0.0010	0.0003
Rural	Vegetation	0.0022	0.0033	0.0011		
T=258°K	Snow	0.0023	0.0036	0.0014		
B=258°K	Sand	0.0020	0.0032	0.0009		
	Soil	0.0020	0.0030	0.0007		
Case 6	Target	0.0018	0.0027	******	0.0007	0.0003
Rural	Vegetation	0.0022	0.0033	0.0007		
T=260°K	Snow	0.0023	0.0036	0.0010		
B=258°K	Sand	0.0020	0.0032	0.0005		
	Soil	0.0020	0.0030	0.0004		

Table XIX. Continued

Case	Source	SCR 3.3-3.8 μm Band	SCR 3.8-4.2 μm Band	SCR Vector Distance	Average Vector Distance	Std Dev
Case 7	Target	0.0104	0.0153	******	0.0063	0.0018
Tropical	Vegetation	0.0144	0.0208	0.0068		
T=298°K	Snow	0.0151	0.0225	0.0086		
B=298°K	Sand	0.0134	0.0199	0.0054		
	Soil	0.0134	0.0188	0.0045		
Case 8	Target	0.0163	0.0211	******	0.0015	0.0013
$\rho(\lambda)$-0.2	Vegetation	0.0173	0.0219	0.0014		
T=298°K	Snow	0.0181	0.0238	0.0033		
B=298°K	Sand	0.0161	0.0210	0.0002		
	Soil	0.0161	0.0198	0.0013		
Case 9	Target	0.0088	0.0113	******	0.0131	0.0019
$\rho(\lambda)$+0.2	Vegetation	0.0173	0.0219	0.0136		
T=298°K	Snow	0.0181	0.0238	0.0156		
B=298°K	Sand	0.0161	0.0210	0.0121		
	Soil	0.0161	0.0198	0.0112		
			Overall Average		0.0046	

T = Target Temperature.

B = Background Temperature.

of bands, the 3.3-to-4.2 μm and 4.5-to-5.0 μm band combination gives significantly larger distances, therefore indicating better contrast. This supports the previous conclusion that the 4.5-to-5.0 μm band contributes very little to target discrimination from the background. Based on this, remote sensing should use only the 3.3-to-4.2 μm band. Figure 33 compares the daytime PtSi SCR distances for both combinations of bands for the baseline case.

Indium Antimonide. Using the same rationale as for PtSi, the same two combinations of bands were examined for InSb. The overall average distance between the target and the backgrounds for the 3.3-to-4.2 μm and 4.5-to-5.0 μm band combination is 3.3049 during the day and 0.9194 at night. For the 3.3-to-3.8 μm and 3.8-to-4.2 μm band combination, the overall average is 2.355 for the day and 0.3677 at night. As with PtSi, the 3.3-to-4.2 μm and 4.5-to-5.0 μm band combination has substantially larger values than the other combination, indicating better target discrimination. However, unlike PtSi, both bands within the 3.0-to-5.0 μm region contribute significantly and, hence, the 3.3-to-4.2 μm and 4.5-to-5.0 μm multiband combination is the best choice for remote sensing. This is primarily due to the higher quantum efficiency and, therefore, higher thermal sensitivity in the 4.5-to-5.0 μm band. Tables XI and XIII, previously shown, contain all of the detailed data for day and night, respectively, for the 3.3-to-4.2 μm and

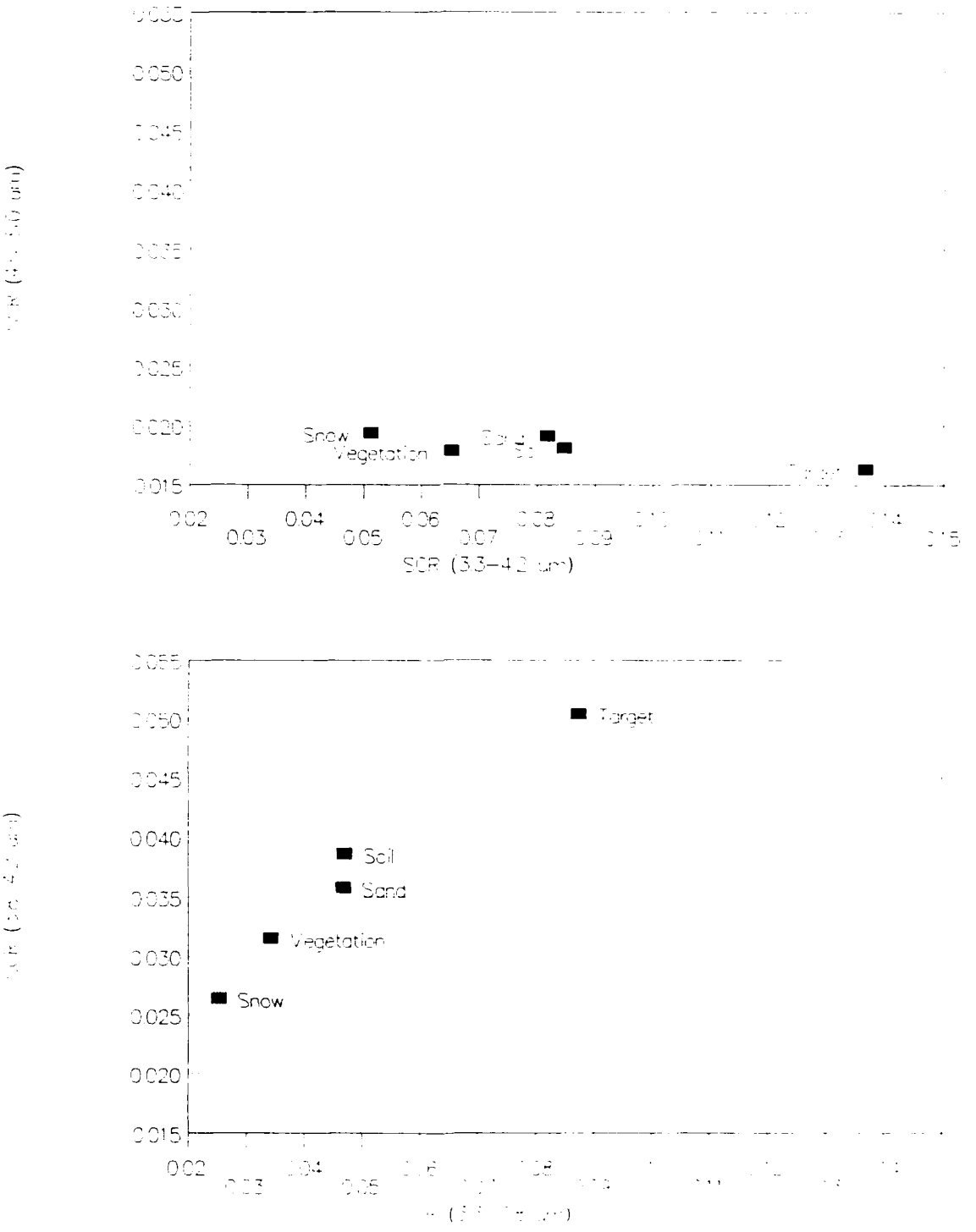

Figure 33. PtSi Daytime Baseline Vector Distance Plots

4.5-to-5.0 μm band combination. Tables XX and XXI contain all of the detailed data for day and night, respectively, for the 3.3-to-3.8 μm and 3.8-to-4.2 μm band combination. Figure 34 compares the daytime InSb SCR distances for both combinations of bands for the baseline case.

Table XX. InSb Daytime SCR Vector Distances for the 3.3-to-3.8 μm and 3.8-to-4.2 μm Bands

Case	Source	SCR 3.3-3.8 μm Band	SCR 3.8-4.2 μm Band	SCR Vector Distance	Average Vector Distance	Std Dev
Baseline	Target	3.4735	3.1404	******	2.1915	0.5240
Rural	Vegetation	1.3774	2.0141	2.3795		
T=298°K	Snow	1.0203	1.6372	2.8462		
B=298°K	Sand	1.8879	2.2547	1.8162		
	Soil	1.9000	2.4364	1.7239		
Case 1	Target	3.5212	3.2282	******	2.2754	0.5256
Rural	Vegetation	1.3774	2.0141	2.4637		
T=300°K	Snow	1.0203	1.6972	2.9323		
B=298°K	Sand	1.8879	2.2547	1.9014		
	Soil	1.9000	2.4364	1.8043		
Case 2	Target	3.7516	3.6433	******	2.6918	0.5293
Rural	Vegetation	1.3774	2.0141	2.8794		
T=308°K	Snow	1.0203	1.6972	3.3536		
B=298°K	Sand	1.8879	2.2547	2.3241		
	Soil	1.9000	2.4364	2.2102		
Case 3	Target	3.2835	2.7820	******	2.3085	0.5575
Rural	Vegetation	1.1146	1.5291	2.5047		
T=288°K	Snow	0.7448	1.1709	3.0068		
B=288°K	Sand	1.6440	1.7890	1.9168		
	Soil	1.6568	1.9981	1.8057		
Case 4	Target	3.3157	2.8439	******	2.3675	0.5587
Rural	Vegetation	1.1146	1.5291	2.5638		
T=290°K	Snow	0.7448	1.1709	3.0674		
B=288°K	Sand	1.6440	1.7890	1.9767		
	Soil	1.6568	1.9981	1.8621		
Case 5	Target	3.0259	2.2554	******	2.4779	0.6067
Rural	Vegetation	0.7583	0.8171	2.6853		
T=258°K	Snow	0.3711	0.3978	3.2403		
B=258°K	Sand	1.3134	1.1047	2.0632		
	Soil	1.3273	1.3544	1.9229		
Case 6	Target	3.0341	2.2736	******	2.4945	0.6071
Rural	Vegetation	0.7583	0.8171	2.7020		
T=260°K	Snow	0.3711	0.3978	3.2574		
B=258°K	Sand	1.3134	1.1047	2.0802		
	Soil	1.3273	1.3544	1.9386		

Table XX. Continued

Case	Source	SCR 3.3-3.8 μm Band	SCR 3.8-4.2 μm Band	SCR Vector Distance	Average Vector Distance	Std Dev
Case 7	Target	2.5211	2.8563	******	2.2186	0.3891
Tropical	Vegetation	1.0701	1.8790	2.0920		
T=298°K	Snow	0.8186	1.6015	1.7299		
B=298°K	Sand	1.4320	2.0846	2.4562		
	Soil	1.4415	2.2456	2.5965		
Case 8	Target	1.8203	2.2130	******	0.4385	0.3808
$\rho(\lambda)$-0.2	Vegetation	1.3774	2.0141	0.4855		
T=298°K	Snow	1.0203	1.6972	0.9518		
B=298°K	Sand	1.8879	2.2547	0.0795		
	Soil	1.9000	2.4364	0.2372		
Case 9	Target	5.1268	4.0679	******	4.0860	0.5249
$\rho(\lambda)$+0.2	Vegetation	1.3774	2.0141	4.2750		
T=298°K	Snow	1.0203	1.6972	4.7416		
B=298°K	Sand	1.8879	2.2547	3.7118		
	Soil	1.9000	2.4364	3.6158		
			Overall SCR Average		2.3550	

T = Target Temperature.

B = Background Temperature.

Table XXI. InSb Nighttime SCR Vector Distances for the 3.3-to-3.8 μm and 3.8-to-4.2 μm Bands

Case	Source	SCR 3.3-3.8 μm Band	SCR 3.8-4.2 μm Band	SCR Vector Distance	Average Vector Distance	Std Dev
Baseline	Target	0.5125	1.0456	******	0.3944	0.1144
Rural	Vegetation	0.7090	1.4139	0.4175		
T=298°K	Snow	0.7435	1.5352	0.5414		
B=298°K	Sand	0.6577	1.3589	0.3454		
	Soil	0.6557	1.2782	0.2732		
Case 1	Target	0.5602	1.1333	******	0.2946	0.1143
Rural	Vegetation	0.7090	1.4139	0.3176		
T=300°K	Snow	0.7435	1.5352	0.4417		
B=298°K	Sand	0.6577	1.3589	0.2458		
	Soil	0.6557	1.2782	0.1735		
Case 2	Target	0.7905	1.5484	******	0.1849	0.1082
Rural	Vegetation	0.7090	1.4139	0.1573		
T=308°K	Snow	0.7435	1.5352	0.0488		
B=298°K	Sand	0.6577	1.3589	0.2314		
	Soil	0.6557	1.2782	0.3020		
Case 3	Target	0.3225	0.6871	******	0.2569	0.0748
Rural	Vegetation	0.4462	0.9289	0.2717		
T=288°K	Snow	0.4680	1.0088	0.3531		
B=288°K	Sand	0.4138	0.8932	0.2254		
	Soil	0.4125	0.8399	0.1774		
Case 4	Target	0.3547	0.7490	******	0.1872	0.0748
Rural	Vegetation	0.4462	0.9289	0.2019		
T=290°K	Snow	0.4680	1.0088	0.2834		
B=288°K	Sand	0.4138	0.8932	0.1558		
	Soil	0.4125	0.8399	0.1077		
Case 5	Target	0.0649	0.1605	******	0.0585	0.0173
Rural	Vegetation	0.0898	0.2169	0.0616		
T=258°K	Snow	0.0943	0.2357	0.0807		
B=258°K	Sand	0.0832	0.2088	0.0517		
	Soil	0.0830	0.1962	0.0399		
Case 6	Target	0.0730	0.1787	******	0.0386	0.0172
Rural	Vegetation	0.0898	0.2169	0.0417		
T=260°K	Snow	0.0943	0.2357	0.0608		
B=258°K	Sand	0.0832	0.2088	0.0318		
	Soil	0.0830	0.1962	0.0201		

Table XXI. Continued

Case	Source	SCR 3.3-3.8 μm Band	SCR 3.8-4.2 μm Band	SCR Vector Distance	Average Vector Distance	Std Dev
Case 7	Target	0.4310	0.9927	******	1.4295	0.1077
Tropical	Vegetation	0.5963	1.3420	1.4502		
T=298°K	Snow	0.6257	1.4574	1.5679		
B=298°K	Sand	0.5526	1.2905	1.3856		
	Soil	0.5508	1.2133	1.3142		
Case 8	Target	0.6658	1.3607	******	0.0877	0.0761
$\rho(\lambda)$-0.2	Vegetation	0.7090	1.4139	0.0685		
T=298°K	Snow	0.7435	1.5352	0.1910		
B=298°K	Sand	0.6577	1.3589	0.0082		
	Soil	0.6557	1.2782	0.0831		
Case 9	Target	0.3592	0.7304	******	0.7446	0.1146
$\rho(\lambda)$+0.2	Vegetation	0.7090	1.4139	0.7679		
T=298°K	Snow	0.7435	1.5352	0.8919		
B=298°K	Sand	0.6577	1.3589	0.6958		
	Soil	0.6557	1.2782	0.6229		
		Overall SCR Average			0.3677	

T = Target Temperature.

B = Background Temperature.

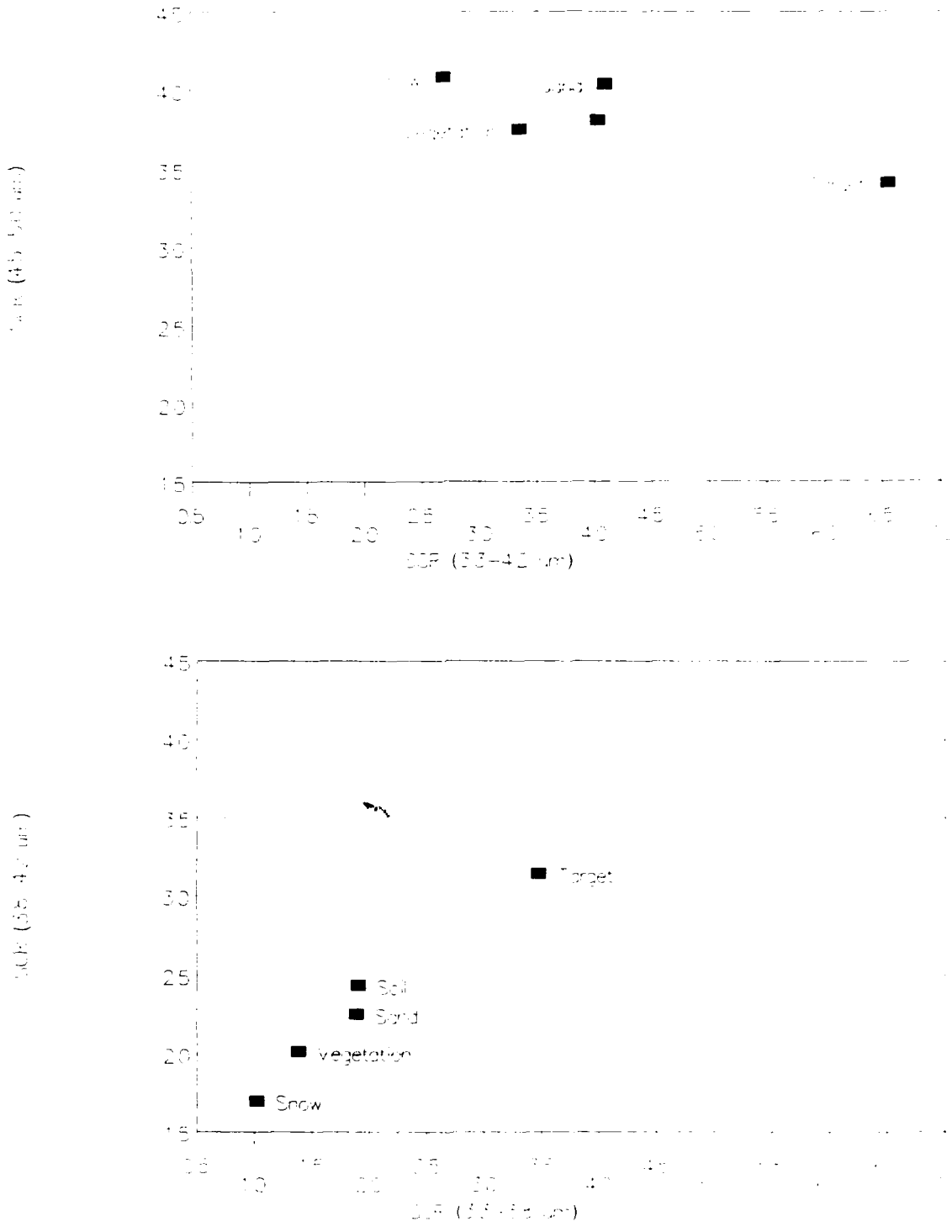

Figure 34. InSb Daytime Baseline Vector Distance Plots

V. Conclusions and Recommendations

Platinum Silicide

Day. The 3.3-to-4.2 μm band appears to be the band of choice for PtSi for daytime remote sensing under most atmospheric and temperature conditions. The main reason for this is that the SCRs for the target and background in the 3.3-to-4.2 μm band are driven by reflectivity, which is higher for the target, thereby producing good contrast. The 4.5-to-5.0 μm band, which contributes very little to discriminating between target and background, can be combined with the 3.3-to-4.2 μm band for multiband remote sensing, but is probably unnecessary. Table XXII summarizes the day and night SCR differences between target and background for PtSi.

Target/background temperatures play a small role in daytime applications because of the dominance of the reflected portion of target and background signatures. In fact, as temperatures are reduced, the reflectance maintains the contrast. Increased target temperature above background temperatures actually often tends to reduce contrast in the 4.5-to-5.0 μm band. Table XXIII summarizes the effects for day and night an increase in target temperature has on contrast.

Target reflectivity plays an important role in detection. Results indicate that as the target reflectivity drops below 0.3 (emissivity greater than 0.7), contrast in

Table XXII. Summary of PtSi SCR Differences Between Target and Average Background for the 3.3-to-4.2 μm and 4.5-to-5.0 μm Bands

Case	Diff 3.3-4.2 μm Band	Diff 4.5-5.0 μm Band	% Diff 3.3-4.2 μm Band	% Diff 4.5-5.0 μm Band
Day				
Baseline (Rural, T=298°K, B=298°K)	-0.0659	0.0023	-48.24	13.98
1 (T=300°K)	-0.0684	0.0013	-49.17	7.79
2 (T=308°K)	-0.0804	-0.0030	-53.21	-13.70
3 (T=288°K, B=288°K)	-0.0693	0.0010	-54.85	7.88
4 (T=290°K)	-0.0711	0.0003	-55.46	2.05
5 (T=258°K, B=258°K)	-0.0742	-0.0012	-66.21	-20.87
6 (T=260°K)	-0.0747	-0.0015	-66.35	-24.29
7 (Tropical)	-0.0479	0.0018	-44.75	17.67
8 ($\rho(\lambda)$-0.2)	-0.0088	0.0002	-11.10	1.27
9 ($\rho(\lambda)$+0.2)	-0.1229	0.0043	-63.49	30.34
Night				
Baseline (Rural, T=298°K, B=298°K)	0.0097	0.0044	34.17	32.93
1 (T=300°K)	0.0072	0.0034	23.28	24.18
2 (T=308°K)	-0.0048	-0.0009	-11.18	-4.61
3 (T=288°K, B=288°K)	0.0063	0.0031	34.15	32.92
4 (T=290°K)	0.0045	0.0024	22.55	23.58
5 (T=258°K, B=258°K)	0.0014	0.0009	34.10	32.89
6 (T=260°K)	0.0009	0.0006	19.89	21.37
7 (Tropical)	0.0087	0.0029	34.10	33.20
8 ($\rho(\lambda)$-0.2)	0.0012	0.0005	3.19	2.69
9 ($\rho(\lambda)$+0.2)	0.0183	0.0083	91.72	88.43

Difference calculations use the target SCR in each case as the reference point. Therefore, positive values are above the target SCR and negative values are below.

T = Target Temperature.

B = Background Temperature.

Case description indicates changes from the baseline.

Table XXIII. Increased Target Temperature Effects on Contrast for PtSi and InSb

Background Temperature	Band	Target Temperature Increase Above Background Temperature	
	Day	1-5°K	5°K +
298°K	3.3-4.2 μm	I	I
	4.5-5.0 μm	D	I
288°K	3.3-4.2 μm	I	I
	4.5-5.0 μm	D	I
258°K	3.3-4.2 μm	I	I
	4.5-5.0 μm	I	I
	Night	1-7°K	7°K +
298°K	3.3-4.2 μm	D	I
	4.5-5.0 μm	D	I
288°K	3.3-4.2 μm	D	I
	4.5-5.0 μm	D	I
258°K	3.3-4.2 μm	D	I
	4.5-5.0 μm	D	I

I = Increase in Contrast.

D = Decrease in Contrast.

The crossover temperature, where a target SCR becomes larger than the background SCR, varies with conditions. On average it is about 5°K during the day and 7°K at night.

both the 3.3-to-4.2 μm and 4.5-to-5.0 μm bands is reduced, particularly in the 4.5-to-5.0 μm band. While target detection may still be possible in the 3.3-to-4.2 μm band, it probably is much more difficult in the 4.5-to-5.0 μm band. On the other hand, targets with reflectivities of 0.3 and above are more easily detectable in both bands. Table XXIV summarizes the effects target reflectivity has on contrast for day and night.

Night. With a few exceptions, the 3.3-to-4.2 μm band is the best choice for nighttime PtSi remote sensing. Targets and backgrounds with colder temperatures around 260°K and lower provide little, if any, contrast for discrimination purposes.

Targets with reflectivities lower than 0.3 (emissivities greater than 0.7) are another cause for reduced contrast in both bands. As with the day, targets with relectivities greater than 0.3 are more easily detectable.

Indium Antimonide

Day. The 3.3-to-4.2 μm band or a combination of this band and the 4.5-to-5.0 μm band can be chosen for most daytime remote sensing needs. The high reflectivity of the target provides good contrast in the 3.3-to-4.2 μm band, while the thermal sensitivity of InSb provides fairly good contrast in the 4.5-to-5.0 μm band. Table XXV summarizes

Table XXIV. Effects of Reflectivity Changes on Contrast for PtSi and InSb

Reflectivity	3.3-4.2 μm Day	3.3-4.2 μm Night	4.5-5.0 μm Day	4.5-5.0 μm Night
0.0-0.3	D	D	D	D
0.3-1.0	I	I	I	I

I = Increase in Contrast.

D = Decrease in Contrast.

Table XXV. Summary of InSb SCR Differences Between Target and Average Background for the 3.3-to-4.2 μm and 4.5-to-5.0 μm Bands

Case	Diff 3.3-4.2 μm Band	Diff 4.5-5.0 μm Band	% Diff 3.3-4.2 μm Band	% Diff 4.5-5.0 μm Band
Day				
Baseline (Rural, T=298°K, B=298°K)	-2.9366	0.5094	-44.85	14.94
1 (T=300°K)	-3.0708	0.3119	-45.96	8.65
2 (T=308°K)	-3.7104	-0.5918	-50.68	-13.12
3 (T=288°K, B=288°K)	-3.1216	0.2356	-51.99	9.16
4 (T=290°K)	-3.2148	0.0867	-52.72	3.19
5 (T=258°K, B=258°K)	-3.3858	-0.2209	-64.77	-18.78
6 (T=260°K)	-3.4119	-0.2760	-64.95	-22.42
7 (Tropical)	-2.2105	0.3724	-41.52	18.41
8 ($\rho(\lambda)$-0.2)	-0.3819	0.0495	-9.56	1.28
9 ($\rho(\lambda)$+0.2)	-5.4913	0.9694	-60.33	32.85
Night				
Baseline (Rural, T=298°K, B=298°K)	0.5251	0.9210	34.00	32.66
1 (T=300°K)	0.3908	0.7235	23.28	23.98
2 (T=308°K)	-0.2488	-0.1803	-10.73	-4.60
3 (T=288°K, B=288°K)	0.3401	0.6472	33.99	32.65
4 (T=290°K)	0.2468	0.4983	22.56	23.38
5 (T=258°K, B=258°K)	0.0759	0.1907	33.94	32.62
6 (T=260°K)	0.0497	0.1356	19.93	21.19
7 (Tropical)	0.4791	0.5720	33.95	32.98
8 ($\rho(\lambda)$-0.2)	0.0608	0.0934	3.03	2.56
9 ($\rho(\lambda)$+0.2)	0.9893	1.7486	91.61	87.78

Difference calculations use the target SCR in each case as the reference point. Therefore, positive values are above the target SCR and negative values are below.

T = Target Temperature.

B = Background Temperature.

Case description indicates changes from the baseline.

the day and night SCR differences between target and background for InSb. Table XXIII, previously shown, summarizes the effects an increase in target temperature has on contrast for day and night.

Changes in target reflectivity have considerable impact on target detection when using InSb. A decrease in target reflectivity below 0.3 reduces the contrast in the 3.3-to-4.2 μm band and even more so in the 4.5-to-5.0 μm band. On the other hand, a target reflectivity increase above 0.3 increases contrast in both bands, and therefore, increases target detection. Table XXIV, previously shown, summarizes the effects target reflectivity has on contrast for day and night.

Night. For most cases, the contrast in the 4.5-to-5.0 μm band is better than that for the 3.3-to-4.2 μm band. Moreover, for most cases, the contrast in the 4.5-to-5.0 μm band at night is better than it is during the day. With few exceptions, a combination of the 3.3-to-4.2 μm and 4.5-to-5.0 μm bands is the best choice for nighttime remote sensing.

A decrease in target reflectivity below 0.3 reduces the contrast in both bands and, hence, the possibility of target detection. An increase in target reflectivity above 0.3 results in increased contrast in both bands, thereby improving target detection.

Mercury Cadmium Telluride

Although HgCdTe was not examined as part of this investigation, it should be noted that the InSb results are applicable to HgCdTe. As was explained in Chapter II, the only major difference between the two materials is their quantum efficiency. However, since both materials have nearly constant quantum efficiencies across the MWIR, the findings for InSb should hold for HgCdTe.

Recommendations For Future Efforts

This investigation revealed several important facts about the use of PtSi and InSb as detector materials for space-based remote sensing in the MWIR. However, study of these two materials is far from being complete. The following paragraphs discuss a few possible follow-on efforts that should prove valuable.

Actual Sensor. This study was designed to be generic in that the sensor outputs calculated are not definitive, and only point out possible ranges of where target discrimination may or may not be possible. Because these calculations are non-sensor specific, signal-to-noise (S/N) ratios cannot be calculated. By designing a specific sensor, S/N ratios can be calculated allowing for a more definitive measure of target discrimination.

Real Targets. The target chosen for this study was generic, in that it was a combination of various paints that

could be used on real objects under surveillance. Although this target was useful for this study, its reflectivity was relatively flat across the MWIR. By using specific targets, results particular to that target may be realized, especially if the reflectivity of the such targets varies more with wavelength over the MWIR.

Viewing Geometry. This entire study used a vertical line-of-sight to the target. Another study investigating various look angles could prove useful in seeing how the current results change, as well as, establishing viewing limits or boundaries. This could also be combined with the design of an actual sensor.

Bibliography

1. Alkezweeny, A.J. and P.V. Hobbs. "The Reflection Spectrum of Ice in the Near Infrared," Journal of Geophysical Research, 71: 1083-1086 (15 February 1966).

2. Amber Engineering, Inc. "Amber 128 x 128 InSb Focal Plane Array Description and Performance Summary." Presentation to WRDC on 3 August 1989.

3. Berger, Roger H. Snowpack Optical Properties in the Infrared, Hanover, New Hampshire: Cold Regions Research And Engineering Laboratory, May 1979 (AD-A071004).

4. Cantella, M.J. Space Surveillance Application Potential of Schottky Barrier IR Sensors. Contract F19628-85-C-0002. Lexington, Massachusetts: Lincoln Laboratory, 9 April 1987 (AD-A180848).

5. Contini, Casey and Richard Honzik. "Staring FPA Modeling Capability," Proceedings of the SPIE Conference on Thermal Imaging, 3-4 April 1986, Orlando, Florida. Volume 636. 60-70. Bellingham, Washington: SPIE, 1986.

6. Denda, Masahiko et al. "4 x 4096-Element SW IR Multispectral Focal Plane Array," Proceedings of SPIE on Infrared Technology XIII, 18-20 August 1987, San Diego, California. Volume 819. 279-286. Bellingham, Washington: SPIE, 1987.

7. Elliot, C.T. "Detectors of Thermal Infrared Radiation," Proceedings of the SPIE Conference on Recent Developments in Infrared Components and Subsystems, 7-8 June 1988, London, England. Volume 915. 9-19. Bellingham, Washington: SPIE, 1988.

8. Höhn, D.H. et al. "Atmospheric IR Propagation," Infrared Physics, 25: 445-456 (February 1985).

9. Holz, Robert K. The Surveillant Science: Remote Sensing of the Environment (Second Edition). New York: John Wiley & Sons, 1985.

10. Hudson, Richard D., Jr. and Jacqueline W. Hudson. "The Military Applications of Remote Sensing by Infrared," Proceedings of the IEEE. Volume 63. 104-128. New York: IEEE Press, 1975.

11. Hughes, David. "Platinum Silicide Detectors Incorporated Into New Generation of Missile Seekers," Aviation Week & Space Technology, 130: 51-62 (March 27, 1989).

12. Jamieson, John A. "Infrared Technology: Advances 1975-84, Challenges 1985-94," Proceedings of the SPIE Conference on Infrared Technology X, 23-24 August 1984, San Diego, California. Volume 510. 56-68. Bellingham, Washington: SPIE, 1984.

13. Johnson, R. Barry. "Relative Merits of the 3-5 μm and 8-12 μm Spectral Bands," Proceedings of the SPIE Conference on Recent Developments in Infrared Components and Subsystems, 7-8 June 1988, London, England. Volume 915. 106-115. Bellingham, Washington: SPIE, 1988.

14. Jost, S.R. et al. "InSb: A Key Material for IR Detector Applications," Materials Research Society Symposia Proceedings on Materials for Infrared Detectors and Sources, 1-5 December 1986, Boston, Massachusetts. Volume 90. 429-435. Pittsburgh, Pennsylvania: Materials Research Society, 1987.

15. Joyce, Richard R. "Indium Antimonide Detectors for Ground-based Astronomy," Proceedings of SPIE on Infrared Detectors, 25-26 August 1983, San Diego, California. Volume 443. 50-58. Bellingham, Washington: SPIE, 1983.

16. Kimata, Masafumi et al. "A 512 x 512-Element PtSi Schottky-Barrier Infrared Image Sensor," IEEE Journal of Solid-State Circuits, SC-22: 1124-1129 (December 1987).

17. -----. "High Density Schottky-Barrier Infrared Image Sensor," Critical Reviews of Optical Science and Technology by SPIE on Infrared Detectors and Arrays, 6-7 April 1988, Orlando, Florida. Volume 930. 11-25. Bellingham, Washington: SPIE, 1988.

18. Kneizys, F.X. et al. Atmospheric Transmittance/Radiance: Computer Code LOWTRAN 6, Hanscom AFB, Massachusetts: Air Force Geophysics Laboratory, 1 August 1983 (AD-A137786).

19. Kosonocky, Walter F. et al. "160 x 244 Element PtSi Schottky-Barrier IR-CCD Image Sensor," IEEE Transactions on Electron Devices, ED-32: 1564-1573 (August 1985).

20. Kruer, M.R. et al. "Navy Infrared Focal Plane Array Development," Proceedings of SPIE on Infrared Technology XIII, 18-20 August 1987, San Diego, California. Volume 819. 270-278. Bellingham, Washington: SPIE, 1987.

21. Lange, Maj James J. and Lt Col Howard E. Evans. Elements of Remote Sensing (Version B). Course Notes for PHYS 521, Space Surveillance. Department of Engineering Physics, Air Force Institute of Technology (AU), Wright-Patterson AFB, Ohio, May 1985.

22. Milton, A.F. et al. "Influence of Nonuniformity on Infrared Focal Plane Array Performance," Optical Engineering, 24: 855-862 (September/October 1985).

23. Mooney, Jonathan M. and Eustace L. Dereniak. "Comparison of the Performance Limit of Schottky-barrier and Standard Infrared Focal Plane Arrays," Optical Engineering, 26: 223-227 (March 1987).

24. Neel, Riley. "Challenges in Processing Data From Mosaic Sensors," Proceedings of SPIE on Mosaic Focal Plane Methodologies II, 27-28 August 1981, San Diego, California. Volume 311. 84-90. Bellingham, Washington: SPIE, 1981

25. "Non-Line-of-Sight Missile Will Use Platinum Silicide Infrared Detectors," Aviation Week & Space Technology, 130: 67-70 (March 27, 1989).

26. Orias, B. et al. "58 x 62 InSb Focal Plane Array for Infrared Astronomy," Proceedings of SPIE on Instrumentation in Astronomy, 4-8 March 1986, Tucson, Arizona. Volume 627. 408-417. Bellingham, Washington: SPIE, 1986.

27. Pellegrini, P.W. et al. "A Comparison of Iridium Silicide and Platinum Silicide Photodiodes," Proceedings of SPIE on Infrared Sensors and Sensor Fusion, 19-21 May 1987, Orlando, Florida. Volume 782. 147-160. Bellingham, Washington: SPIE, 1987.

28. Pommerrenig, D.H. "Extrinsic Silicon Focal Plane Arrays," Proceedings of SPIE on Infrared Detectors, 25-26 August 1983, San Diego, California. Volume 443. 144-150. Bellingham, Washington: SPIE, 1983.

29. Richason, Benjamin F., Jr. Introduction to Remote Sensing of the Environment (Second Edition). Dubuque, Iowa: Kendall/Hunt Publishing Company, 1983.

30. Sabins, Floyd F., Jr. Remote Sensing, Principles and Interpretation. New York: W. H. Freedman & Company, 1987.

31. Schaaf, Joel W. and Dudley Williams. "Optical Constants of Ice in the Infrared," Journal of the Optical Society of America, 63: 726-732 (June 197?).

32. Schoon, Capt Neil F. An Analysis of Platinum Silicide and Indium Antimonide for Remote Sensors in the 3 to 5 Micrometer Wavelength Band. MS Thesis AFIT/GSO/ENP/88D-4. School of Engineering, Air Force Institute of Technology (AU), Wright-Patterson AFB OH, December 1988.

33. Scribner, D.A. et al. "Measurement, Characterization, and Modeling of Noise in Staring Infrared Focal Plane Arrays," Proceedings of SPIE on Infrared Sensors and Sensor Fusion, 19-21 May 1987, Orlando, Florida. Volume 782. 147-160. Bellingham, Washington: SPIE, 1987.

34. Shepherd, F.D. "Recent Advances in Silicide Detectors," Proceedings of SPIE on Recent Developments in Infrared Components and Subsystems, 7-8 June, London, England. Volume 915. 98-104. Bellingham, Washington: SPIE, 1988.

35. -----. "Silicide Infrared Staring Sensors," Critical Reviews of Optical Science and Technology by SPIE on Infrared Detectors and Arrays, 6-7 April 1988, Orlando, Florida. Volume 930. 2-10. Bellingham, Washington: SPIE, 1988.

36. Slater, Philip N. Remote Sensing: Optics and Optical Systems, Reading, Massachusetts: Addison-Wesley Publishing Company, Inc. 1980.

37. Tsaur, B.-Y. et al. "Pt-Ir Silicide Schottky-Barrier IR Detectors," IEEE Electron Device Letters, 9: 100-102 (February 1988).

38. Turner, Robert E. Thermophysical Properties of Natural Surface Materials: Interim Report, June 1984 - May 1985. Contract F33615-80-C-1206. Dayton, Ohio: Science Applications International Corporation, October 1985 (AD-B102596).

39. Wyatt, Clair L. Radiometric System Design, New York: Macmillan Publishing Company, 1987.

40. Zhang, Y.-X. "Two Kinds of 'Blueward Shift' in the NEP Spectral Curves of InSb Detectors," Infrared Physics, 25: 579-582 (May 1985).

Vita

Captain Ralph R. Sandys [redacted] He graduated from high school in Junction City, Kansas, in 1979. He then attended the University of Michigan, where he graduated in 1983 with a Bachelor of Science in Aerospace Engineering. Upon graduation he received a commission in the USAF through the AFROTC program. He was then assigned to the Foreign Technology Division at Wright-Patterson AFB, Ohio. Initially he served as an analyst in the Future Systems Division forecasting future Soviet ballistic missiles. Later he was assigned as the Division Chief of the Future Systems Division with technical and supervisory responsibility for the Division until entering the School of Engineering, Air Force Institute of Technology in May 1988.

[redacted]

UNCLASSIFIED

SECURITY CLASSIFICATION OF THIS PAGE

REPORT DOCUMENTATION PAGE

Form Approved OMB No. 0704-0188

1a. REPORT SECURITY CLASSIFICATION UNCLASSIFIED	1b. RESTRICTIVE MARKINGS
2a. SECURITY CLASSIFICATION AUTHORITY	3. DISTRIBUTION/AVAILABILITY OF REPORT Approved for public release; distribution unlimited.
2b. DECLASSIFICATION/DOWNGRADING SCHEDULE	
4. PERFORMING ORGANIZATION REPORT NUMBER(S) AFIT/GSO/ENP/ENS/89D-6	5. MONITORING ORGANIZATION REPORT NUMBER(S)
6a. NAME OF PERFORMING ORGANIZATION School of Engineering 6b. OFFICE SYMBOL (If applicable) AFIT/ENP	7a. NAME OF MONITORING ORGANIZATION
6c. ADDRESS (City, State, and ZIP Code) Air Force Institute of Technology Wright-Patterson AFB, OH 45433-6583	7b. ADDRESS (City, State, and ZIP Code)
8a. NAME OF FUNDING/SPONSORING ORGANIZATION WRDC 8b. OFFICE SYMBOL (If applicable) AARI	9. PROCUREMENT INSTRUMENT IDENTIFICATION NUMBER
8c. ADDRESS (City, State, and ZIP Code) Wright-Patterson AFB, OH 45433-6543	10. SOURCE OF FUNDING NUMBERS PROGRAM ELEMENT NO. / PROJECT NO. / TASK NO. / WORK UNIT ACCESSION NO.

11. TITLE (Include Security Classification)
Evaluation of Platinum Silicide and Indium Antimonide as Detector Materials for Space-Based Remote Sensing in the 3.0-to-5.0 Micrometer Wavelength Band

12. PERSONAL AUTHOR(S)
Ralph R. Sandys, B.S., Capt, USAF

13a. TYPE OF REPORT	13b. TIME COVERED	14. DATE OF REPORT (Year, Month, Day)	15. PAGE COUNT
MS Thesis	FROM _____ TO _____	1989 December	154

16. SUPPLEMENTARY NOTATION

17. COSATI CODES			18. SUBJECT TERMS (Continue on reverse if necessary and identify by block number)
FIELD	GROUP	SUB-GROUP	Infrared Detection, Remote Sensing, Platinum Silicide, MWIR, Indium Antimonide
17	05	01	

19. ABSTRACT (Continue on reverse if necessary and identify by block number)
Thesis Advisor: James J. Lange, Maj, USAF
Adjunct Professor
Department of Engineering Physics

20. DISTRIBUTION/AVAILABILITY OF ABSTRACT	21. ABSTRACT SECURITY CLASSIFICATION
☒ UNCLASSIFIED/UNLIMITED ☐ SAME AS RPT. ☐ DTIC USERS	UNCLASSIFIED
22a. NAME OF RESPONSIBLE INDIVIDUAL James J. Lange, Maj, USAF	22b. TELEPHONE (Include Area Code) (513) 255-9613
	22c. OFFICE SYMBOL WRDC/AARI

DD Form 1473, JUN 86 *Previous editions are obsolete.*

SECURITY CLASSIFICATION OF THIS PAGE

UNCLASSIFIED

19. Abstract

Platinum Silicide and Indium Antimonide are evaluated as detector materials for space-based remote sensing of man-made ground targets in the 3.0-to-5.0 μm band. The evaluation compares a generic target to each of four backgrounds including vegetation, snow, sand, and soil. A spectral count rate for the target and each background is calculated taking into account the material's quantum efficiency, the source's reflectivity/emissivity, and the atmospheric transmission. A baseline case and nine excursions were examined. The baseline case has the target and backgrounds at a temperature of 298°K. The atmospheric transmission used in this case is for a rural setting with a 23 km visibility and a vertical path through the atmosphere. The nine additional cases are produced by varying the baseline one parameter at a time — target and background temperatures, target reflectivity, and atmospheric humidity. Based on these cases, an evaluation was made of the remote sensing potential of each material as the various parameters were varied. In addition, an assessment was made of the multiband remote sensing possibilities in the 3.0-to-5.0 μm band available for each material.